UNIVERSITY OF Hull

Effects of dietary fats on heart-liver lipid compositions

Yaser Alnaam

MSc (Biomedical Science)

Submitted in accordance with the requirements for the degree of

PhD (Medicinal Chemistry)

Department of Chemistry

University of Hull

March 2018

Risk Assessment

All experiments were carried out in accordance with the University of Hull's Health and Safety guidelines. A full COSHH and risk assessment was carried out for each new experiment, signed by the undertaking student, supervisor, Prof Mark Lorch and the departmental safety officer (Dr T. McCreedy) before any practical work started. The COSHH forms carry the reference numbers MLY01-04.

Acknowledgements

I would like to thank my supervisors Prof Mark Lorch, Dr. A. M. Seymour and Dr. Anthony D Walmsley for giving me the opportunity to work on this project.

My sincere thanks go to Prof Lorch for his friendly, patience guidance, encouragement and advice during my study.

I am very grateful to Mrs. Kath Bulmer for technical assistance. Kath managed all lab facilities in a professional way that made life easy for us researchers. In addition, I would like to thank Mrs. Laura Goodlass and Mr. Mathew Sanderson for excellent care of the experimental animals. My thanks go to all my friends, including Mr. Othman Alfahad, Mr. Saeed Alqarni, Mr. Khalid Al-Thubati, Mr. Usman Bamji and Dr. Hamza Al-Sheheri for their friendship and help. I am particularly indebted to my colleague Dr. Rahul Saurabh for his constant help and support throughout my research. I also appreciate Dr. Kanika Kanchan for her help and good wishes.

Most importantly, I would like to give my heartiest thanks to my childern (Ghaliah, Leen, Fahad, Abdulaziz and Dana) as well as everyone among my family and friends for their love, support, advice and encouragement. A special thanks to The Government of the Kingdom of Saudi Arabia and The Ministry of Defence, Saudi Arabia, for their care and support.

This thesis is dedicated to

My Parents

Mr. Abdul Aziz Alnaam and Mrs. Zahwa Aljorafany

&

My beloved wife

Mrs. Nawal Alshammari

Abstract

Accumulation of lipids in various organs causes many diseases such as obesity, cardiac disorder and dysfunction of the liver. The intake of fats from the diet influences the way that lipids are metabolised in the heart and liver. This provides an energy source and is a route for the production of hormones. However, excess fats may also cause abnormal metabolic pathways that lead to disease. Altered lipid metabolism is also observed because of heart failure. The aim of this project is to investigate the effect of high fat diets and heart failure on the lipid compositions of both heart and liver tissues.

Rats were maintained for nine weeks. At this point they underwent aortic constriction surgery (to mimic hypertrophied heart) or control surgery (Sham). Post-surgery animals were fed either a Western diet (WD; 45% kcal of lipids) or a high fat diet (HFD; 60% kcal of lipids). Subsequently, lipid accumulation and compositions of heart and liver tissues were investigated by histological lipid stains and nuclear magnetic resonance spectroscopy methods. Data were analysed by using principal component analysis (PCA).

Hematoxylin and eosin (H & E) and oil red O stain sections of the heart and liver tissue showed lipid accumulating, in the form of droplets, inside the cells in all animals. On initial inspection, NMR data showed little obvious difference between any of the animal groups. However, PCA was employed differences in the triglyceride (TG) and unsaturated lipids of animals fed WD and HFD were revealed. Surgery, however, appeared to have no effect on the organ's lipid compositions.

In conclusion, small but potentially significant changes in lipid compositions of WD and HFD were found in heart and liver tissues. The results of this study also suggest that the lipid diet composition may not be directly involved to propagate cardiac diseases and toxicity in the liver, which may need further investigation. However, the TG and FA unsaturated group may give an insight to develop as a biomarker to understand the mechanism between dietary surplus fat intake and lipid profiles of heart and liver and their clinical applications.

Contents

List of Figures

List of Tables

Abbreviations

AC	Aortic Constriction
ACAT	Acetyl-Coenzyme A acetyltransferase.
ACSL1	Acyl Coenzyme A synthetase Ligase 1
	(Long-chain-fatty-acid—CoA ligase 1)
ADC	Analogue to Digital Converter
ALD	Alcoholic Liver Disease
ATGL	Adipose Triglyceride Lipase
ATP	Adenosine Triphosphate
AUP1	Ancient Ubiquitous Protein 1
B0	External Magnetic Field
BN	Nucleus Magnetic Field
CGI-58	Comparative Gene Identification-58
CIDE	Cell-death Inducing DFFA-like Effector
CVD	Cardiovascular Disease
DAG	DiAcylGlycerols
DFFA	DNA Fragmentation Factor A
DGAT	Diacylglycerol Acyltransferase
DIO	Diet Induced Obesity

DNA	Deoxyribonucleic Acid
DNL	De Novo Lipogenesis
ER	Endoplasmic Reticulum
FA	Fatty Acid
FAO	Fatty Acid β-Oxidation
FATP	Fatty Acid Transport Protein
FFA Free	Free Fatty Acid
FID	Free Induction Decay
FIP2	Fat Induced Protein 2
FT	Fourier Transformation
GPC	Glycero Phospho Choline
H & E	Hematoxylin-Eosin
HF	Heart Failure
HFD	High Fat Diet
HR	High Resolution
HSL	Hormone Sensitive Lipase
LCFA	Long Chain Fatty Acid
LD	Lipid Droplet
LRAT	Lecithin Retinol Acyl Transferase
LVH	Left Ventricular Hypertrophy

LysoPC	Lyso-Phosphatidyl Choline
LysoPE	Lyso-Phosphatidyl Ethanolamine
MAPK	Mitogen Activated Protein Kinase
MAS	Magic Angel Spinning
MCTG	Medium Chain Triglyceride
MGL	Monoacylglycerol Lipase
MI	Myocardial Infarction
MRI	Magnetic Resonance Imaging
MS	Mass Spectrometry
MVA	Multivariate Analysis
NASH	Non-alcoholic Steatohepatitis
NMR	Nuclear Magnetic Resonance
ORO	Oil Red O
PA	Phosphatidic Acid
PC	Phosphatidyl Choline
PCA	Principal Component Analysis
PE	Phosphatidyl Ethanolamine
PI	Phosphatidyl Inositol
PI3K	PhosphoInositide-3-kinase
PKC	Protein Kinase C

PLIN	Perilipins
PS	Phosphatidyl Serine
PUFA	Polyunsaturated Fatty Acids
RF	Radio Frequency
ROS	Reactive Oxygen Species
SE	Sterol Esters
SFA	Saturated Fatty Acids
SM	Sphingo Myelin
TAG	Triacylglycerol
TG	Triglyceride
TMS	Tetra Methyl Silane
UBXD8	Ubiquitination X-domain-containing protein 8
VLDL	Very Low-Density Lipoprotein
WD	Western Diet
WHO	World Health Organization

Chapter 1

Introduction

The excess consumption of exogenous fats and distribution of the specific fatty acids in the tissues may be a strong marker for chronic diseases.[1-4] Fats exhibit significant roles as energy storage units, membrane structural units and eicosanoids (hormones prostaglandins and their related compounds) precursors. Therefore, they are found in the membranes, serum and adipocytes.[1-4] The body's lipids together with triglycerides and cholesterol accumulate in various fat storage tissues and organs.[1, 2] In human tissue, fats are produced endogenously and largely supplied from dietary sources.[1-4]

Fats are also stored in non-adipose tissues of muscle, liver, pancreas and heart. Over depositing of triglycerides, cholesterol and free fatty acids (FFAs) produced via *de-novo* synthetic pathway and released when triglycerides and phospholipids are hydrolyzed by cellular lipases) in these organs, is commonly known as ectopic fat deposition or steatosis.[5-7] When cells deposit more excess fats than are required for metabolic processes then the surplus lipid is esterified and stored as triglyceride in lipid droplets. The lipid droplets are intracellular organelles for the storage of fats/lipids. The excessive accumulation of lipid droplets in the cytoplasm cause cell dysfunction or cell death and this phenomenon is termed lipotoxicity.[5-10]

Atherogenic dyslipidemia (serum elevations of triglycerides, apolipoprotein B, small low-density lipoprotein and low high-density lipoprotein cholesterol), elevated blood pressure, elevated glucose associated with insulin resistance, prothrombotic and proinflammatory conditions are all linked with metabolic abnormalities.[12] These may be triggered when there is an imbalance between food uptake and energy outflow, which results in deposition of lipids in non-adipose tissues.[13]

Lipids deposition in the cardiac tissues promote cardiomyopathy (disease related to heart muscle). The overload of lipids in the heart may cause heart failure via alterations in the mitochondrial fatty acid oxidation pathways.[14] Elevated plasma lipids contribute to intramyocellular lipid accumulation in skeletal muscle that may encourage insulin resistance and type 2 diabetes.[15-19] The lipid accumulation in the liver is linked with non-alcoholic steatohepatitis (NASH) that damages the hepatocytes and promotes fibrosis leading to cirrhosis (prolonged inflammation and damage of liver tissue).[20, 21]

Subsequently, fat composition has been developed as a significant measurement mainly as a marker for metabolic syndrome, predictor of insulin resistance, low-grade inflammation, fatty liver, dyslipidemia, cancer, high blood pressure, hyperglycemia, type 2 diabetes, risk factors for both liver and cardiovascular diseases.[1-4]

1.1 Fats

Dietary fats either from plants or animals, mostly contain triacylglycerol made up of three individual fatty acids that are linked by an ester bond to a glycerol backbone[22] as shown in figure 1.1. A saturated fat comprises single bonds between the carbon atoms. In contrast, unsaturated fat possesses double bonds between the carbon atoms. Based on the number of double bonds, the unsaturated fats are classified into monounsaturated (single double bond), and polyunsaturated (more than one double bond)[23] as shown in figure 1.1.

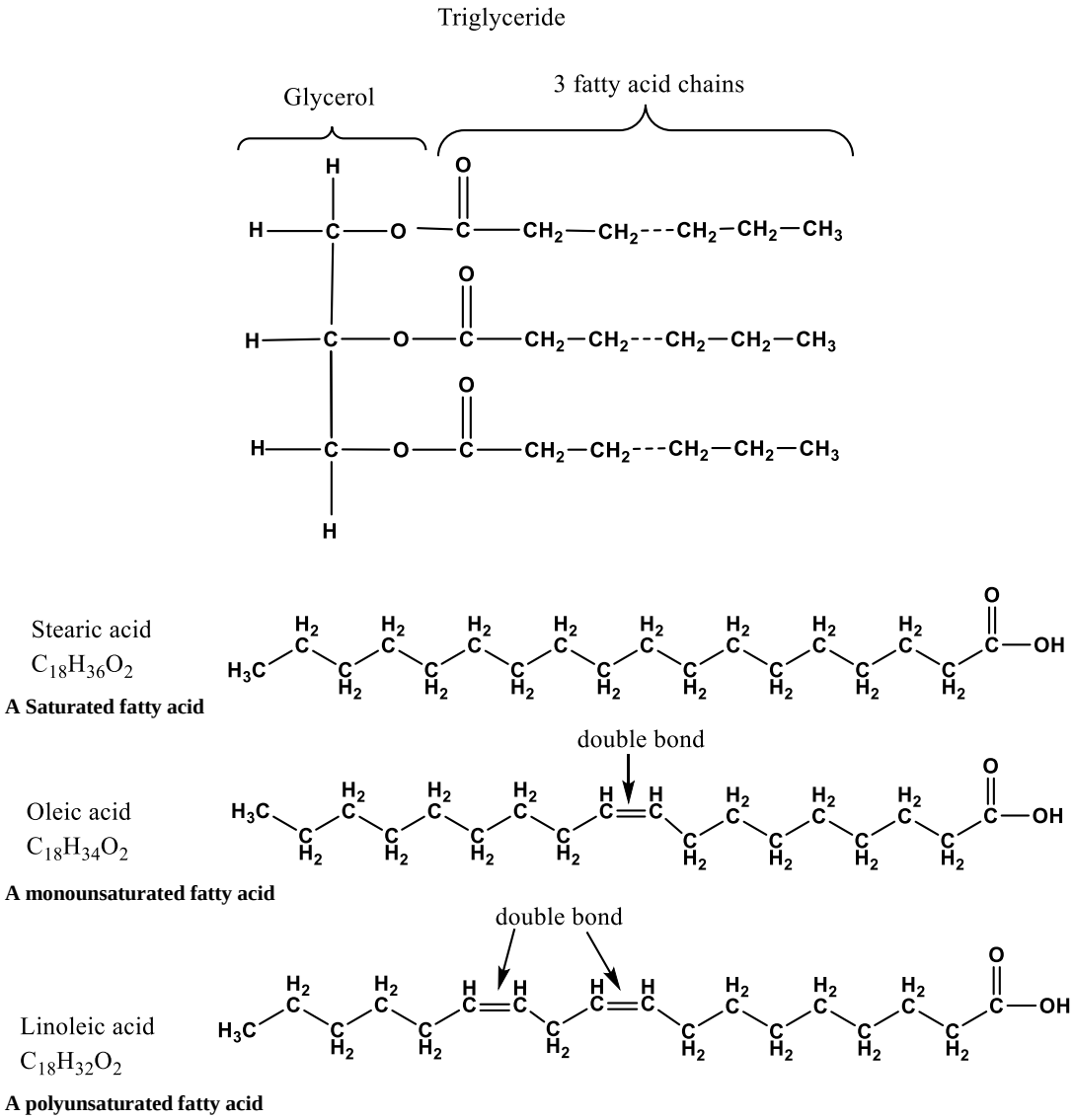

Figure 1.1 Chemical structures of triglyceride, saturated, monounsaturated, and polyunsaturated fatty acids.

The common fats in our diets are saturated, monounsaturated, polyunsaturated and *trans* fats. Dietary fats containing mainly saturated fatty acids remain solid at room temperature, particularly with long chain fatty acids (i.e. long 30 carbon chains). Whereas monounsaturated (one double bond in the fatty acid chain) or polyunsaturated (more than one double bond in the fatty acid chain) fatty acids are generally liquid at room temperature. Virtually all fatty acids in the diet and the body are long-chain forms.[23]

Nutritional guidelines usually suggest low intake of saturated fats and high use of polyunsaturated fatty acids with a double bond (C=C) at the third carbon atom from the end of the carbon chain, commonly known as omega-3 (fish or plant sources) in the diet. The guidelines also warn against eating *trans* fats to avoid diseases especially cardiovascular and liver diseases.[24, 25]

Trans fatty acids occur naturally in low amount in red meat (3-9%) and dairy products (2-5%) such as cheese, butter and milk from ruminant animals (cattle, sheep and goats).[26, 27] Artificial *trans* fats are produced by adding hydrogen (hydrogenation process) to vegetable oils, making them solid or semi solid, such as those used in margarines and shortenings. In the *cis* isomer, the hydrogen atoms are on the same side of the double bond. During hydrogenation process, the *cis* isomers of the unsaturated fat convert to a *trans* isomer of the unsaturated fat. In the *trans* isomers, the hydrogen atoms are on the opposite side ot the double bond.[28, 29] Numerous animal studies suggest that great quantities of *trans* fats lead to negative effects on insulin and glucose function.[30-32]

Fatty acids are the fundamental structural constituents of triglycerides that are also observed in phospholipids and cholesterol esters.[33] The common fatty acids of human tissues are listed in table 1.1. The polyunsaturated fats are essential for life, one double bond containing polyunsaturated fats are usually liquid (i.e., oils) at room temperature. The most dominant polyunsaturated fats in the human tissues are dihomo-γ-linolenate, linoleate, eicosapentanoate and arachidonate. Subsequently the selective storage, metabolism and digestion of dietary fats may influence tissue levels and body profiling.[33]

Table 1.1 List of common fatty acids found in human tissues[33]

Saturated fatty acids	Unsaturated fatty acids
Laurate, Myristate, Palmitate, Stearate, Arachidate, Behenate, Lignocerate	Lauroleate, Oleate, Myristoleate, Palmitoleate, Elaidate, α-Linolenate Linoleate, γ-Linolenate, Gadoleate, Gondoate, Eicosapentanoate, Dihomo-γ-linoleate, Arachidonate, Euricate, Docosahexanoate, Docosapentanoate, Docosapentanoate, Docosahexanoate

Fatty acids with fewer than 8 carbons are considered to be short chain. These fatty acids are usually water soluble. The fatty acids with 8–15 carbons are known as medium chained and found in mainly milk and coconut fat.[33] The medium chained fatty acids are normally intermediaries in the biosynthesis of long-chain fatty acids. These above-mentioned types of fatty acids are commonly deposited in substantial amounts in body lipids.[33] More than 15 carbons chain fatty acids are known as long chain fatty acids, such as palm oil, animal fat, butter and peanut fats. Predominantly long-chain polyunsaturated fatty acids are found in sperm, retinal membranes and brain synapses.[33]

1.2 Fats and modern diets

Excess fat in the diet is the basic determining factor contributing to store the fat/lipid in the body and initiating lipid metabolic diseases and disorders.[34, 35] The present day or modern diet frequently involves a high intake of fats and sugar-based foods. Such a modern lifestyle causes considerable risk factors for either obesity and lipid disorders or dyslipidemia that have an independent and collective impact on the body.[34, 35]

The adipose tissues of the body are complicated structures that regulate fatty acid balance, clearing and release process.[36] The biological data support that the fatty acids of the diet are one of the major underlying factors increasing the risk of cardiac and liver diseases.[37] According to the World Health Organization (WHO) obesity is the 5th major cause of global mortality and an important risk factor for chronic diseases, such as coronary disorders, hypertension and diabetes.[38]

1.2.1 Standard Diet

As per the American Heart Association,[39] standard diets are those diets where the total energy obtained from fats in the overall per day calorie intake does not exceed 7% Kcal. One can calculate one's per day fat intake in grams as shown in an example of a 2000 calorie per day diet. This total calorific intake of 2000 is multiplied by the recommended percentage of fat intake (that is 0.07 or 7%) to get 140 calories. Now the obtained calories is further divided by 9, since one gram of fat contains 9 calories (140 divided by 9 gives 15). Thus, in a daily diet of 2000 calories, the amount of saturated fat should be around 15 grams to maintain a standard diet with 7% Kcal fat.[39] Animal or rat models have served as helpful tools for research studies on lipid metabolism. Many commercial companies like Research Diets, Inc. and Purina have developed a standard diet formula with 7% Kcal fat that is called normal laboratory chow, or is referred to as standard diet, maintenance diet or control diet .This standard diet is used in the control group of animal models during obesity and lipid metabolism research as well as experimentation.[40]

1.2.2 Western Diet

Nutritional shift towards a more Western diet with 45% Kcal fat has resulted in more adiposity, but it is still not clear whether it is the Western diet that accelerates the growth of obesity in combination with other factors such as metabolic syndrome and vascular

function. It is still unexplained how the fat compositions of Western diet are responsible for affecting the lipid metabolism and promoting diseases such as obesity, overweight, vascular dysfunction and metabolic syndrome.[41]

Western diet can enhance obesity, cause fatty liver and lipid metabolic disease. The dietary fat percentage could be an important marker for assessment of obesity and related risk factors.[41] Heinonen *et al*. studied the impact of a high fat diet with even more than 45% kcal fat and compared it with a Western diet (of the same calorie content but with elevated levels of fat and cholesterol) using animal models (nine-week-old male mice were fed *ad libitum* standard diets, either low fat (10%) diet or Western diet for eight weeks).[41] It was found that the animals that were given the excess fat diet and the Western diet had significantly more adipose tissue as compared to the control and animals that were given a low-fat diet with 10% Kcal fat.[41] The level of liver triglycerides, cholesterol as well as oxidative damage were far more in the animals given the Western diet as compared to those given the low-fat diet.[41] They also found that the level of serum triglycerides was higher in Western diet animals in comparison with low fat diet groups. The circulating cholesterol was ten-fold higher in Western diet groups of mice and harmed the livers.[41] The data collected in this study demonstrates that without causing any changes in the total body weight, the Western diet leads to significant levels of full-body oxidative stress and increases body adiposity levels which are associated with endothelial functions involved in arterial resistance.[41]

1.2.3 High fat Diet

High fat diet contains 60% Kcal fat. These kinds of diets were originally created for use in research studies that were examining the kind of nutritional diet required to induce obesity and lipid metabolic disorders.[42] The original high fat diet was created by Research

Diets Inc. (USA) as diet induced obesity (DIO) series diets contaning matched purified ingredients, which would be used for reporting valid results from any research study, unlike those obtained using a grain-based chow diet. High fat diets with up to 60% Kcal fat are, in the context of human nutrition, bordering on the extreme. As such, these high fat diets are mostly utilized in obesity inducing studies to examine metabolic compounds within a smaller time frame.[43, 44]

1.3 Heart and lipids

The mammalian heart needs energy to perform the contractile function and maintain blood transport. During healthy physiological conditions, cardiac energy mainly comes from the oxidative catabolism of fatty acids, 70% of total cardiac energy comes from fatty acids and glucose is the second source of cardiac energy (20 %), the remaining 10% is derived from substrates such as lactate and ketones.[45] To perform the contractile function under different physiological conditions, the myocardium has developed critical molecular mechanisms which match the energy supply requirement that depend upon the availability of nutrients.[46] For example, the foetus heart functions at low oxygen pressure and mainly relies on glucose as well as lactate, while the mature heart uses fatty acids but conserves the ability to shift to other substrates. Meanwhile, aged mammals, including humans, utilize a comparatively smaller amount of fatty acids and massive amounts of glucose.[47] High glucose level and excess fatty acids may cause the lipotoxicity in various organs such as the liver, pancreas and heart.[48]

1.3.1 Sources and delivery of lipids to myocardium

Myocardial tissues readily obtain lipids from circulating free non-esterified fatty acids as well as esterified fatty acids which are bound to lipo-proteins[47] (Figure 1.2). The esterified

fatty acids are a major source of lipids for the mammalian heart.[47, 49] The fatty acids delivered to the heart come from nutritional fats.[49-51]

There are three possible ways to deliver lipid into cardio-myocytes. (1) The endothelial cell surface transporter CD36 carries fatty acids inside the cardio-myocytes. This route was identified in CD36 knockout mice studies.[52-56] Whereas, Fukuchi *et al*. reported that the genetic abnormalities in CD36 may alter the delivery of fatty acids inside the cardio myocyte and they also suggested that in this condition glucose uptake increased up to three times more than the normal condition in the cardio-myocytes. (2) Non-receptor mechanisms such as biophysical diffusion transporting fatty acids inside the heart tissues. (3) The transporter protein known as fatty acid transport protein (FATP) is also reported to deliver fatty acid inside the cardiac myocytes. [57-59]

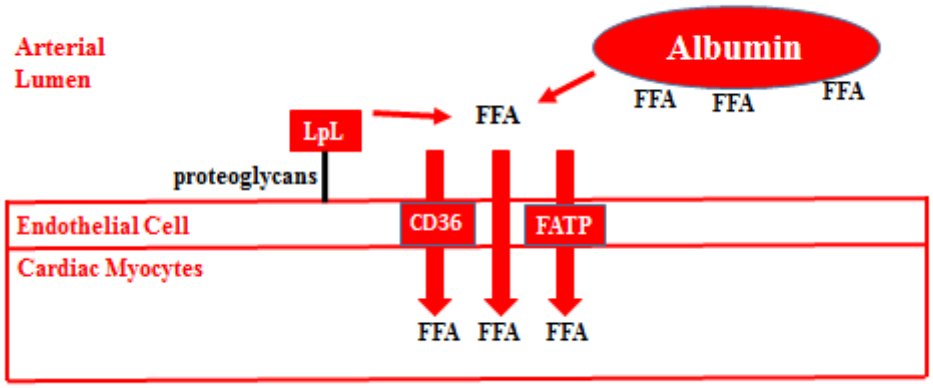

Figure 1.2 Schematic diagram of source and delivery of myocardium fatty acids.
Lipoprotein lipase (LpL) is linked with proteoglycans on the lumen surface of endothelial cells. Lipoprotein derived fatty acids and non-esterified free fatty acids (FFA) with albumin are internalised by membrane transporters such as CD36 or other transporters such as fatty acid transport protein (FATP) or non-receptor diffusion via membrane.

1.3.2 Lipid accumulation in myocardium

Extra lipid, mainly TG accumulates in the form of lipid droplets as shown in figure 1.3. in the myocardium.[47] Lipid droplet formation is dependent on a family of lipid droplet proteins commonly known as perilipin. In the myocardium, the expression of perilipin is a principal factor in lipotoxicity,[60, 61] and regulation of TG oxidation. [62]

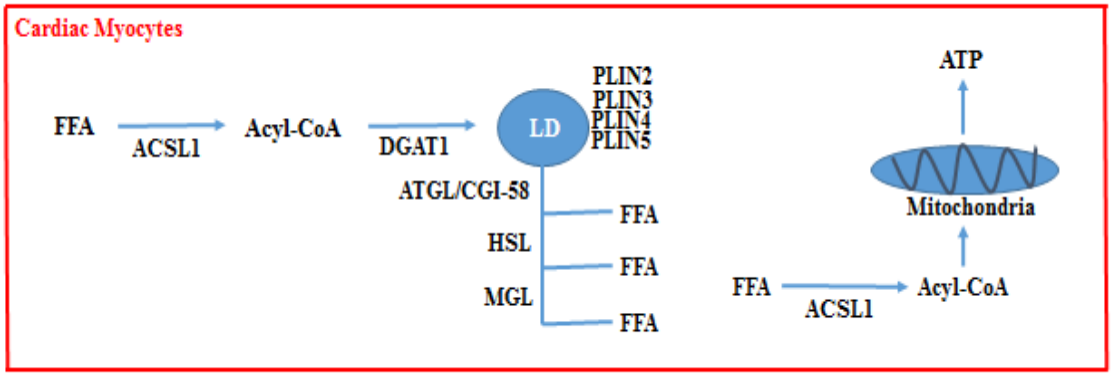

Figure 1.3 Schematic diagram of lipid storage inside the heart.

The fatty acids inside the cardiac myocytes are esterified to acetyl-CoA and either accumulate in the form of lipid droplet (LD) by the action of fatty acid CoA ligase 1(ACSL1) and signalling lipid molecules diacylglycerols (DAGs) or utilize for ATP formation by mitochondria. Lipid droplet proteins family, perilipins (PLIN) are expressed in the heart which is very important for the formation of LD. LD deliveries oxidative fatty acids by the action of enzymes ATGL, HSL and MGL. CGI-58 is the co-activator of ATGL.

The quantity of lipid-droplet is regulated by various cytosolic proteins and enzymes such as lipid-droplet-associated proteins, acyl transferases and intracellular lipases.[63] Lipid metabolism in cardiac myocytes has a similar regulatory mechanism to skeletal myocytes. TG lipid-droplet may be hydrolysed by cardiac expressed enzymes such as adipose triglyceride lipase (ATGL) as well as hormone sensitive lipase (HSL). In the lipid droplets containing adipose tissue, the lipolysis process is inhibited by insulin and stimulated by

catecholamines, thyroid hormone, and glucagon, but such a regulatory mechanism is not yet found in the heart.[47]

1.3.3 Effects of dietary fats on heart

Saturated long chain fatty acids, mainly palmitic acids are reported to cause more toxicity than unsaturated long chain fatty acids, for example oleic acids.[48] Park *et al*. found that mice fed a high-fat diet rapidly developed heart insulin resistance, which further suggested that the storage of lipids altered the metabolism of the heart, permitting it to become more dependent on fatty acids as its energy source. However, the effect of dietary fats on heart function are diverse.[64] For example, Okere *et al*. found that rats feed a 60% fat diet had minor left ventricular hypertrophy as well as systolic dysfunction in comparison to rats feed a 10% fat diet.[65] In the same way, the rats fed a high-fat diet dealt with this by rising the oxidation of fatty acids, while the rats feed a low fat and a high carbohydrate Western diets developed cardiac dysfunction.[66]

1.3.4 Heart hypertrophy and lipid metabolism

Hypertrophy, enlargement of the heart, is seen as a response to physiological and metabolic stress.[67] During stress, the mammalian heart adapts to become hypertrophied, resulting in a decrease in functional cardiac output and eventually leading to heart failure (HF).[67, 68] Left ventricular hypertrophy (LVH) was believed to be the first response to stress although this is now known to be an oversimplification.[69] Since then, two other processes have been recognised in the heart during stress – concentric and eccentric hypertrophy modelling. The eccentric hypertrophy is characterised by inconsistences in cardiac cells length against cell width.[70] It is generally noticed in the left ventricle of post-myocardial infarction (MI) hearts.[71] Whereas, concentric hypertrophy is recognised as a

growth in the width of myocyte relative to the cardiac cell length, exhibiting an increase in ventricular mass and a smaller ventricular cavity.[70]

Metabolic remodelling is a primary characteristic in the progression of cardiac hypertrophy.[71, 72] Particularly, this type of remodelling is well recognised in both experimental models and patients with LVH and heart failure. Two main cardiac hypertrophy models are well established in the study of metabolic hypertrophy heart – the aortic constriction (AC) rat and the MI rat – exhibit decreased long chain fatty acid (LCFA) oxidation associated with FA uptake and oxidation.[73] Sack *et al.* reported that a gene regulatory pathway controlled the cardiac energy and fatty acid β-oxidation (FAO) derived energy was reduced during hypertrophied heart and the development of HF.[74] Further, Doenst *et al.* demonstrated that remodelling of the heart via AC or MI reduced CD36 expression in hypertrophied hearts, suggesting impairment in LCFA uptake.[75] However, Iemitsu *et al.* found that the function of the hypertrophied heart improved with a diet supplement of medium chain TG (MCTGs).[76] In addition, Allard *et al.* observed a significant increase in FAO rates in hypertrophied hearts with palmitate intake.[77] Collectively, these findings suggest precise disturbance to the uptake and oxidation of FA in the hypertrophied heart. Therefore, a hypertrophied heart may exhibit noticeable changes in its lipid composition.

1.4 Liver and lipids

The incidence of fatty liver diseases is growing worldwide in both youth and older persons.[78] Adipose tissues play a vital role in protecting against lipids flux during the postprandial (the phase directly after a meal) period. Once the protecting ability of adipose tissue reduces, at that point non- adipose tissues, for example, skeletal muscle

and liver are exposed to extra lipids.[78] The liver contributes a significant role in metabolic regulation of dietary nutrients together with fats and carbohydrates. [79-81]

The deposition of intra-hepatic fats is immediately identified as a contributor to the pathogenesis of metabolic diseases.[82] However, the mechanism by which the liver initiates fat accumulation is not well understood. It has been hypothesised that once the fatty acid levels surpass the capacity of the liver to process then through different pathways, such as secretion or oxidation, then these excess fatty acids are deposited as triglyceride (TG).[83-85] The majority of lipids involved in hepatic metabolic diseases are TG.[86] Elevated levels of FFA, free cholesterol, diacylglycerol, ceramide, cholesterol ester and phospholipids also cause abnormalities and toxicity in the liver.[86, 87]

1.4.1 Fatty acids uptake in the liver

The liver does not act as a fat storage organ under stable physiological conditions and when the concentration of TG is low, as in a normal healthy state. However, the concentration of TG and fatty acids in the liver also depend on feeding and fasting states. Dietary fats are absorbed by the small intestine and further accumulated as TG and then secreted into plasma. The excess fatty acids are stored in adipose tissues and any remaining fatty acids are taken up by the liver.[88-90] Excess carbohydrates are synthesized de novo within the liver and stored as fatty acids.[91] These fatty acids are then converted into glycerolipids, glycerophospholipids and sterols that are stored as very low-density lipoprotein (VLDL) particles secreting from the liver into the plasma, as shown in figure 1.4.[91]

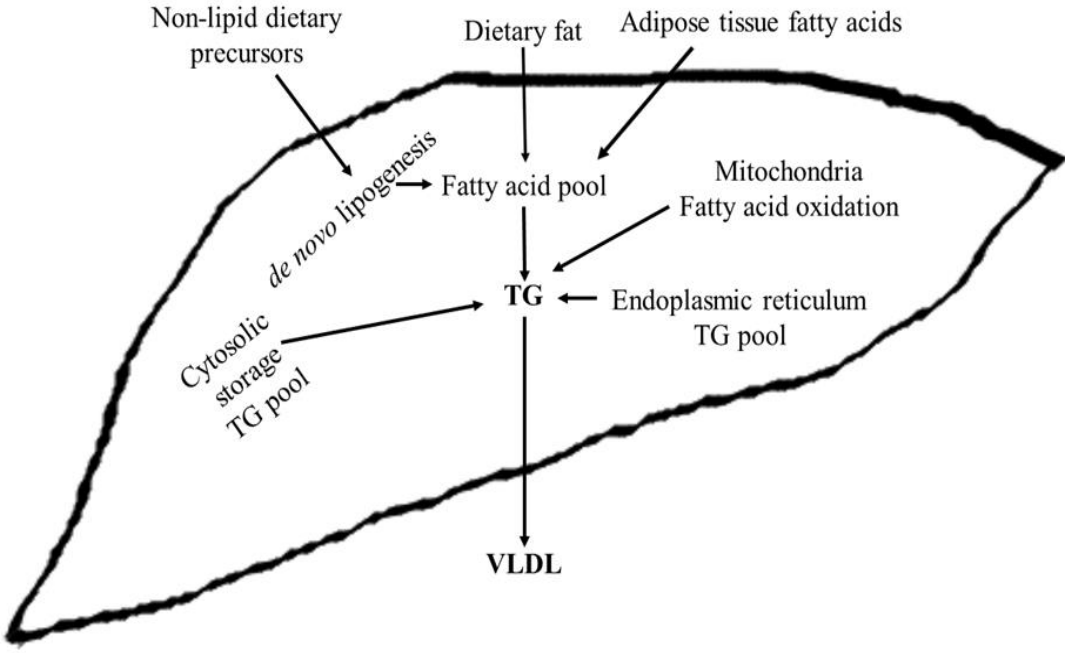

Figure 1.4 Schematic diagram of liver lipid accumulation. [92]

Fatty acids enter in the liver in a common pool or fatty acids pool. Fatty acids are utilised in different pathway, such as esterification or oxidation in mitochondria. Esterified fatty acids accumulate as triglyceride (TG) in the cytosolic storage pool and in endoplasmic reticulum (ER) pools. Then the ER secretory pool releases very low-density lipoprotein (VLDL) in the plasma.[92]

Non-esterified fatty acids, obtained from the lipolysis of adipose TG, pass into the liver. Here they function as a main substrate for oxidation of fatty acid.[93] Fatty acids derived from the adipose tissue, fatty acids from the intrahepatic de novo lipogenesis (DNL) and cytosol fatty acids are used together to produce VLDL-TG.[94] Experimental studies on rodent hepatocytes suggest that most fatty acids enter the liver via a common pool.[95, 96] The dietary fatty acids taken up by the liver mix with existing fatty acids in the common pool. Further fatty acids are segregated into different pathways, such as esterification or oxidation. Esterified fatty acids accumulate as TG in the cytosol as a storage pool and in endoplasmic reticulum lumen as secretory pools.[97, 98] TG accumulation in the liver signifies a possible imbalance between fatty acid input and removal pathways.[99, 100] Dietary fats play a key role for TG metabolism in the liver. [101]

1.4.1.1 de novo lipogenesis

The ability to synthesize fatty acids endogenously apart from fat sources such as carbohydrates is called *de novo* lipogenesis (DNL). It is an important biosynthetic process of fatty acids synthesis from acetyl-CoA subunits that are produced from carbohydrate catabolism contributing to store lipid in the hepatocyte.[102] The surplus carbohydrates that are not stored as glycogen in the liver are converted into fatty acids and esterified into triglycerides.[103] This pathway is a complex metabolic physiological process within the liver primarily through glycolysis and the metabolism of carbohydrates. A high-carbohydrate diet can boost the DNL process and increase lipid storage in the hepatocytes.[104]

When fatty acids are esterified to become TGs for storage, a number of enzymatic reactions are associated in the course of carbons from glucose to fatty acids.[105, 106] Mainly four major steps are involved in all the process. In the first step, glucose from carbohydrates goes through two main biological processes: glycolysis and Krebs cycle to generate citrate in the mitochondria - later brought to cytosol and releasing acetyl-CoA by ATP-citrate lyase (ACLY).[105, 106] In the second step, the acetyl-CoA converts to malonyl-CoA by acetyl-CoA carboxylases (ACC). In the third step, the fatty acid synthase (FASN) converts malonyl-CoA into palmitate that is the first fatty acid product in the process of DNL. In the fourth and final step, palmitate goes through elongation and desaturation process to produce the fatty acids (stearic acid, palmitoleic acid, and oleic acid).[105, 106]

The DNL process begins with the generation of malonyl-CoA from an acetyl-CoA precursor, under the enzymatic activity of acetyl-CoA carboxylase (ACC).[105, 106] Then

malonyl-CoA is transferred to the prosthetic phosphopantetheine group of acyl carrier protein (ACP) by the activity of the malonyl/acetyl transferase (MAT). Further, ACP is bound to a β-ketoacyl intermediate. ACP transports the β-ketoacyl intermediate to the NADPH-dependent β-ketoreductase (KR).[105, 106] The β-carbon ketone is reduced and generates a hydroxyl group. This step is a resulted of dehydration through dehydratase (DH) and further reduction by NADPH-dependent enoyl-reductase. Then a saturated acyl-ACP is produced that binds the thiol-group of the cysteine at the catalytic site of ketoacyl synthase (KS). The ACP is replaced with CoA and the acyl-CoA released from FAS by the activity of thioesterase (TE).[105, 106] The DNL process is summarised in figure 1.5.

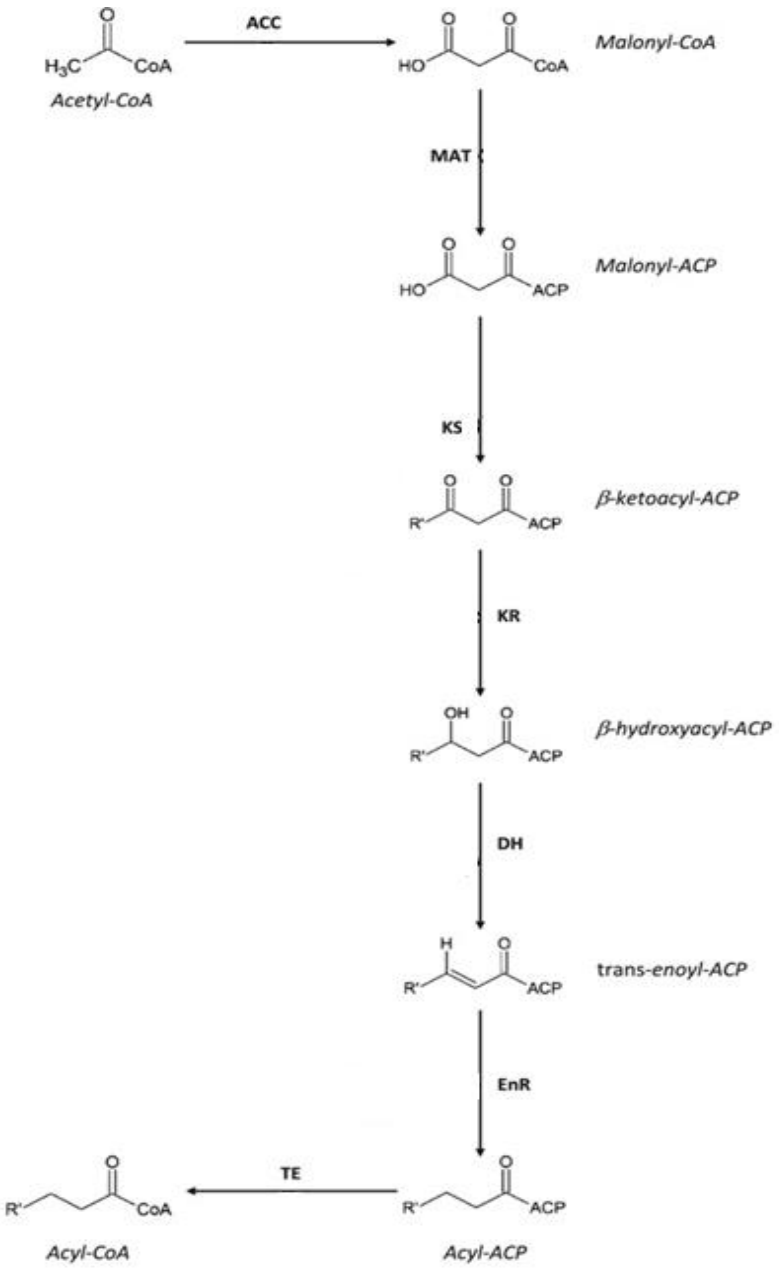

Figure 1.5 De novo lipogenesis.

Malonyl-CoA is produced from acetyl-CoA by the catalytic activity of ACC. Then the acetyl-malonyl substrates are transferred to ACP. The β-ketone group of β-ketoacyl-ACP is reduced using NADPH by KR, producing a β-hydroxyacyl-ACP intermediate. Then dehydration of the β-carbon, generates a trans-enoyl-ACP. The trans double bond between the α- and β-carbons is reduced under EnR and forms acyl-ACP. Then the ACP is replaced with CoA and the acyl-CoA released from FAS by the action of TE. ACC, acetyl-CoA carboxylase; ACP, acyl carrier protein; CoA, coenzyme A; DH, dehydratase; DNL, de novo lipogenesis; EnR, enoyl-reductase; FAS, fatty acid synthase; KR, β-ketoreductase; KS, β-ketoacyl synthase; MAT, malonyl acetyl transferase; TE, thioesterase.

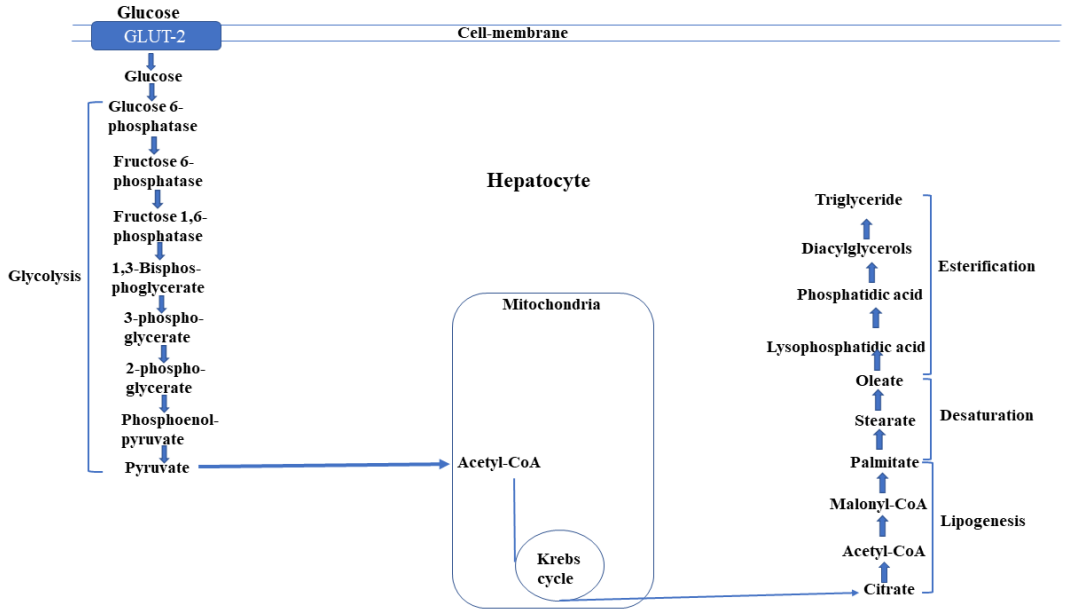

Figure 1.6 Hepatic glycolysis and triglyceride synthesis.

Glucose goes through the multistep during glycolysis to produce pyruvate. This pyruvate is further transported to mitochondria and utilise in Krebs cycle to form citrate. The citrate is then used in lipogenesis to form acetyl-CoA and then malonyl-CoA is produced. Malonyl-CoA then undergoes desaturation and elongation reactions to generate complex fatty acids and TG is synthesised in the hepatocytes.

Glucose is the key substrate for DNL. After the consumption of carbohydrates, the surplus circulating glucose is entered into the hepatocytes through insulin-stimulated glucose transporter 2 (GLUT2, a member of transmembrane carrier protein, which permits protein enabled glucose to transport across cell membrane).[105, 106] Then glucose is converted to pyruvate through the glycolysis process in the cytosol. Further pyruvate is carried into the mitochondria for oxidation in the Krebs cycle. Citrate, an intermediate of the Krebs cycle, is transported into cytosol and this is an important substrate for de novo lipogenesis. During the DNL process, citrate converts into acetyl-CoA and then malonyl-CoA into palmitate which undergoes elongation and desaturation reactions to generate complex fatty acids and TG is synthesised in the hepatocytes as shown in figure 1.6. The TGs are then packed into very low-density lipoproteins (VLDLs) for export from the liver or are stored within the hepatocytes.[105, 106]

Insulin is secreted by pancreatic β cells that is an important hormone for the regulation of lipid and carbohydrate homeostasis. Insulin is responsible for increasing the level of circulating glucose after a meal. A large amounts of glucose molecules are absorbed from the small intestine, which are instantly absorbed by the hepatocytes that convert them into glycogen.[102] Once the liver is flooded with glycogen (nearly 5% mass of liver), any surplus glucose molecules absorbed by the hepatocytes is propelled into physiological processes leading to the synthesis of FA that are further esterified into TG to be distributed to adipose tissue as VLDLs. Insulin also has the ability to constrain lipolysis in adipose tissue via preventing hormone-sensitive lipase (HSL) and this enzyme regulates FFA that is released from adipose tissue.[107] Insulin has a "fat-sparing" outcome by driving maximum cells to specially oxidize carbohydrates rather than fatty acids for energy.[102, 107]

1.4.2 Role of TG and FFA in liver diseases

The accumulation of elevated levels of TG in the hepatic cells is a primary cause of hepatic disease development.[108, 109] Diacylglycerol acyltransferase (DGAT) 2 is an enzyme which basically catalyses the formation of TG at the last stage in the liver. DGAT induces elevated TG level in the liver.[110] The accumulation of TG in the liver may not damage the liver, but it may provide defence against FFA-encouraged lipotoxicity.[111] However, it is also reported that unsaturated FFA in hepatic cells significantly increases the amount of TG without reduction in cell viability. However, saturated fatty acids in the liver significantly increase apoptosis of hepatic cells due to lack of TG.[112] Further it has been established that blocking of TG synthesis increases the level of FFA, which increases oxidative stress, apoptosis, inflammatory activity and fibrosis, damaging hepatic cells and causing lipo-toxicity in the liver.[113]

Together these studies suggest that FFA may enter the non-adipose cells via harmful pathways leading to lipotoxicity.[112] The proportion of unsaturated fatty acids to saturated fatty acids may decide whether the hepatic cells are harmed by the accumulation of extracellular FFA. Hence the types of FFA may be more responsible for determining hepatic dysfunction or stress rather than the absolute amount of FFA. Data from dietary model and cell model of excess fat suggest that the stearoyl-CoA desaturase-1 (SCD1) may convert saturated fatty acid to monounsaturated fatty acid, show a significant role to damage to hepatocytes.[114]

1.5 Metabolomics and NMR

Metabolomics is the multiparametric analysis of the metabolic reaction of biological systems to pathological or physiological stimuli and reveals the metabolic patterns of living beings to disease.[115] Metabolites are the final outcomes of metabolism that characterise the functional responses of tissues or organs[116] and give information about the fundamental mechanisms of metabolism or metabolic state of organisms.[117, 118] In other words, metabolomics establishes the associations between phenotype and metabolic responses that are important characteristics of patho-physiological function. These approaches have been used to detect the metabolic markers participating in various diseases such as, obesity, diabetes and heart disease. Animal models, such as Zucker$^{fa/fa}$ obese rats and high-fat-diet induced obesity in mice are used to examine the comparative alterations in the patterns of metabolite between control and diseased samples.[119-125]

Metabolic responses may be affected by several factors, for example, life style, ethnic-race, age, food habits or drugs and these factors also influence to gain information about metabolic diseases.[126]

Biofluid and tissue samples are used to examine metabolic responses. The most common biofluid samples for metabolomics studies are urine and blood serum or plasma. Other biofluids, for example, saliva, cerebrospinal fluids, seminal fluids, bile, and synovial fluids are also used to examine metabolites profiling.[127-129] Biofluids integrate the metabolic profile changes happening in an organ.[117, 130] Tissue samples are employed to examine the metabolic fingerprints of a specific organ. The intact tissues and its extracts such as lipids are used as biomarker to detect the metabolic disorders or sites of toxicity[131] causing obesity and cardiovascular disease. [132, 133]

Various analytical techniques are used to analyse the metabolic or toxicity profiling, but NMR spectroscopy is one of the suitable instruments to collect evidence on hundreds or thousands of metabolites of a sample in a single run.[134-136] NMR spectra are important to analyse multivariate metabolic profiling and metabolic structural clarification. NMR analyses of biofluid metabolomics provide deeper insight in to pathogenesis and recognition of metabolic biomarkers valuable for diagnosis or treatment of diseases.[137-139] NMR spectroscopy has established positive results to determine the metabolic sections and their environments, both *in vivo* and *in vitro*. Application of NMR on intact tissues metabolomics helps to detect, diagnose, and characterise the toxicity or pathophysiology of diseases, for example, human prostate cancer. [140, 141]

^{1}H NMR spectroscopy is used to examine the toxic response to drugs, as reflected in biofluid, and further it helps to figure out the metabolic markers of organ specific toxicity.[142] Using NMR, metabolomics studies of urine, liver, and serum revealed the alteration in lipid metabolic profiling.[143] Then Griffin *et al* employed high-resolution ^{1}H magic angle spinning (MAS) NMR spectroscopy to investigate the alteration of lipid

metabolites of kidney tissues exposed to cadmium.[144, 145] Further Kauppinen *el al* used NMR to determine the metabolites of the sections of brain.[146, 147] and similar studies have been performed on muscle and cardiac tissue to determine the nature of metabolites and their link to diseases.[148, 149] Together all these experimental conditions suggest that NMR-spectroscopy may be a useful diagnostic tool to detect changes in metabolomic profiling.[126] Additionally, the analysis of the metabolic profiling obtained from NMR spectra by multivariate statistical analysis methods provide a detail mechanism of diseases that may help to discover biomarkers for diagnosis and treatment.[126]

1.6 Nuclear magnetic resonance (NMR) spectroscopy

NMR is a significant and useful method to analyse structural and functional information on biomolecules.[156] The advantage of this technique is that it is non-invasive allowing molecular constituents to be analysed in a native or native-like state.[151]

The effect of magnetic resonance on atomic nucleus was first discovered by Edward M. Purcell and Felix Bloch in 1945 and for this they received the Nobel Prize for physics in 1952.[152] Then the chemical shift (the resonant frequency of a nucleus corresponding to a standard in a magnetic field) was first determined by Packard and Arnold in 1951.[153] Further, Overhauser discovered the effect of electron spin population and the first ^{13}C NMR method was employed by Lauterbur and Holm.[154-156] Later, Richard R. Ernst discovered fourier transform NMR and for this invention, he too received a Nobel prize, this time for chemistry, in 1991.[157] All these rapid developments in NMR made it possible to determine the structure of macromolecules. Using these techniques, the NMR spectrum of protein structure was first determined by Kurt Wüthrich for which he was awarded the Nobel Prize for chemistry in 2002.[152]

1.6.1 Basic principle of NMR

The basic principle of NMR is based on the fact that atomic nuclei have magnetic field. This is important to gather chemical information. As we know, atoms contain three basic or fundamental subatomic particles; electrons, protons and neutrons and these particles having four fundamental properties; charge, mass, spin and magnetism.[159-162]

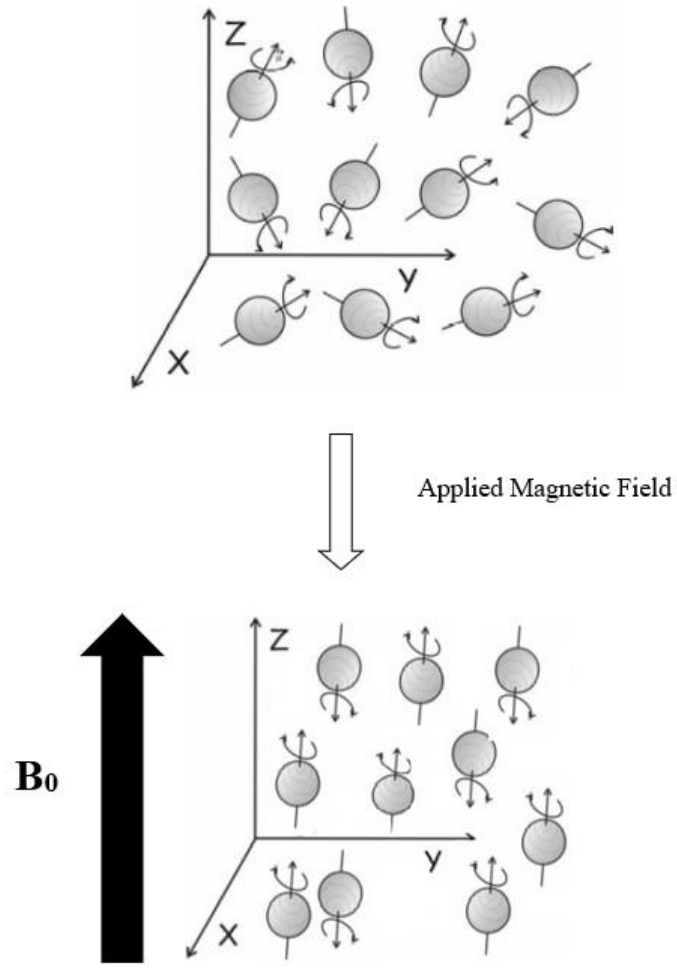

Figure 1.7 Schematic diagram of nuclei orientation under external magnetic field. Orientation of nuclei are randomly oriented and after application of an external magnetic field the random nuclei align themselves in a magnetic field.[163]

In the atomic nucleus, the source of magnetic field and spin is present as an angular momentum that is useful to produce signals of NMR. The zero spin nuclei (^{12}C, ^{16}O) carry paired spin (atomic mass and neutrons are even numbers) that cancel each other. These nuclei lack spin and thus are unable to produce NMR signals. The non-zero spin nuclei

(^{1}H, ^{13}C, ^{15}N, ^{19}F, ^{31}P etc.) are NMR active nuclei having angular momentum to produce NMR signals. The sum of protons and neutrons of these nuclei are odd number.[158-162] These types of atomic nuclei are considered as a small bar magnet. These nuclei are orientated randomly (pointing in any direction) with their own local magnetic field that are degenerative. When a strong external (z-axis oriented) magnetic field (B_0) applies the magnetic field of the nuclei align themselves either parallel or antiparallel to B_0 and spin around z-orientation as shown in figure 1.7.[158-162]

The parallel orientated nuclei possess low energy or α state with spin +1/2, whereas the anti-parallel nuclei have high energy or β state with spin -1/2. Further it generates a net magnetic field (M_0) directing in the same orientation as B_0.[159, 160, 162]

^{1}H, ^{13}C, ^{15}N, ^{19}F and ^{31}P are commonly used in NMR. Because the spin quantum number (I) of these nuclei are ½, meaning that their magnetic quantum number (m) may adopt m=1/2 or -1/2 (figure 1.8) that similar to α and β state as mentioned above.[159, 160]

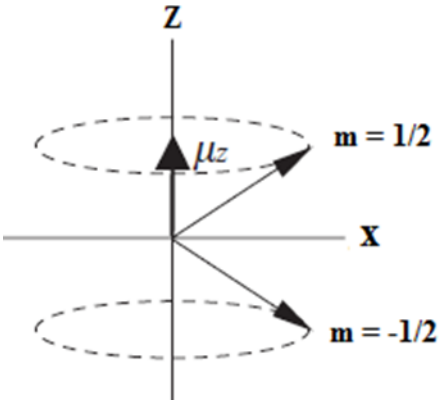

Figure 1.8 Schematic diagram of angular momentum.
The angular momentum of spin ½ has Z axis and -Z axis orientations.[158, 159, 162]

The non-zero spin nuclei orient along specific orientations relative to the magnetic field. These nuclei precession around the magnetic field at a rate dependent on the nuclear

magnetic moment (μ) induced by the nuclei. This alignment situation is known as Zeeman or spin states. The energy is correlated to individual nuclei alignment characterized by the precession frequency.[158, 159, 162] The Zeeman energy state with magnetic quantum number (m) is expressed as the following equation 1:

$$E = -\mu_z B_0 = -m\hbar\gamma B_0 = m\hbar\omega$$

Equation 1: The energy of the Zeeman state. Where, E = energy; μ_z = nuclear moment of Z component; B_0 = magnetic field; m = magnetic quantum number; ħ = Plank's constant; γ = gyromagnetic ratio and ω = Larmor frequency.[158, 159, 162]

The NMR signals appear due to the transition between two Zeeman states. The energy population is regulated by the Boltzmann distribution.[158-163] The population ratio in the energy states is described by the Boltzmann equation 2:

$$N\beta/N\alpha = e^{-\Delta E/kT} = e^{-\hbar\gamma B_0/kT} = 1/\ e^{\hbar\gamma B_0/kT}$$

Equation 2: Boltzmann distribution for the population of energy states; where Nα = lower energy state; Nβ = higher energy states; T = absolute temperature and k = Boltzmann constant.

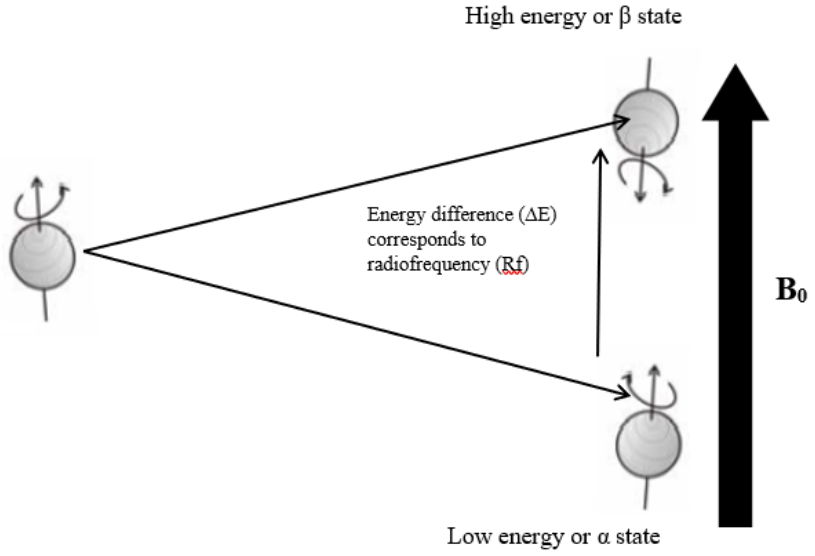

Figure 1.9 Schematic diagram of Boltzmann energy distribution.
Energy population difference between the lower and higher energy state.[163]

The difference of energy population (ΔE) between the low and high energy state is relatively small, although a massive number of nuclei is present in a sample. The energy population difference (ΔE) is related to the strength of the external magnetic field (B_0) (Figure 1.9). That is why strong magnets are used in NMR spectroscopy.[158-163]

To gain the NMR signals, the net magnetization is perturbed by irradiation of nuclei of the sample with short pulses of frequency in the megahertz (MHz) radiofrequency. This phenomenon induces transitions between the α- and β-states from the equilibrium position of nuclei that perturb net magnetization. Along with alignment of nuclei to an external magnetic field or NMR magnet (B_0), the magnetic field of each nuclei also precesses around the NMR magnet (B_0) with a frequency called the Larmor frequency. The Larmor frequency is different for different nuclei, and nuclei in different chemical and physical environments.[158-163]

1.6.1.1 Magnetic moment, Larmor frequency, Magnetization and Chemical shift

The magnetic field of the nucleus (B_N) can be determined by the magnetic moment (μ), which is expressed as the following equation 2:

$$\mu = \gamma Ih/2\pi = \hbar\gamma I$$

Equation 2: Equation of the magnitude of magnetic moment; where, μ=magnetic moment; ħ= h /2π Planck constant; and γ =gyromagnetic ratio that is a nuclear constant. Each nucleus has a precise γ value. For example, γ of $^1H = 2.67x10^4$ $gauss^{-1}sec$.[159, 160, 162]

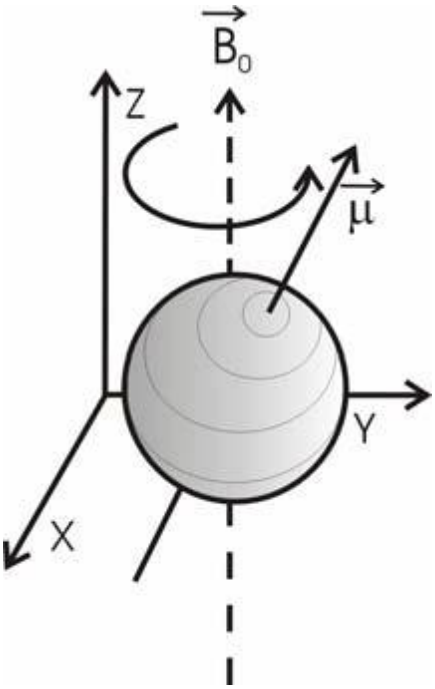

Figure 1.10 Schematic diagram of the precession of nucleus.

The external magnetic field (B_0) around Z-axis with precession frequency of Larmor frequency (ω).[163]

The frequency of precession or Larmor frequency (ω) is a little slanted away from the axis of the magnetic field around the z-axis as shown in figure 1.10 with an angular velocity that can be measured as the following equation 3:

$$\omega = \gamma B_0$$

Equation 3: Equation of the frequency of precession. Where ω = Larmor frequency; γ = magnetogyric ratio and B_0 = external magnetic field. Subsequently the gyromagnetic ratio varies for each nucleus, the Larmor frequency is precise for each nucleus.[159, 160, 162, 163]

When the nuclei are aligned to the external magnetic field (B_0) or projected on the z-axis; this phenomenon is known as net magnetisation (M). The nuclei aligned along with external magnetic field of z-axis further experience another magnetic field that is applied perpendicularly to the external magnetic field for a brief period, known as the pulse.[158-163] In other words, the radio frequency allows the nuclei to absorb energy at a specific

frequency. The absorbed frequency at the Larmor frequency is directly proportional to the external magnetic field.[159, 160, 162, 163] At 90° pulse, this frequency allows the nuclei of magnetisation to orient into the XY-plane with new magnetisation (M1) as shown in figure 1.11. After stopping this pulse, the new magnetisation nuclei re-align to the orientation of magnetization (M) of the z-axis. During this process, an induced magnetic field produces a radio frequency (Rf) that is captured by receiver coils and after a computational process, these signals are produced as a spectrum.[158-163]

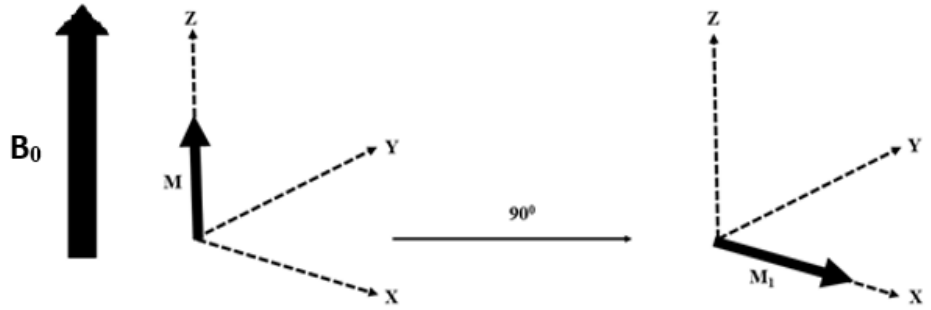

Figure 1.11 The effect of a 90° pulse on net magnetisation.

The nuclei align along with the external magnetic field (B_0), called net magnetisation (M) at the Z-axis. After a Rf frequency pulse 90°, the M is rotated into XY-direction, perpendicular to B_0, referred to as new magnetisation M_1.[159]

Subsequently the signal known as the free induction decay is given in the time domain. To present this in a more native pattern, a Fourier transformation (FT) is applied that transforms the time domain to the frequency domain.[158-163] The following steps are involved in generating NMR signals:

Initialization: Prior to the experiment, the computer copies commands to the pulse programmer and to other components of hardware, for example, the frequency synthesizer (source of Rf to produce constant frequency) and analogue to digital

converters (ADCs; convert NMR signals to binary system), scheduling the carrier frequency and the sampling frequency, etc.[159]

Excitation: When the experiment begins, the pulse programmer implements a timed progression of commands to establish the phase of the Rf synthesizer and set off the pulse gate or channel. More precisely, since Rf is employed for a very short period, the frequency source (synthesizer) is gated to the Rf pulse. The Rf pulse passes through the probe from the amplifier.[159] The length of the Rf is controlled by the programmer. Then the Rf pulse establishes resonant oscillations in the tuned circuit of the probe, exposing the sample to a Rf resembling the Larmor frequency of measuring nuclei. This Rf pulse interrupts the equilibrium of the nuclear spin system and produces transverse nuclear magnetization.[159]

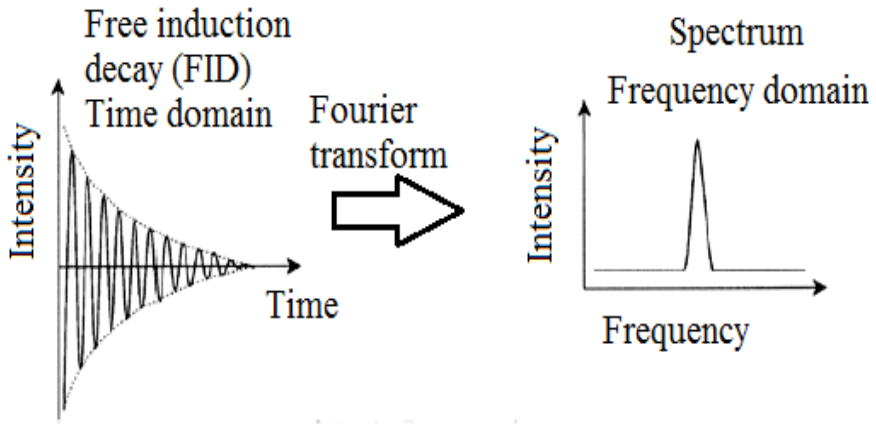

Figure 1.12 Schematic diagram of Fourier Transformation. [164]

The signals emitted from excited atoms are received in the form of free induction decay (FID) and Fourier transformed by the spectrometer and further obtained as spectrum after computational manipulation. The process of receiving the NMR signals is called acquisition. FID is the time domain. Spectrum is the frequency domain.[159]

Detection, processing and display: Further the Rf pulse is stopped and after few microseconds, the pulse frequencies of the tuned circuit disintegrate, and are ready to

collect as NMR signals. The precession of the nuclear spin magnetization produces Rf NMR signal in the form of free induction decay (FID).[159] Further, this signal is amplified and converted by ADCs to computational languages and stored in the memory of the computer. These signals are manipulated by various mathematical and numerical calculations called Fourier transformation (FT). Finally, FT transforms the NMR signal, which is a function of time, into an NMR spectrum, which is a function of frequency (Figure 1.12).[159]

The number of pulses (NP) employed to give a well resolved FID is directly proportional to the signal-to-noise (S/N) ratio in the Fourier transformed spectrum. Generally, the ideal number of pulses to be applied during an experiment is that which gives a useful S/N ratio in a moderate time. After FT, two valuable pieces of information; the chemical environment and number of nuclei generating the signal, are usually obtained.[158-163] The numerous NMR spectral signals are also known as chemical shifts that are generated from the real-time interface of a nuclei with electrons or the electrons with the external magnetic field. The association between nuclei and electromagnetic fields can be expressed as in the following equation 4:

$$\omega = \gamma B_0 (1 - \sigma)$$

or

$$\upsilon = \gamma/2\pi \, B_0 (1- \sigma) \text{ Since } \omega = 2\pi\upsilon$$

Equation 4: Equation of the relationship between nuclei and electromagnetic field or chemical shift. Where, σ = shielding tensor; ω = Larmor frequency; γ = magnetogyric ratio, B_0 = external magnetic field and ν = chemical shift expressed in Hz and strongly dependent on the strength of the external magnetic field. The electron density is directly proportional to the shielding tensor (σ) thus providing small Larmor frequency (ω) values.[158-163]

1.7 Multivariate analysis

Multivariate analysis (MVA) includes a group of methods that are used when numerous dimensions are produced on each entity in one or many samples. Variables are represented by the dimensions and the entities as 'units' (investigation units, specimen units, or experimental units) or 'observations'.[165] MVA allows the groups to generate information and further predict or progress the conclusion. In other words, it refers to all statistical methods that simultaneously analyse more than two variables that are loosely considered multivariate analysis.[166] Multivariate techniques are useful for (a) simplification and reduction of data without disturbing valuable information; (b) grouping or sorting similar objects or variables based on measured characteristics; (c) investigation of the nature of the associations among variables; (d) predicting the values of variables based on observations; (e) testing and constructing specific statistical hypotheses.[167]

MVA is a constantly growing method that can be further classified into many types, such as multiple regression, multiple discriminant analysis, canonical correlation, multivariate analysis of variance and covariance, conjoint analysis, cluster analysis, perceptual mapping and principal component analysis.

Multiple regression is applied when the investigation problems include a single metric dependent variable supposed to be associated to two or more metric independent variables. This method may help to predict the changes in the dependent variable in response to variations in the independent variables.[165]

Multiple discriminant analysis is useful when the single dependent variable is nonmetric, such as dichotomous (e.g., male-female) or multichotomous (e.g., high-medium-low). It is applicable in a sample that may be distributed into groups of a nonmetric dependent

variable describing numerous identified categories. This type of MVA can help to recognise group differences and to predict the probability that an individual or object will belong to a class or group based on several nonmetric variables.[165]

Canonical correlation can be used to correlate the numerous metric dependent and independent variables. The main objective of this method to obtain a linear combination of each independent and dependent variable to maximize the correlation between two sets.[165]

Multivariate analysis of variance and covariance can be useful to simultaneously analyse the correlations between many independent variables (e.g., treatments) and two or more metric dependent variables.[165]

Conjoint analysis is a popular marketing research analytical method to determine features of objects, such as a new product, idea or service.[165]

Cluster analysis is a type of MVA that can be using to develop significant subgroups of objects or individuals. In this analysis, the groups are not predefined. Therefore, it helps to identify the groups.[165]

Perceptual mapping is a multidimensional scaling method to convert buyer perceptions of similarities or liking into distances characterised in multidimensional space.[165]

Principal component analysis can be used to analyse interdependence among many variables and to describe these variables in terms of their mutual underlying dimensions.[165]

1.7.1 Principal component analysis (PCA)

Principal component analysis (PCA) is a statistical tool that can be used to transform the dimension of a large data set of correlated variables into a small data set of uncorrelated variables.[165, 167] It has been described as one of the most significant results achieved from the application of linear algebra.[167] Thus, it is widely used in all form of biological data analysis, such as molecular genetics, marine biology, ecology, pharmacy, metabolomics, neurosciences, agriculture and health sciences.[167, 168] It is a powerful tool to identify the pattern of data in such a manner as to spot similarities and differences that can be difficult to find in a data set of large dimensions, where the comfort of graphical illustration is unavailable.[169] Hence, PCA is used as a tool in experimental data analysis to find the variables that explain the maximum variance in the data set. Therefore, PCA can be used to analyse a large volume of the variable data and create predictive models.[170]

The main concept upon which PCA is based is to decrease dimensionality of any data set that is made up of a sizeable number of interconnected variables, while keeping any variations that may exist within the data set variables. This is achieved through the transformation into a new set of variables, the main or principal components that are not correlated, and then placing it in such a way that the starting few data points still have most of the existing variation that is present in all the original variables. It is used to analyse the data set and decrease the number of dimensions, without a significant loss of information.[171]

1.7.1.1 What is PCA?

PCA is a statistical method related to explaining the covariance arrangement of a group of variables. Specifically, it allows recognition of the main direction wherein the data

differs.[172] It measures data regarding its principal components (PCs) instead of a normal x-y axis. Basically, PCs are the underlying components in the set of data that directions are the most variance and spread out.[170, 172]

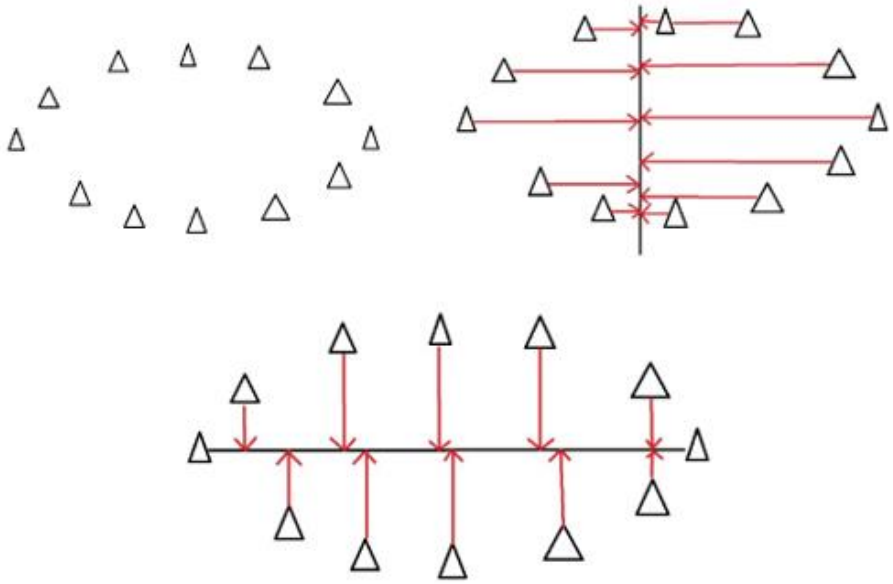

Figure 1.13 Schematic diagram of two-dimensional variable space and PCA.
Oval shape triangles represent points of data. The vertical line data figure shows less variance with less spread in comparison to the horizontal line data figure. Hence, the horizontal line data figure can be considered as principal components.[173]

Here, in figure 1.13, some triangles are arranged in an oval shape. Let us suppose that these triangles are points of data. To understand the most variance in direction, vertical and horizontal straight lines project the data spread. Here, the vertical line projected data does show a small spread, hence it does not possess a large variance.[173] Therefore, it is most likely not a principal component. On the other hand, in the horizontal line projected figure, the data points are more spread out with a large variance. Therefore, this may be a principal component.[173]

In figure 1.14, the plots represent two variable sets of data measured on the X-Y axis. The principal directions of the data set of the U axis and V axis. By transforming each data point of the X-Y axis into its corresponding U-V axis value, the points of data are de-

correlated, denoting that the co-variance between the U and V variables is zero.[174] PCA finds the coordinate system represented by the principal directions of variance i.e. the U-V coordinate system. The directions of the U and V coordinates are called the principal components. PCA gives a way of reducing the dimensionality of a data set. As shown in figure 1.14B, the two variables are related linearly. However, in figure 1.14A, the principal direction of the data differs between the U and V axis. In this case, the points of the V axis are very close to zero. It can be considered non-zero only because of experimental noise. Hence in this system, the data set of one variable U is considered and the data points of the V axis are discarded. Therefore, PCA reduces the dimensionality of the data set.[174]

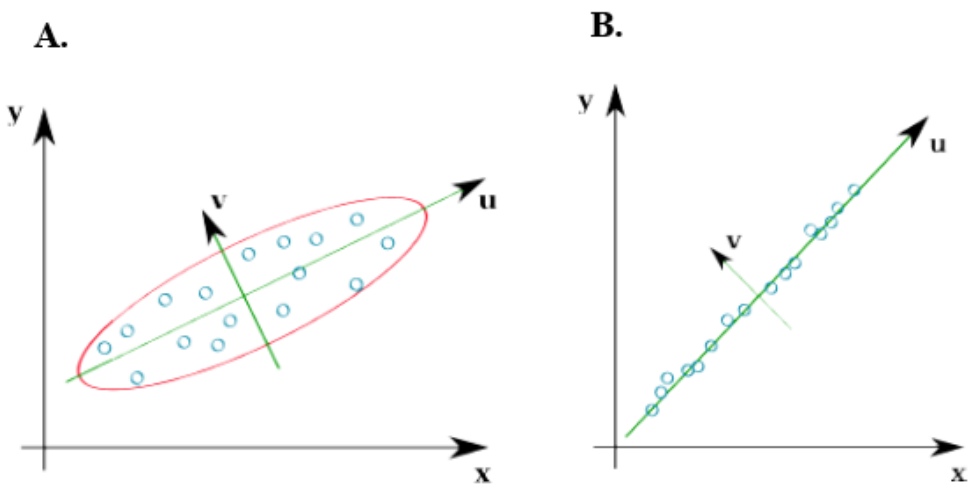

Figure 1.14 Schematic representation of two variable data sets in the X-Y axis.
The principal directions of the data set of the U axis and V axis. PCA detects the coordinate system signified by the principal directions of variance of the U-V coordinate system, called the principal components.[174]

1.7.1.2 NMR and PCA

PCA recognises the group variances from a multivariate dataset. The variance could be a group of any biologically related category, for example, organisms treated with a specific

nutrition or medicine; or tissues/organ exposed to stress. An NMR or MS spectrum of a biological extract (fluids/lipids/serum etc.) is an observation of variables for each spectrum that signifies an individual entity. The observations create the data matrix. PCA then classifies a grouping of the variables that describes the class separation.[175]

Generally, metabolic datasets have more observed variables than observations, i.e. large numbers of variables and small numbers of observations class make for difficulties in statistics.[175] These characteristics cause traditional linear regression methods (predictive methods that describe the association between one dependent variable and one or more independent variables) to be unachievable where the data matrix is singular.[176] For this reason, metabolomics data need multivariate analysis that can deal with significant amounts of collinearity (two or more variables are highly correlated) in the data matrix.[176] The multivariate method, PCA, is capable to develop a linear transformation that keeps maximum variance in the original dataset.[175, 176]

The selection of the MVA method is essential to achieve the experimental goals of metabolic studies.[176] The application of PCA gives early information about the experimental unknown or unpredictable groups of the metabolic data sets.[176] PCA analysis results are important to formulate a preliminary biological conclusion. The difference between groups in the scores of PCA is detected when the variation within the group is considerably less than between group variation in the data sets. Therefore, PCA outcomes have a significant chance of generating biologically applicable results.[176]

Pre-processing of raw NMR or MS spectral data is essential for producing consistent, interpretable standard patterns using MVA methods. The procedures for pre-processing of metabolic data sets have been completely defined to normalise the methods.[177, 178]

However, implementation of some standard processes is vital to acquire an optimal method for analysing those raw data obtained from different instrumental techniques.[177, 178]

The binning process is one of the important steps to overcome the chemical shift differences and spectral noise, then covers substantial fluctuations of low-intensity peaks close to strong-intensity peaks. In proton NMR, the chemical shifts sometimes differ with factors such as temperature, pH, ionic strength and another electronic environment.[179-181] The metabolic data sets of NMR also experience inaccuracies in chemical shifts, and consequently in the variables. The MVA method, PCA is unable to recognise separations between classes of spectra of full resolution proton NMR of metabolic samples.[179-181] The loading process of these data sets may be disturbed and the interpretation can be affected because of the excess- load of variables. These problems from chemical shift variations could be diminished by consistently dividing each spectrum into 'bins' comprising standard spectral widths (0.04ppm) and adding signal intensities within each bin to generate a small set of variables.[179-181]

Normalisation of metabolomic data sets is crucial. To signify the variable dilution factors of metabolic samples arising from differences in the size of tissues, volume of biofluids, or number of cells, each observation can be normalized to confirm that all observations are precisely comparable.[182, 183] Normalization of data sets is achieved by computational means via internal standards such as using TMS in NMR or externally through measurements of the optical density of cell culture or protein contents.[182, 183] The procedure of internal normalization is known as constant-sum normalization, where each spectrum can be normalized such a way that its integral value is equal to one.[182, 183] Noise and baseline removal is the scaling process to eliminate instrumental errors prior to

multivariate analysis.[184] The main drawback of data scaling is its tendency to intensify instrumental noise, to which PCA has been shown to be sensitive.[185, 186]

The most commonly used chemometric method for the interpretation of NMR data sets of biological or pharmaceutical samples is PCA. It provides great advantages in terms of accurate visualization of large data sets.[187] This is the main reason why PCA is used to analyse the complexity of NMR data of metabolites and body fluids.[126, 187-189] PCA is used to analyse NMR data of samples to determine the principal components. The first principal component or principal component one (PC1) gives a description of a majority of the variance, while the second principal component or principal component two (PC2) describes the second most common amongst the orthogonal variation in relation to another imposed component.[165]

The decision on the right number of components is an issue of basic consequence when using the PCA to analyse NMR data. This decision is usually not critical in the case of exploratory research studies. Because the first principal component does not undergo any further change as a function of the number of components that are selected later. The principal components have two main components, scores and loadings.[165, 187, 190] Loadings have all the information related to the variables or chemical shifts of the data sets. Scores give information related to the biological samples or their concentrations as seen in the data sets. In the context of any specific principal component, the loading vector means the spectral profile while the score of a sample refers to the quantity of that specific component in the sample expressed in a least squares sense. Therefore, a sum of loadings weighted according to a sample's score values will give an approximate evaluation of the spectral profile of that sample.[165, 187, 190]

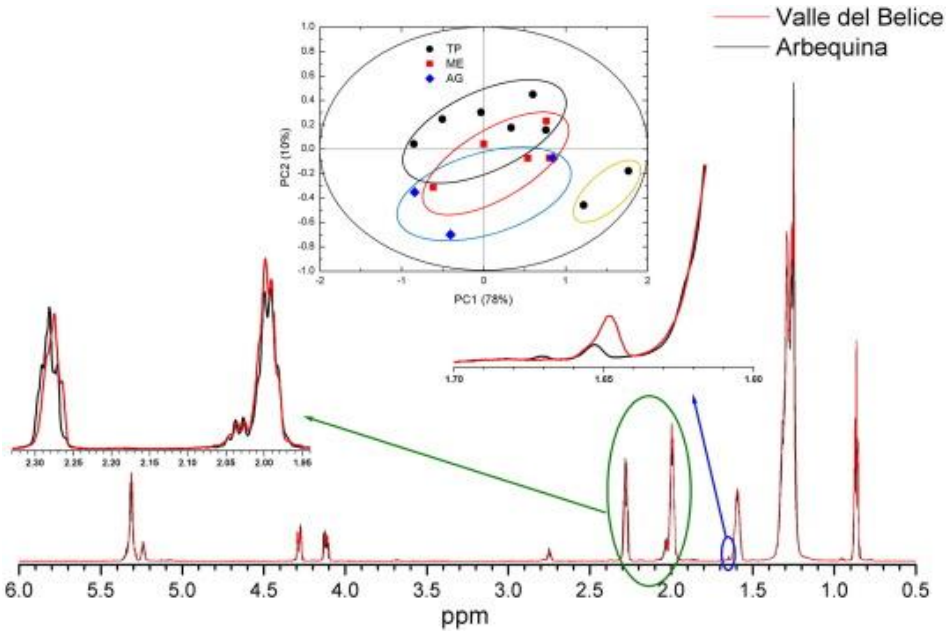

Figure 1.15 ^{1}H MAS NMR spectra and PCA.

The scattered score plot of the PCA analysis performed on extra virgin olive oil varieties Valle del Belice and Arbequina of Sicilian regions; Trapani (TP), Messina (ME) and Agrigento (AG). The results from different Sicilian regions: are superimposed on each other. The orange ellipse on the bottom right side refers to two Spanish cultivars, Arbosana and Arbequina grown in the province of Trapani (TP). (Adapted from Corsaro *et al*., 2015)[191]

These scores are usually made into a graphical plot which is then represented in a scatter plot (Figure 1.15) that provides a map of every sample. Samples which are classed together in the score plot have similar spectra in the context of the chosen principal components in the PCA analysis. A major advantage of PCA is that it gives fast and unsupervised viewing of the samples and the identification of samples that show variant features, also known as outliers. This helps in the identification of trends and patterns, as well as any existing groups within the samples. Before the PCA tool, NMR-based data was arranged by the subtraction (from each chemical shift value) of the average value at any specific shift calculated across every sample.[84, 165, 187]

In lipidomics, PCA gives information and identification of molecules of lipid and their structural and functional role as metabolites.[192, 193] PCA provides new insights in to several pathologies of lipid abnormalities causing cardiovascular disease, obesity and diabetes.[188, 194] Lipid profiling by PCA is one of the latest methods used in functional genomics to identify the possible lipid biomarkers that characterize any particular dysfunctional gene.[195, 196]The use of ^{1}H NMR spectroscopy with PCA promises great advantages in lipid metabolomic profiling research studies.[196] Together NMR and PCA will be important in the research of functional genomics, lipidomics, metabolomics, plant chemistry, pharmaceuticals studies, proteomics, epidemiology and food research.[196]

1.8 Objectives

The main objective of this study is to investigate whether high fats diets and heart hypertrophy result in changes in lipid composition in rat hearts and livers using liquid and solid state ^{1}H NMR. Due to the complexity of the NMR data it will be analysed by PCA software to obtain a clear view of the variables effecting the data. This will allow the changes in the spectra to be observed and then correlated with specific lipids.

Rats will be assigned to either Western diet (WD) or high fat diet (HFD). Further, to see the of effect the dietary lipid composition during stress, the aortic constriction (AC) surgery rat models will be used. For normal condition, Sham surgery rat models will be used.

1) To confirm the presence of lipids in the heart and liver tissues as lipid droplets - the histological sections of heart and liver tissues will be stained by Oil O Red and hematoxylin-eosin (H & E) and observed under light microscope.

2) The lipid samples collected from rat hearts and livers will be analysed by ^{1}H NMR liquid state and intact tissues will be analysed by MAS ^{1}H NMR solid state.

3) The data gained from peak intensity of NMR spectra will be analysed by PCA statistical tool to give a clear view of the group classification and the most effective variables in the data, which will help identifying the different lipid metabolites of WD and HFD.

1.9 References

1. H. E. Bays, P. P. Toth, P. M. Kris-Etherton, N. Abate, L. J. Aronne, W. V. Brown, J. M. Gonzalez-Campoy, S. R. Jones, R. Kumar, R. La Forge and V. T. Samuel, *Journal of clinical lipidology*, 2013, **7**, 304-383.
2. E. D. Rosen and B. M. Spiegelman, *Cell*, 2014, **156**, 20-44.
3. X. Yang and U. Smith, *Diabetologia*, 2007, **50**, 1127-1139.
4. U. J. Jung and M. S. Choi, *International journal of molecular sciences*, 2014, **15**, 6184-6223.
5. N. A. van Herpen and V. B. Schrauwen-Hinderling, *Physiology & behavior*, 2008, **94**, 231-241.
6. R. H. Unger and L. Orci, *FASEB journal: official publication of the Federation of American Societies for Experimental Biology*, 2001, **15**, 312-321.
7. J. E. Schaffer, *Current opinion in lipidology*, 2003, **14**, 281-287.
8. T. Fujimoto and R. G. Parton, *Cold Spring Harbor perspectives in biology*, 2011, **3**.
9. Y. Guo, K. R. Cordes, R. V. Farese, Jr. and T. C. Walther, *Journal of cell science*, 2009, **122**, 749-752.
10. A. R. Thiam, R. V. Farese and T. C. Walther, *Nature reviews. Molecular cell biology*, 2013, **14**, 775-786.
11. A. Avalos-Soriano, R. De la Cruz-Cordero, J. L. Rosado and T. Garcia-Gasca, *Molecules (Basel, Switzerland)*, 2016, **21**.
12. S. M. Grundy, *The Journal of clinical endocrinology and metabolism*, 2004, **89**, 2595-2600.
13. R. Yang and L. A. Barouch, *Circulation research*, 2007, **101**, 545-559.
14. P. C. Schulze, K. Drosatos and I. J. Goldberg, *Circulation research*, 2016, **118**, 1736-1751.

15. M. P. Corcoran, S. Lamon-Fava and R. A. Fielding, *American Journal of Clinical Nutrition*, 2007, **85**, 662-677.

16. P. M. Coen, J. J. Dube, F. Amati, M. Stefanovic-Racic, R. E. Ferrell, F. G. Toledo and B. H. Goodpaster, *Diabetes*, 2010, **59**, 80-88.

17. S. M. Kitessa and M. Y. Abeywardena, *Nutrients*, 2016, **8**.

18. A. Giacca, C. T. Xiao, A. I. Oprescu, A. C. Carpentier and G. F. Lewis, *American Journal of Physiology-Endocrinology and Metabolism*, 2011, **300**, E255-E262.

19. G. C. Yaney and B. E. Corkey, *Diabetologia*, 2003, **46**, 1297-1312.

20. J. K. Dowman, J. W. Tomlinson and P. N. Newsome, *QJM: monthly journal of the Association of Physicians*, 2010, **103**, 71-83.

21. Q. Liu, S. Bengmark and S. Qu, *Lipids in health and disease*, 2010, **9**, 42.

22. W. M. Ratnayake and C. Galli, *Annals of nutrition & metabolism*, 2009, **55**, 8-43.

23. A. M. Smith and A. L. Collene, *Wardlaw's Contemporary Nutrition*, McGrow-Hill, New York, 10 edn., 2016.

24. L. A. Smit, D. Mozaffarian and W. Willett, *Annals of nutrition & metabolism*, 2009, **55**, 44-55.

25. S. Stanner, *Cardiovascular Disease: Diet, Nutrition and Emerging Risk Factors*, Blackwell Publishing, Oxford, United Kingdom, 1 edn., 2005.

26. A. Aro, J. M. Antoine, L. Pizzoferrato, O. Reykdal and G. van Poppel, *Journal of Food Composition and Analysis*, 1998, **11**, 150-160.

27. A. M. O'Donnell-Megaro, D. M. Barbano and D. E. Bauman, *Journal of dairy science*, 2011, **94**, 59-65.

28. D. C. Klonoff, *Journal of diabetes science and technology*, 2007, **1**, 415-422.

29. G. List, *Lipid Technology*, 2014, **26**, 131-133.

30. K. V. Axen, A. Dikeakos and A. Sclafani, *The Journal of nutrition*, 2003, **133**, 2244-2249.

31. A. Ibrahim, S. Natrajan and R. Ghafoorunissa, *Metabolism: clinical and experimental*, 2005, **54**, 240-246.

32. S. Natarajan and A. Ibrahim, *The British journal of nutrition*, 2005, **93**, 829-833.

33. L. Arab, *The Journal of nutrition*, 2003, **133 Suppl 3**, 925s-932s.

34. D. T. Jamison, R. G. Feachem, M. W. Makgoba, E. R. Bos, F. K. Baingana, H. K.J. and K. O. Rogo, in *Disease and Mortality in Sub-Saharan Africa*, eds. K. Steyn and A. Damasceno, World Bank, Washington (DC), 2 edn., 2006, ch. 18.

35. B. A. Franklin, J. L. Durstine, C. K. Roberts and R. J. Barnard, *Best practice & research. Clinical endocrinology & metabolism*, 2014, **28**, 405-421.

36. K. M. Platt, R. J. Charnigo and K. J. Pearson, *Journal of developmental origins of health and disease*, 2014, **5**, 229-239.

37. S. M. Innis, *Current opinion in endocrinology, diabetes, and obesity*, 2007, **14**, 359-364.

38. S. K. Muthuri, C. E. Francis, L. J. Wachira, A. G. Leblanc, M. Sampson, V. O. Onywera and M. S. Tremblay, *PloS one*, 2014, **9**, e92846.

39. R. M. Krauss, R. H. Eckel, B. Howard, L. J. Appel, S. R. Daniels, R. J. Deckelbaum, J. W. Erdman, Jr., P. Kris-Etherton, I. J. Goldberg, T. A. Kotchen, A. H. Lichtenstein, W. E. Mitch, R. Mullis, K. Robinson, J. Wylie-Rosett, S. St Jeor, J. Suttie, D. L. Tribble and T. L. Bazzarre, *Circulation*, 2000, **102**, 2284-2299.

40. M. A. Cole, A. J. Murray, L. E. Cochlin, L. C. Heather, S. McAleese, N. S. Knight, E. Sutton, A. Abd Jamil, N. Parassol and K. Clarke, *Basic Research in Cardiology*, 2011, **106**, 447-457.

41. I. Heinonen, P. Rinne, S. T. Ruohonen, S. Ruohonen, M. Ahotupa and E. Savontaus, *Acta physiologica (Oxford, England)*, 2014, **211**, 515-527.

42. C. Y. Wang and J. K. Liao, *Methods in molecular biology (Clifton, N.J.)*, 2012, **821**, 421-433.

43. H. S. Cheng, S. H. Ton, S. C. W. Phang, J. B. L. Tan and K. Abdul Kadir, *Journal of advanced research*, 2017, **8**, 743-752.

44. S. L. Johnston, D. M. Souter, B. J. Tolkamp, I. J. Gordon, A. W. Illius, I. Kyriazakis and J. R. Speakman, *Obesity (Silver Spring, Md.)*, 2007, **15**, 600-606.

45. G. D. Lopaschuk, J. R. Ussher, C. D. Folmes, J. S. Jaswal and W. C. Stanley, *Physiological reviews*, 2010, **90**, 207-258.

46. D. A. Prosdocimo, P. Anand, X. Liao, H. Zhu, S. Shelkay, P. Artero-Calderon, L. Zhang, J. Kirsh, D. Moore, M. G. Rosca, E. Vazquez, J. Kerner, K. M. Akat, Z. Williams, J. Zhao, H. Fujioka, T. Tuschl, X. Bai, P. C. Schulze, C. L. Hoppel, M. K. Jain and S. M. Haldar, *The Journal of biological chemistry*, 2014, **289**, 5914-5924.

47. I. J. Goldberg, C. M. Trent and P. C. Schulze, *Cell metabolism*, 2012, **15**, 805-812.

48. A. R. Wende and E. D. Abel, *Biochimica et biophysica acta*, 2010, **1801**, 311-319.

49. K. Drosatos and P. C. Schulze, *Current heart failure reports*, 2013, **10**, 109-121.

50. E. D. Bartels, J. M. Nielsen, L. I. Hellgren, T. Ploug and L. B. Nielsen, *PloS one*, 2009, **4**, e5300.

51. K. G. Bharadwaj, Y. Hiyama, Y. Hu, L. A. Huggins, R. Ramakrishnan, N. A. Abumrad, G. I. Shulman, W. S. Blaner and I. J. Goldberg, *The Journal of biological chemistry*, 2010, **285**, 37976-37986.

52. J. A. Villena, S. Roy, E. Sarkadi-Nagy, K. H. Kim and H. S. Sul, *The Journal of biological chemistry*, 2004, **279**, 47066-47075.

53. R. Zimmermann, J. G. Strauss, G. Haemmerle, G. Schoiswohl, R. Birner-Gruenberger, M. Riederer, A. Lass, G. Neuberger, F. Eisenhaber, A. Hermetter and R. Zechner, *Science (New York, N.Y.)*, 2004, **306**, 1383-1386.

54. N. H. Banke, A. R. Wende, T. C. Leone, J. M. O'Donnell, E. D. Abel, D. P. Kelly and E. D. Lewandowski, *Circulation research*, 2010, **107**, 233-241.

55. P. C. Kienesberger, T. Pulinilkunnil, M. M. Sung, J. Nagendran, G. Haemmerle, E. E. Kershaw, M. E. Young, P. E. Light, G. Y. Oudit, R. Zechner and J. R. Dyck, *Molecular and cellular biology*, 2012, **32**, 740-750.

56. C. T. Coburn, F. F. Knapp, Jr., M. Febbraio, A. L. Beets, R. L. Silverstein and N. A. Abumrad, *The Journal of biological chemistry*, 2000, **275**, 32523-32529.

57. R. E. Gimeno, A. M. Ortegon, S. Patel, S. Punreddy, P. Ge, Y. Sun, H. F. Lodish and A. Stahl, *The Journal of biological chemistry*, 2003, **278**, 16039-16044.

58. J. K. Kim, R. E. Gimeno, T. Higashimori, H. J. Kim, H. Choi, S. Punreddy, R. L. Mozell, G. Tan, A. Stricker-Krongrad, D. J. Hirsch, J. J. Fillmore, Z. X. Liu, J. Dong, G. Cline, A. Stahl, H. F. Lodish and G. I. Shulman, *The Journal of clinical investigation*, 2004, **113**, 756-763.

59. J. Yang, N. Sambandam, X. Han, R. W. Gross, M. Courtois, A. Kovacs, M. Febbraio, B. N. Finck and D. P. Kelly, *Circulation research*, 2007, **100**, 1208-1217.

60. A. Paul, L. Chan and P. E. Bickel, *Current hypertension reports*, 2008, **10**, 461-466.

61. K. Fukuchi, S. Nozaki, T. Yoshizumi, S. Hasegawa, T. Uehara, T. Nakagawa, T. Kobayashi, Y. Tomiyama, S. Yamashita, Y. Matsuzawa and T. Nishimura, *Journal of nuclear medicine: official publication, Society of Nuclear Medicine*, 1999, **40**, 239-243.

62. N. H. Son, T. S. Park, H. Yamashita, M. Yokoyama, L. A. Huggins, K. Okajima, S. Homma, M. J. Szabolcs, L. S. Huang and I. J. Goldberg, *The Journal of clinical investigation*, 2007, **117**, 2791-2801.

63. R. C. Meex, P. Schrauwen and M. K. Hesselink, *American journal of physiology. Regulatory, integrative and comparative physiology*, 2009, **297**, R913-924.

64. S. Y. Park, Y. R. Cho, H. J. Kim, T. Higashimori, C. Danton, M. K. Lee, A. Dey, B. Rothermel, Y. B. Kim, A. Kalinowski, K. S. Russell and J. K. Kim, *Diabetes*, 2005, **54**, 3530-3540.

65. I. C. Okere, M. E. Young, T. A. McElfresh, D. J. Chess, V. G. Sharov, H. N. Sabbah, B. D. Hoit, P. Ernsberger, M. P. Chandler and W. C. Stanley, *Hypertension (Dallas, Tex.: 1979)*, 2006, **48**, 1116-1123.

66. C. R. Wilson, M. K. Tran, K. L. Salazar, M. E. Young and H. Taegtmeyer, *The Biochemical journal*, 2007, **406**, 457-467.

67. M. Maillet, J. H. van Berlo and J. D. Molkentin, *Nature reviews. Molecular cell biology*, 2013, **14**, 38-48.

68. E. D. Abel and T. Doenst, *Cardiovascular research*, 2011, **90**, 234-242.

69. D. Lazzeroni, O. Rimoldi and P. G. Camici, *Circulation journal: official journal of the Japanese Circulation Society*, 2016, **80**, 555-564.

70. I. Kehat and J. D. Molkentin, *Circulation*, 2010, **122**.

71. B. A. French and C. M. Kramer, *Drug discovery today. Disease mechanisms*, 2007, **4**, 185-196.

72. M. van Bilsen, F. A. van Nieuwenhoven and G. J. van der Vusse, *Cardiovascular research*, 2009, **81**, 420-428.

73. A. Akki, K. Smith and A. M. Seymour, *Molecular and cellular biochemistry*, 2008, **311**, 215-224.

74. M. N. Sack, T. A. Rader, S. Park, J. Bastin, S. A. McCune and D. P. Kelly, *Circulation*, 1996, **94**, 2837-2842.

75. T. Doenst, G. Pytel, A. Schrepper, P. Amorim, G. Farber, Y. Shingu, F. W. Mohr and M. Schwarzer, *Cardiovascular research*, 2010, **86**, 461-470.

76. M. Iemitsu, N. Shimojo, S. Maeda, Y. Irukayama-Tomobe, S. Sakai, T. Ohkubo, Y. Tanaka and T. Miyauchi, *American journal of physiology. Heart and circulatory physiology*, 2008, **295**, H136-144.

77. M. F. Allard, H. L. Parsons, R. Saeedi, R. B. Wambolt and R. Brownsey, *American journal of physiology. Heart and circulatory physiology*, 2007, **292**, H140-148.

78. K. N. Frayn, *Diabetologia*, 2002, **45**, 1201-1210.

79. S. A. Parry and L. Hodson, *Journal of investigative medicine: the official publication of the American Federation for Clinical Research*, 2017, **65**, 1102-1115.

80. D. B. Jump, *Current opinion in clinical nutrition and metabolic care*, 2011, **14**, 115-120.

81. P. Nguyen, V. Leray, M. Diez, S. Serisier, J. Le Bloc'h, B. Siliart and H. Dumon, *Journal of animal physiology and animal nutrition*, 2008, **92**, 272-283.

82. H. Yki-Jarvinen, *Digestive diseases (Basel, Switzerland)*, 2010, **28**, 203-209.

83. F. Diraison and M. Beylot, *The American journal of physiology*, 1998, **274**, E321-327.

84. P. J. Babin and G. F. Gibbons, *Progress in lipid research*, 2009, **48**, 73-91.

85. L. S. Sidossis, B. Mittendorfer, E. Walser, D. Chinkes and R. R. Wolfe, *American journal of physiology. Endocrinology and metabolism*, 1998, **275**, E798-e805.

86. J. D. Browning and J. D. Horton, *The Journal of clinical investigation*, 2004, **114**, 147-152.

87. O. Cheung and A. J. Sanyal, *Seminars in liver disease*, 2008, **28**, 351-359.

88. Y. Kawano and D. E. Cohen, *Journal of gastroenterology*, 2013, **48**, 434-441.

89. P. J. Nestel, R. J. Havel and A. Bezman, *The Journal of clinical investigation*, 1962, **41**, 1915-1921.

90. K. L. Donnelly, C. I. Smith, S. J. Schwarzenberg, J. Jessurun, M. D. Boldt and E. J. Parks, *The Journal of clinical investigation*, 2005, **115**, 1343-1351.

91. J. C. Cohen, J. D. Horton and H. H. Hobbs, *Science (New York, N.Y.)*, 2011, **332**, 1519-1523.

92. C. J. Green and L. Hodson, *Nutrients*, 2014, **6**, 5018-5033.

93. R. J. Havel, J. P. Kane, E. O. Balasse, N. Segel and L. V. Basso, *The Journal of clinical investigation*, 1970, **49**, 2017-2035.

94. L. Hodson and B. A. Fielding, *Clinical Lipidology*, 2010, **5**, 131-144.

95. G. F. Gibbons, S. M. Bartlett, C. E. Sparks and J. D. Sparks, *The Biochemical journal*, 1992, **287 (Pt 3)**, 749-753.

96. G. F. Gibbons and D. Wiggins, *Advances in enzyme regulation*, 1995, **35**, 179-198.

97. G. F. Gibbons, *The Biochemical journal*, 1990, **268**, 1-13.

98. V. A. Zammit, *The Biochemical journal*, 1996, **314 (Pt 1)**, 1-14.

99. S. E. McQuaid, L. Hodson, M. J. Neville, A. L. Dennis, J. Cheeseman, S. M. Humphreys, T. Ruge, M. Gilbert, B. A. Fielding, K. N. Frayn and F. Karpe, *Diabetes*, 2011, **60**, 47-55.

100. T. Ruge, L. Hodson, J. Cheeseman, A. L. Dennis, B. A. Fielding, S. M. Humphreys, K. N. Frayn and F. Karpe, *The Journal of clinical endocrinology and metabolism*, 2009, **94**, 1781-1788.

101. G. K. Pot, C. J. Prynne, C. Roberts, A. Olson, S. K. Nicholson, C. Whitton, B. Teucher, B. Bates, H. Henderson, S. Pigott, G. Swan and A. M. Stephen, *The British journal of nutrition*, 2012, **107**, 405-415.

102. M. Yilmaz, K. C. Claiborn and G. S. Hotamisligil, *Diabetes*, 2016, **65**, 1800-1807.

103. C. Postic and J. Girard, *J. Clin. Invest*., 2008, **118**, 829-838.

104. J. M. Schwarz, P. Linfoot, D. Dare and K. Aghajanian, *Am J Clin Nutr*, 2003, **77**, 43-50.

105. F. W. B. Sanders and J. L. Griffin, *Biol Rev Camb Philos Soc*., 2016, **91**, 452-468.

106. Z. Song, A. M. Xiaoli and F. Yang, *Nutrients*, 2018, **10**, E1383.

107. G. Y. Carmen and S. M. Victor, *Cellular Signalling*, 2006, **18**, 401-408.

108. C. P. Day and O. F. James, *Gastroenterology*, 1998, **114**, 842-845.

109. A. Wieckowska and A. E. Feldstein, *Current opinion in pediatrics*, 2005, **17**, 636-641.

110. M. Monetti, M. C. Levin, M. J. Watt, M. P. Sajan, S. Marmor, B. K. Hubbard, R. D. Stevens, J. R. Bain, C. B. Newgard, R. V. Farese, Sr., A. L. Hevener and R. V. Farese, Jr., *Cell metabolism*, 2007, **6**, 69-78.

111. C. J. McClain, S. Barve and I. Deaciuc, *Hepatology (Baltimore, Md.)*, 2007, **45**, 1343-1346.

112. L. L. Listenberger, X. Han, S. E. Lewis, S. Cases, R. V. Farese, Jr., D. S. Ory and J. E. Schaffer, *Proceedings of the National Academy of Sciences of the United States of America*, 2003, **100**, 3077-3082.

113. K. Yamaguchi, L. Yang, S. McCall, J. Huang, X. X. Yu, S. K. Pandey, S. Bhanot, B. P. Monia, Y. X. Li and A. M. Diehl, *Hepatology (Baltimore, Md.)*, 2007, **45**, 1366-1374.

114. Z. Z. Li, M. Berk, T. M. McIntyre and A. E. Feldstein, *The Journal of biological chemistry*, 2009, **284**, 5637-5644.

115. J. C. Lindon, J. K. Nicholson, E. Holmes and J. R. Everett, *Concepts in Magnetic Resonance*, 2000, **12**, 289-320.

116. C. Y. Lin, H. Wu, R. S. Tjeerdema and M. R. Viant, *Metabolomics*, 2007, **3**, 55-67.

117. E. Holmes, A. W. Nicholls, J. C. Lindon, S. C. Connor, J. C. Connelly, J. N. Haselden, S. J. Damment, M. Spraul, P. Neidig and J. K. Nicholson, *Chemical research in toxicology*, 2000, **13**, 471-478.

118. W. Weckwerth, *Annual review of plant biology*, 2003, **54**, 669-689.

119. C. B. Newgard, J. An, J. R. Bain, M. J. Muehlbauer, R. D. Stevens, L. F. Lien, A. M. Haqq, S. H. Shah, M. Arlotto, C. A. Slentz, J. Rochon, D. Gallup, O. Ilkayeva, B. R. Wenner, W. S. Yancy, Jr., H. Eisenson, G. Musante, R. S. Surwit, D. S. Millington, M. D. Butler and L. P. Svetkey, *Cell metabolism*, 2009, **9**, 311-326.

120. J. T. Brindle, H. Antti, E. Holmes, G. Tranter, J. K. Nicholson, H. W. Bethell, S. Clarke, P. M. Schofield, E. McKilligin, D. E. Mosedale and D. J. Grainger, *Nature medicine*, 2002, **8**, 1439-1444.

121. R. Williams, E. M. Lenz, A. J. Wilson, J. Granger, I. D. Wilson, H. Major, C. Stumpf and R. Plumb, *Molecular bioSystems*, 2006, **2**, 174-183.

122. Y. Bao, T. Zhao, X. Wang, Y. Qiu, M. Su, W. Jia and W. Jia, *Journal of proteome research*, 2009, **8**, 1623-1630.

123. N. J. Serkova, M. Jackman, J. L. Brown, T. Liu, R. Hirose, J. P. Roberts, J. J. Maher and C. U. Niemann, *Journal of hepatology*, 2006, **44**, 956-962.

124. X. Zhang, Y. Wang, F. Hao, X. Zhou, X. Han, H. Tang and L. Ji, *Journal of proteome research*, 2009, **8**, 5188-5195.

125. J. Shearer, G. Duggan, A. Weljie, D. S. Hittel, D. H. Wasserman and H. J. Vogel, *Diabetes, obesity & metabolism*, 2008, **10**, 950-958.

126. J. K. Nicholson, J. C. Lindon and E. Holmes, *Xenobiotica; the fate of foreign compounds in biological systems*, 1999, **29**, 1181-1189.

127. G. A. Gowda, B. S. Somashekar, O. B. Ijare, A. Sharma, V. K. Kapoor and C. L. Khetrapal, *Lipids*, 2006, **41**, 577-589.

128. M. E. Bollard, E. G. Stanley, J. C. Lindon, J. K. Nicholson and E. Holmes, *NMR in biomedicine*, 2005, **18**, 143-162.

129. L. Bala, U. C. Ghoshal, U. Ghoshal, P. Tripathi, A. Misra, G. A. Gowda and C. L. Khetrapal, *Magnetic resonance in medicine*, 2006, **56**, 738-744.

130. W. H. Heijne, R. J. Lamers, P. J. van Bladeren, J. P. Groten, J. H. van Nesselrooij and B. van Ommen, *Toxicologic pathology*, 2005, **33**, 425-433.

131. S. Garrod, E. Humpher, S. C. Connor, J. C. Connelly, M. Spraul, J. K. Nicholson and E. Holmes, *Magnetic resonance in medicine*, 2001, **45**, 781-790.

132. M. A. Anwar, K. N. Adesina-Georgiadis, K. Spagou, P. A. Vorkas, J. V. Li, J. Shalhoub, E. Holmes and A. H. Davies, *Scientific reports*, 2017, **7**, 2989.

133. G. A. Gowda, S. Zhang, H. Gu, V. Asiago, N. Shanaiah and D. Raftery, *Expert review of molecular diagnostics*, 2008, **8**, 617-633.

134. E. M. Lenz and I. D. Wilson, *Journal of proteome research*, 2007, **6**, 443-458.

135. I. D. Wilson, R. Plumb, J. Granger, H. Major, R. Williams and E. M. Lenz, *Journal of chromatography. B, Analytical technologies in the biomedical and life sciences*, 2005, **817**, 67-76.

136. I. D. Wilson, J. K. Nicholson, J. Castro-Perez, J. H. Granger, K. A. Johnson, B. W. Smith and R. S. Plumb, *Journal of proteome research*, 2005, **4**, 591-598.

137. T. Gebregiworgis and R. Powers, *Combinatorial chemistry & high throughput screening*, 2012, **15**, 595-610.

138. A.-H. M. Emwas, R. M. Salek, J. L. Griffin and J. Merzaban, *Metabolomics*, 2013, **9**, 1048-1072.

139. I. F. Duarte, S. O. Diaz and A. M. Gil, *Journal of pharmaceutical and biomedical analysis*, 2014, **93**, 17-26.

140. E. M. DeFeo, C. L. Wu, W. S. McDougal and L. L. Cheng, *Nature reviews. Urology*, 2011, **8**, 301-311.

141. I. Garcia-Alvarez, A. Fernandez-Mayoralas and L. Garrido, *Current topics in medicinal chemistry*, 2011, **11**, 27-42.

142. J. K. Nicholson and I. D. Wilson, *Progress in Nuclear Magnetic Resonance Spectroscopy*, 1989, **21**, 449-501.

143. M. Coen, E. Holmes, J. C. Lindon and J. K. Nicholson, *Chemical research in toxicology*, 2008, **21**, 9-27.

144. J. L. Griffin, L. A. Walker, R. F. Shore and J. K. Nicholson, *Chemical research in toxicology*, 2001, **14**, 1428-1434.

145. J. G. Bundy, D. J. Spurgeon, C. Svendsen, P. K. Hankard, J. M. Weeks, D. Osborn, J. C. Lindon and J. K. Nicholson, *Ecotoxicology (London, England)*, 2004, **13**, 797-806.

146. R. A. Kauppinen and S. R. Williams, *Journal of neurochemistry*, 1991, **57**, 1136-1144.

147. R. A. Kauppinen, T. R. Pirttila, S. O. Auriola and S. R. Williams, *The Biochemical journal*, 1994, **298 (Pt 1)**, 121-127.

148. J. Schneider, E. Fekete, A. Weisser, S. Neubauer and M. von Kienlin, *Magnetic resonance in medicine*, 2000, **43**, 497-502.

149. J. L. Griffin, H. J. Williams, E. Sang and J. K. Nicholson, *Magnetic resonance in medicine*, 2001, **46**, 249-255.

150. J. C. Chatham and S. J. Blackband, *ILAR journal*, 2001, **42**, 189-208.

151. N. Merkley, I. Burton, T. Karakach and R. T. Syvitski, in *Using Old Solutions to New Problems - Natural Drug Discovery in the 21st Century*, ed. M. Kulka, InTech, Rijeka, 2013, ch. 3, pp. 62-91.

152. M. A. Shampo, R. A. Kyle and D. P. Steensma, *Mayo Clinic proceedings*, 2012, **87**, e73.

153. Y. Xia and P. Stilbs, *Cartilage*, 2016, **7**, 293-297.

154. A. W. Overhauser, *Physical Review*, 1953, **89**, 689-700.

155. N. Muller and D. E. Pritchard, *The Journal of Chemical Physics*, 1959, **31**, 768-771.

156. C. Holm, *The Journal of Chemical Physics*, 1957, **26**, 707-708.

157. C. Boesch, *Journal of magnetic resonance imaging: JMRI*, 2004, **20**, 177-179.

158. A. G. Palmer and D. J. Patel, *Structure (London, England: 1993)*, 2002, **10**, 1603-1604.

159. M. H. Levitt, *Spin Dynamics: Basics of nuclear magnetic resonance*, John Wiley and Sons, West Sussex, UK, 2 edn., 2002.

160. J. N. S. Evans, *Biomolecular NMR Spectroscopy*, Oxford University Press, New York, 1995.

161. Q. Teng, *Structural Biology: Practical NMR Applications*, Springer, 2 edn., 2013.

162. P. J. Hore, *Nuclear Magnetic Resonance*, Oxford Science Publication, New York, 1995.

163. P. Conte and A. Piccolo, *Opt. Pura Apl*, 2007, **40**, 215-226.

164. Chapter 3. Introductory Theory and Terminology, http://triton.iqfr.csic.es/guide/man/beginners/chap3-9.htm

165. I. T. Jolliffe, *Principal Component Analysis*, Springer, London, 2 edn., 2002.

166. S. Karamizadeh, S. M. Abdullah, A. A. Manaf, M. Zamani and A. Hooman, *Journal of Signal and Information Processing*, 2013, **Vol.04No.03**, 3.

167. J. Shlens, A TUTORIAL ON PRINCIPAL COMPONENT ANALYSIS Derivation, Discussion and Singular Value Decomposition, https://www.cs.princeton.edu/picasso/mats/PCA-Tutorial-Intuition_jp.pdf

168. *Principal Component Analysis - Multidisciplinary Applications*, InTech, London,, 2012.

169. L. I. Smith, A tutorial on Principal Components Analysis, http://www.cs.otago.ac.nz/cosc453/student_tutorials/principal_components.pdf

170. X. Chen, C. Chen and L. Jin, *Advances in Anthropology*, 2011, **Vol.01No.02**, 6.

171. I. T. Jolliffe and J. Cadima, *Philosophical transactions. Series A, Mathematical, physical, and engineering sciences*, 2016, **374**, 20150202.

172. H. Abdi and L. J. Williams, *Wiley Interdisciplinary Reviews: Computational Statistics*, 2010, **2**, 433-459.

173. https://georgemdallas.wordpress.com/2013/10/30/principal-component-analysis-4-dummies-eigenvectors-eigenvalues-and-dimension-reduction/

174. Principal Component Analysis, http://people.duke.edu/~hpgavin/SystemID/References/Gillies-PCA-notes.pdf

175. I. M. Johnstone and D. M. Titterington, *Philosophical transactions. Series A, Mathematical, physical, and engineering sciences*, 2009, **367**, 4237-4253.

176. B. Worley and R. Powers, *Current Metabolomics*, 2013, **1**, 92-107.

177. J. C. Lindon, J. K. Nicholson, E. Holmes, H. C. Keun, A. Craig, J. T. Pearce, S. J. Bruce, N. Hardy, S. A. Sansone, H. Antti, P. Jonsson, C. Daykin, M. Navarange, R. D. Beger, E. R. Verheij, A. Amberg, D. Baunsgaard, G. H. Cantor, L. Lehman-McKeeman, M. Earll, S. Wold, E. Johansson, J. N. Haselden, K. Kramer, C. Thomas, J. Lindberg, I. Schuppe-Koistinen, I. D. Wilson, M. D. Reily, D. G. Robertson, H. Senn, A. Krotzky, S. Kochhar, J. Powell, F. van der Ouderaa, R. Plumb, H. Schaefer and M. Spraul, *Nature biotechnology*, 2005, **23**, 833-838.

178. L. W. Sumner, A. Amberg, D. Barrett, M. H. Beale, R. Beger, C. A. Daykin, T. W. Fan, O. Fiehn, R. Goodacre, J. L. Griffin, T. Hankemeier, N. Hardy, J. Harnly, R. Higashi, J. Kopka, A. N. Lane, J. C. Lindon, P. Marriott, A. W. Nicholls, M. D. Reily, J. J. Thaden and M. R. Viant, *Metabolomics*, 2007, **3**, 211-221.

179. P. E. Anderson, D. A. Mahle, T. E. Doom, N. V. Reo, N. J. DelRaso and M. L. Raymer, *Metabolomics*, 2011, **7**, 179-190.

180. P. E. Anderson, N. V. Reo, N. J. DelRaso, T. E. Doom and M. L. Raymer, *Metabolomics*, 2008, **4**, 261-272.

181. T. De Meyer, D. Sinnaeve, B. Van Gasse, E. Tsiporkova, E. R. Rietzschel, M. L. De Buyzere, T. C. Gillebert, S. Bekaert, J. C. Martins and W. Van Criekinge, *Analytical Chemistry*, 2008, **80**, 3783-3790.

182. M. Sysi-Aho, M. Katajamaa, L. Yetukuri and M. Oresic, *BMC bioinformatics*, 2007, **8**, 93.

183. A. Craig, O. Cloarec, E. Holmes, J. K. Nicholson and J. C. Lindon, *Anal Chem*, 2006, **78**, 2262-2267.

184. H. C. J. Hoefsloot, M. P. H. Verouden, J. A. Westerhuis and A. K. Smilde, *Journal of Chemometrics*, 2006, **20**, 120-127.

185. J. Trygg and S. Wold, *Journal of Chemometrics*, 2002, **16**, 119-128.

186. S. Halouska and R. Powers, *Journal of magnetic resonance (San Diego, Calif.: 1997)*, 2006, **178**, 88-95.

187. H. Winning, F. H. Larsen, R. Bro and S. B. Engelsen, *Journal of magnetic resonance (San Diego, Calif.: 1997)*, 2008, **190**, 26-32.

188. M. R. Wenk, *Nature reviews. Drug discovery*, 2005, **4**, 594-610.

189. A. Zhou, J. Ni, Z. Xu, Y. Wang, S. Lu, W. Sha, P. C. Karakousis and Y. F. Yao, *Journal of proteome research*, 2013, **12**, 4642-4649.

190. J. K. Nicholson and J. C. Lindon, *Nature*, 2008, **455**, 1054-1056.

191. C. Corsaro, D. Mallamace, S. Vasi, V. Ferrantelli, G. Dugo and N. Cicero, *Journal of Analytical Methods in Chemistry*, 2015, **2015**, 14.

192. C. Wolf and P. J. Quinn, *Progress in lipid research*, 2008, **47**, 15-36.

193. N. W. Lutz, j. v. Sweedler and R. A. Wevers, *Methodologies for Metabolomics: Experimental Strategies and Techniques*, Cambridge University Press New York, 2013.

194. J. L. Griffin, *Philos Trans R Soc Lond B Biol Sci*, 2006, **361**, 147-161.

195. A. Ganna, S. Salihovic, J. Sundstrom, C. D. Broeckling, A. K. Hedman, P. K. Magnusson, N. L. Pedersen, A. Larsson, A. Siegbahn, M. Zilmer, J. Prenni, J. Arnlov, L. Lind, T. Fall and E. Ingelsson, *PLoS genetics*, 2014, **10**, e1004801.

196. M. R. El-Gewely, *Biotechnology Annual Review*, Elsevier, Amsterdam, 2006.

Chapter 2

Materials and Methods

2.1 Surgical induction and dietary manipulation

2.1.1 Surgical induction

The surgery of rats was done by Dr Seymour's group.

Cardiac hypertrophy was induced surgically in adult male Sprague Dawley rats (220-250gm, Charles River Inc., Kent, UK) by abdominal aortic-constriction (AC) as described by Boateng *et al.*, Akki *et al.* and Butler *el al.*[1-4] All procedures were performed using aseptic techniques and were in accordance with UK Home Office Regulation on the operation of animals (Scientific Procedures) Act 1986 and approved by the University of Hull ethical review process.

Prior to surgery, Rimadyl (4mg/kg BW), an analgesic was injected in to the rats for pain relief. Rats were anaesthetised with isoflurance in oxygen (3% in 3L/ min) and anaesthesia maintained with 2% isoflurance in 1L/ min oxygen. A laparotomy was performed, the abdominal aorta exposed and ligated between the left and right renal artery branches using a 0.5mm outer diameter 25-gauge blunted needle (Becton Dickinson, UK) and suture (Mersilk 0, Ethicon, Somerville, USA). Ligation of the aorta caused the left kidney to blanch. Removal of the needle restored the blood flow to the left kidney. Control rats underwent the same procedure but without constriction of the aorta, known as sham intervention. Sterile isotonic saline (Animal Care Ltd, York, UK) was administered directly into the abdominal cavity to compensate for any fluid loss during surgery. Abdominal musculature was closed with an absorbable suture (Ethicon 3-0, Vicryl braided) and the epidermal layer with a non-absorbable suture (Ethicon 3-0, Blue monofilament). Ampifen (42mg/kg Intervet UK Ltd,Cambridge,UK) antibiotic was given immediately after surgery.

2.1.2 Dietary manipulation

Animals were fed and looked after for nine weeks by Dr Seymour's group.

Animals could recover for 48 hrs with food and water *ad libitum* before being assigned to diets containing 61.6% fat and 20.3% sucrose (high-fat diet, HFD) or 45% fat and 15% sucrose (Western diet, WD) (table 2.1). The contributions of carbohydrate, protein, and individual FA species were calculated using heat of combustion values of 4, 4, and 9 kcal/g, respectively. Animals were maintained on each of the diets for 9 weeks. The WD was formulated to mimic Western dietary patterns.

Table 2.1 Dietary constituents

Nutrients	WD (% kcal)	HFD (%kcl)
Carbohydrates	15% (from sucrose)	20% (from sucrose)
Proteins	20% (from casein)	18.1% (from casein)
Fats	45% (from lard and soya Oil)	61.6% (from lard and soya Oil)

HFD, high-fat diet; WD, western diet

2.2 Nuclear magnetic resonance (NMR) Analysis

2.2.1 Tissue extraction of lipid for liquid state ^{1}H NMR

2.2.1.1 Liver tissue

The liver tissue was ground into a fine powder using a liquid nitrogen-cooled pestle and mortar and lipids were extracted using the chloroform and methanol method of Blight and Dyer.[5] Approximately 300mg of liver tissues were kept in the glass tube and after that the glass tube was placed into an ice pot. Liver tissues (300mg) were homogenised with an electrical blender (ULTRA-TURRAX T25) in chloroform-methanol-water (1ml) in the ratio 2:1:0.8(v/v/v) and the mixture was centrifuged (Universal refrigerated centrifuge,

SIGMA 2-16 PK) (g800) at 25°C for 15 minutes. The upper aqueous layer was discarded and the lower chloroform layer containing lipids transferred to a screw top glass vial (Agilent Technologies, Ltd) and dried under a nitrogen stream (BOC Edwards, Surrey, UK). Samples were left overnight in a freeze dryer (Modulyo, BOC Edwards, Crawley, UK) to remove trace amounts of remaining solvent, and then resuspended in 1 ml deuterated chloroform +0.03% TMS, H_2O < 0.01% (euriso-top., France) and stored at -20°C for 24 hours pending NMR analysis.

2.2.1.2 Heart tissue

Heart tissue was ground into a fine powder using a liquid nitrogen-cooled pestle and mortar and lipids were extracted using the chloroform and methanol method of Blight and Dyer.[5] Approximately 300mg of heart tissues were kept in the glass tube and after that the glass tube was placed into an ice pot. The heart tissues (300mg) was homogenised with an electrical blender (ULTRA-TURRAX T25) in chloroform-methanol-water (1ml) in the ratio 2:1:0.8(v/v/v) and the mixture was centrifuged (Universal refrigerated centrifuge, SIGMA 2-16 PK) (g800) at 25°C for 15 minutes. The upper aqueous layer was discarded and the lower chloroform layer containing lipids transferred to a screw top glass vial (Agilent Technologies, Ltd) and dried under a nitrogen stream (BOC Edwards, Surrey, UK). Samples were left overnight in a freeze dryer (Modulyo, BOC Edwards, Crawley, UK) to remove trace amounts of remaining solvent, and then resuspended in 1 ml deuterated chloroform +0.03% TMS, H_2O < 0.01% (euriso-top., France) and stored at -20°C for 24 hours pending NMR analysis.

2.2.2 Preparation of NMR sample

The lipid and chloroform-D mixture (600µl) was transferred into a 5mm thin wall NMR sample tube (Wilmad LabGlass, USA). The level of the sample was checked by the

measurement meter to ensure that it was in the range of the magnetic field and the NMR sample tube was placed into the sample probe holder to be lowered into the NMR machine.

2.2.3 Liquid state NMR experiments

All NMR experiments were carried out on a Bruker Avance II 500 MHz spectrometer operating at a frequency of 500.1025 MHz (^{1}H). All measurements were collected at 288K (Kelvin). ^{1}H spectra were collected using a single $\pi/2$ pulse and 64 scans were accumulated. Spectra were referenced to the ^{1}H peak of TMS at 0ppm. All spectra were processed using Topspin 1.3 (Bruker biospin).

2.2.4 Solid state ^{1}H HR-MAS NMR sample preparation

The ^{1}H HR-MAS NMR experiments on intact heart and liver tissue of the left lobe excised from rats were performed on a Bruker Avance II 500 MHz spectrometer operating at a frequency of 500.1025 MHz (^{1}H). NMR spectrometer at 278 K with spinning speed 8kHZ and 256 scans were accumulated. About 30-40mg tissue (liver or heart) was located between two Kel-F plugs in the MAS rotor and inserted in a commercial 4.0mm MAS probe from Bruker. The spectrum was referenced to the methyl (0.9ppm) in each spectrum.

2.2.5 Lipid histology

Rats were anaesthetised via i/p sodium thiopentone (0.5ml/100g BW) and the heart and liver rapidly excised. The apex of each heart and liver was mounted on cork blocks using Tissue-Tek OCT®. Mounted apex of hearts and livers were placed in pre-cooled 2-methyl-butane for one minute then transferred to liquid nitrogen. Samples were stored at -20°C prior to sectioning.

Small blocks of animal's right lop livers were mounted on cork blocks using Tissue-Tek OCT®. Mounted liver tissue was placed in pre-cooled 2-methyl-butane for 1 minute then transferred to liquid nitrogen. Samples were stored at -20°C prior to sectioning.

A cryostat microtome (Microm HM 505 E Cryostat, Thermo Scientific, Walldorf, Germany) was used to obtain 10µm sections from both heart apex and liver tissue. Lipid deposition was examined using Oil Red O stain (Lipid Stain, ab150678, Abcam plc,UK).Sections were analysed using a light microscope (x20 and x50 magnification, Olympus BX51, Tokyo,Japan).

2.2.6 Statistical methods

In this study multivariate data analysis software was used to perform PCA (SIMCA14.1, Umetrics UK). ^{1}H NMR spectrum data for heart tissues, liver tissues and lipid extractions from heart and liver tissues of rats were analysed by PCA software on the basis of sample grouping. In this part of the experiment, four different groups of samples were analysed. The groups were fed on either WD or HFD. Each group had two types of surgery, AC and Sham, a total of 20 samples. They were analysed and grouped as (WD+AC) 6 samples; (WD+SHAM) 7 samples; (HFD+AC) 3 samples and (HFD+SHAM) 4 samples (Table 2.2.6).

The data was analysed by the PCA having a number of variables that represented peaks intensity of ^{1}H NMR and number of observations (20) representing the samples. The PCA scores of the data were then plotted and loaded in diagrams which could then be easily interpreted.

Table 2.2 List of samples extracted from survived rat heart and liver tissues

Sample Type		Type of Surgery		Total
		AC	SHAM	
Diet	WD	7 +1*	7+1*	14+2*=16
	HF	3+1*	4+0*	7+1*=8
Total survived rats		10	11	21

*Number of mortalities

2.3 References

1. A. Akki and A. M. Seymour, *Cardiovascular research*, 2009, **81**, 610-617.
2. A. Akki, K. Smith and A. M. Seymour, *Molecular and cellular biochemistry*, 2008, **311**, 215-224.
3. T. J. Butler, D. Ashford and A. M. Seymour, *Nutrition, metabolism, and cardiovascular diseases : NMCD*, 2017, **27**, 991-998.
4. S. Y. Boateng, A. M. Seymour, N. S. Bhutta, M. J. Dunn, M. H. Yacoub and K. R. Boheler, *Journal of molecular and cellular cardiology*, 1998, **30**, 2683-2694.
5. E. G. Bligh and W. J. Dyer, *Canadian journal of biochemistry and physiology*, 1959, **37**, 911-917.

Chapter 3

Lipid droplets in heart and liver tissues

3.1 Introduction

Lipid droplets (LDs) are intracellular organelles specialized for storage of neutral lipids. The first speculation about the origin of LD, was made in 19th century when Richard Altmann and E.B. Wilson described them as fat droplets inside cells.[1, 2] For a long time, LDs were considered merely as storage depots; however, recently they have emerged as highly dynamic organelles that participate in several cellular processes and interact with various other cellular compartments. LDs form stable interactions with endoplasmic reticulum (ER) and mitochondria.[3] Other cellular organelles such as the inner nuclear envelope, lysosomes or vacuoles, and endosomes also appear to bind with droplets.[3]

3.1.1 Structure and composition of LDs

Typically, LDs are round; their diameter ranges from 0.1-5μm in non-adipocytes and can exceed over 100μm in white adipocytes. The LD core is composed of neutral lipids mainly triacylglycerol (TG) and sterol esters (SE) enclosed by a monolayer of phospholipids and associated proteins. The phospholipid monolayer of LDs is composed of phosphatidylcholine (PC), phosphatidylethanolamine (PE), phosphatidylinositol (PI), lyso-phosphatidylcholine (lysoPC), lyso-phosphatidylethanolamine (lysoPE), phosphatidic acid (PA), phosphatidylserine (PS) and sphingomyelin (SM).[4] Proteomic studies have revealed numerous LD related proteins that can be classified into nine groups: (i) LD structural proteins including perilipin (PLIN) 1-5, (ii) lipid metabolism enzymes namely diacylglycerol acyltransferase (DGAT) enzymes: DGAT1 and DGAT2, acyl-CoA cholesterol acyltransferase (ACAT) enzymes: ACAT1 and ACAT2, and lecithin retinol acyltransferase (LART), (iii) membrane trafficking proteins such as Rab (Rab8a, Rab18) and SNARE proteins, (iv) signalling proteins, mitogen activated protein kinase (MAPK), protein kinase C (PKC), and phosphoinositide-3-kinase (PI3K),

(V) ubiquitination factors, UBX domain-containing protein 8 (UBXD8), ancient ubiquitous protein 1 (AUP1), and ubiquitin-conjugating enzyme E2 G2 (UBE2G2), (vi) cytoskeletal proteins such as actin, vimentin, tubulin, and myosin, (vii) ribosomal proteins, (vii) histones, and (ix) cell death inducing DFFA-like effector (CIDE) proteins.[5, 6]

3.1.2 LDs formation

Recent studies have suggested that in eukaryotes LDs emerge *de novo* from the ER.[7-9] There are several proposed models of LD formation, including the classical model, budding of the lipid ester globule covered by the cytoplasmic leaflet of the ER membrane[10], a model of diffusion of TGs from the ER into formed LDs contained in a membrane cup[11], an ER "hatching", hypothesizing a bicellar structure and the presence of transmembrane ER proteins in LDs[12], and a model of LDs budding first into the lumen of the ER.[10-12] However, Walther *et. al*., have postulated the most recent model for LD formation.[13] According to this model LDs are formed in four conventional steps:

The first step of LD formation includes TG and SE synthesis within the ER. TG synthesis is catalysed by DGAT1 and DGAT2 enzymes.[14-16] DGAT1 catalyses the esterification reaction to generate a TG from fatty acyl-CoA and an acyl acceptor, while, DGAT2 catalyses TG synthesis from fatty acid substrates derived from de novo lipogenesis.[17] TG synthesis occurs throughout the ER wherever enzyme substrates are found in excess and TGs accumulate within the ER bilayer. SEs are also synthesised in the ER by the ACAT enzymes; however, the mechanism of SE synthesis is not well established yet. In the second step of LD formation, there is a formation of a TG lens. After synthesis and accumulation of TG, biophysical processes drive lens formation in the ER tubules. Some ER proteins are assumed to be involved in the lens formation and regulation; for example, Fat induced protein 2 (FIP2) may be involved in the segregation of neutral lipids and

binds to TGs for LD formation.[18] PLIN3 is suggested to bind nascent lenses and stabilize them.[19] Acyl coenzyme-A synthetase 3(ACS3) and Arf1/COPI complex inhibit TG lens formation in specific regions of ER and mediate targeting of proteins from ER to LDs.[9, 20]

In the third step of LD formation encompasses budding of nascent LD. After TGs lens formation it is converted to a bud on the ER and eventually fission of the droplet in the cytosol occurs. Although budding of LDs from the ER is a biophysical process some proteins are thought to be involved in regulating this step. Seipin protein plays a functional role in the nascent LD formation and helps in their growth and expansion.[21, 22] In addition, seipin also regulates the protein composition of LDs.[22, 23] Since LDs and ER stay in contact even when seipin is absent, it is possible that other proteins are involved in initial budding and growth of nascent LD.[21, 22] The fourth and final step of LD formation involves the growth and expansion of LDs. After initial LDs (iLDs) formation, some LDs are converted to expanding LDs (eLDs) by ARF1 and COP-I/coatamer protein machinery.[20, 24, 25] Subsequently, there is targeting of the proteins to LD surfaces. The proteins that are targeted to the LD surfaces can be classified into two major classes: class I proteins and class II proteins.[26] In drosophila, class I proteins, such as GPAT4, DGAT2, ATGL, UBXD8, and ACSL3, translocate to LD surface by ER-LD membrane bridges. Whereas, class II proteins, such as CCT1 and PLIN target from the cytosol by amphipathic helices or hydrophobic domains.[26] Although the model describes the fundamental steps of TG lens formation and budding into the aqueous cytosol, it remains to be validated.

Some cells, such as adipocytes or hepatocytes, have LDs whose diameter is ≥100μm known as giant LDs. These giant LDs are formed by either coalescence or diffusion

mediated by Ostwald ripening. In coalescence, two LDs fuse very rapidly to form a larger LD and in diffusion mediated by Ostwald ripening, one LD enlarges slowly and concentrates the oil of the adjacent second LD

3.1.3 LDs in health and diseases

Most cell types in the body can store lipids in the form of LDs, including, cardiomyocytes, hepatocytes, myocytes, macrophages, fibroblasts, etc. However, the over accumulation of LDs leads to several diseases such as type II diabetes, obesity, hepatosteatosis, cancer, and atherosclerosis.

3.1.3.1 Heart lipid droplets

The heart uses fatty acids (FAs) as the energy source for continuous myocardial contraction. However, excess FA oxidation generates high amounts of reactive oxygen species (ROS). Free FAs and their derivatives may cause lipotoxicity by disturbing the cellular signalling network. To avoid lipotoxicity, excess FAs are converted to inert triacylglycerol (TAG) and stored in LDs.[27] Since, the FA consumption in the healthy heart is dynamic there are very few LDs. Conversely in pathological conditions when FA influx is higher, numerous enlarged LDs appear in the heart, resulting from the increased conversion of FAs to TAGs. This abnormal retention of lipids in the heart is associated with cardiomyopathies. The TAG stored in LD can be used by lipase mediated lipolysis. Heart lipolysis involves two lipases, adipose triglyceride lipase (ATGL) and hormone-sensitive lipase (HSL) and a co-lipase, comparative gene identification 58(CGI-58) and is regulated by PLIN5.[28] Studies have suggested that TAGs are a safe storage form of FAs whereas free FAs and derived intermediates such as DAG and ceramide may cause lipotoxicity.[29]

3.1.3.2 Liver lipid droplets

One of the physiological functions of the liver is lipid metabolism and distribution of lipids throughout the body. The liver breaks down the lipids into FAs to generate metabolic energy and secretes them as lipoproteins. FAs are esterified by DGAT2 enzyme leading to the formation of TGs and stored in LDs. Further, TGs can be secreted to other organs for energy as very low-density lipoprotein (VLDL).[30] TG catabolism in the liver is mediated by ATGL enzyme. ATGL activity is tightly regulated by activators such as CGI-58 pigment epithelial derived factor and inhibitors namely G0/G1 switch gene 2, fas associated factor 2, cell death-inducing DFFA-like effector c (CIDEC), PLIN2 and PLIN5.[31] In addition to lipase mediated lipid breakdown, LD degradation can also occur through lipophagy.[32] In lipophagy, the autophagic machinery targets LDs for degradation by lysosomal lipase. The mechanism through which the autophagic machinery recognizes hepatic LDs, targets specific LDs and channels the degradation products of lipophagy is not well established. However, recent study identified RAB7, as a key protein involved in hepatic lipophagy.[33] During normal conditions there is a balance between influx of FA, oxidation of FA and export of very low-density lipoprotein (VLDL). Imbalance in the homeostasis of lipid metabolism leads to over-accumulation of TGs in liver LDs. The over-accumulation or steatosis of TGs in LDs may occur from increased TG synthesis combined with LD biogenesis, decreased FA oxidation, or impaired VLDL secretion. Steatosis of LDs in the liver leads to progression of liver diseases such as non-alcoholic fatty liver disease (NAFLD), alcoholic liver disease (ALD) and Hepatitis C virus infection.[34, 35]

3.1.4 Hematoxylin-eosin (H & E) and oil red O (ORO)

Tissues were stained with hematoxylin-eosin (H & E) and oil red O (ORO) for the evidence of lipid accumulation.[36] The histological staining is important to know about the properties of the tissue or structure to visualise under stain solution. Visualization of lipids in the histological section is difficult because they are relatively inert.[36] The ORO is a fat-soluble bright red diazo dye without forming any bond with the lipid components.[37] ORO stains hydrophobic and neutral lipids, such as TG and cholesterol esters but is unable to stain membranes polar lipids, such as phospholipids, sphingolipids, and ceramides. This staining can be used for fresh, frozen, or formalin-fixed samples to visualise the lipids.[37] H & E is colourless and forms a functional dye when oxidized to hematein.[39] H & E solutions produce a blue-purple staining of cell nuclei.[38]

3.2 Aims

To investigate the accumulation of lipids in the rat heart and liver tissues under WD and HFD dietary conditions. The histological sections while be stained with H&E and Oil Red O staining under a light microscope. This will show the accumulation of lipids composition in the form of lipid droplets on the hearts and liver tissues under Oil Red O stain. The cell nuclei and cytoplasm or cellular structure will be determined by H & E stain.

3.3 Materials and methods

Adult male Sprague Dawely rats (220-250 gm, Charles River Inc.,Kent, UK) were maintained on diets containing 61.6% fat and 20.3% sucrose (high-fat diet, HFD); or 45% fat and 15% sucrose (western diet, WD), 48 hours post-surgery, as described in Chapter 2 section 2.1, generating four experimental groups:

- High-fat diet + Sham (HFDSham).
- Western diet + Sham (WDSham).
- High-fat diet + Aortic Constriction (HFDAC).
- Western diet + Aortic Constriction (WDAC).

The apex of heart and liver tissues were mounted on cork blocks using Tissue-Tek OCT®. Mounted apex of hearts and livers were placed in pre-cooled 2-methyl-butane for 1 minute then transferred to liquid nitrogen. Samples were stored at -20°C prior to sectioning as described in Chapter 2 section 2.2.5.

A cryostat microtome (Microm HM 505 E Cryostat, Thermo Scientific, Walldorf, Germany) was used to obtain 10µm sections from both heart and liver tissues. Histological morphology was examined using H&E stain (Hematoxylin and Eosin stain, Sigma-Aldrich, Inc). Lipid deposition was examined using Oil Red O stain (Lipid Stain, ab150678, Abcam plc, UK). Sections were observed using light microscope (x10 and x40 magnification, Olympus IX71, Tokyo, Japan) and imaging software (Olympus cellSens Entry).

3.4 Results

3.4.1 Histology of rat heart and liver tissues

Hematoxylin and eosin (H&E) stain was used to observe the nucleus and cell membrane of the tissues. Under H&E stain, the nucleus appeared as blue-purple colour whereas cytoplasm and cell membrane appeared as red- pink colour. Oil red O stain was used to observe the lipid accumulation in the tissues. Under oil red O stain, the accumulated lipid droplets in tissues appear as red colour whereas nucleus appears as blue colour.

The histological sections of rat heart tissues under H&E nuclei appeared as blue colour whereas cell membrane and cytoplasm emerged as red-pink colour in HFAC (Figure 3.1A), HFSham (Figure3.2A), WDAC (Figure 3.3A) and WDSham (Figure 3.4A). The H&E stain result of heart tissues suggested that there were no cellular abnormalities, such as size of cells, cytoplasmic and nucleus structure under both dietary and surgical conditions. Under Oil red O staining, microscopic images suggested that the lipids were accumulated in the form of lipid droplets in the heart tissues of rat models; HFAC (Figure3.1B), HFSham (Figure3.2B), WDAC (Figure3.3B) and WDSham (Figure3.4B)

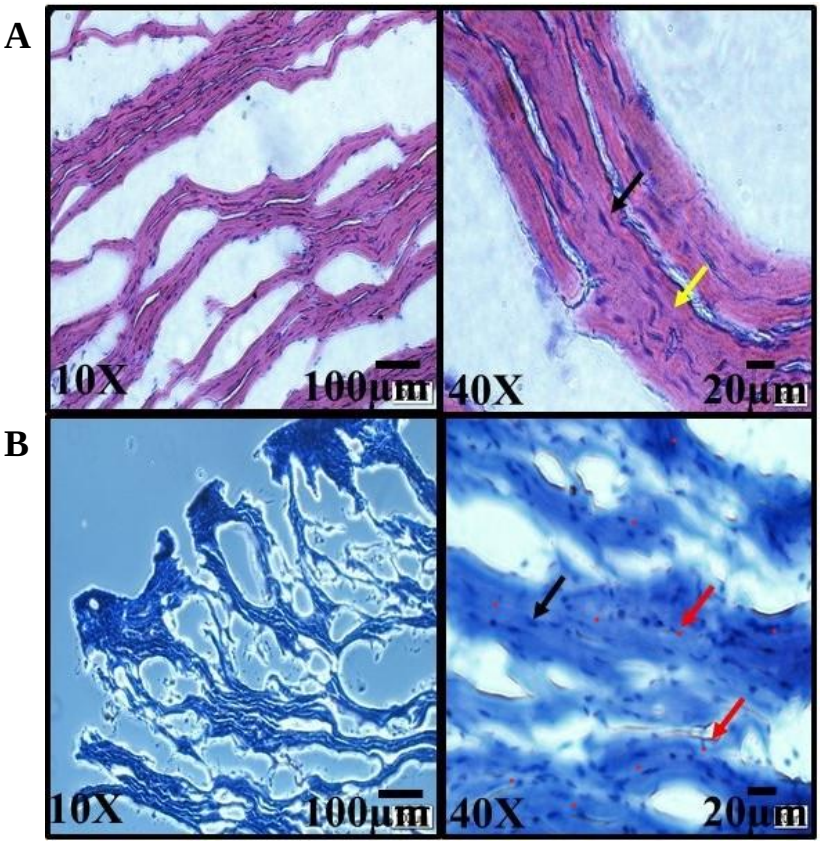

Figure 3.1 Histological section of heart tissues of rat model under HFDAC

(A) H&E stain of nuclei appear as blue (black arrow) and the cytoplasm and cell membrane emerge as red-pink colour (yellow arrow). (B) Under oil red O stain of the heart tissues of HFDAC the nuclei become blue (black arrow) and lipid droplets are stained in red (red arrow). The scale bar represents 100µm at X10 magnification and 20µm at X40 magnification.

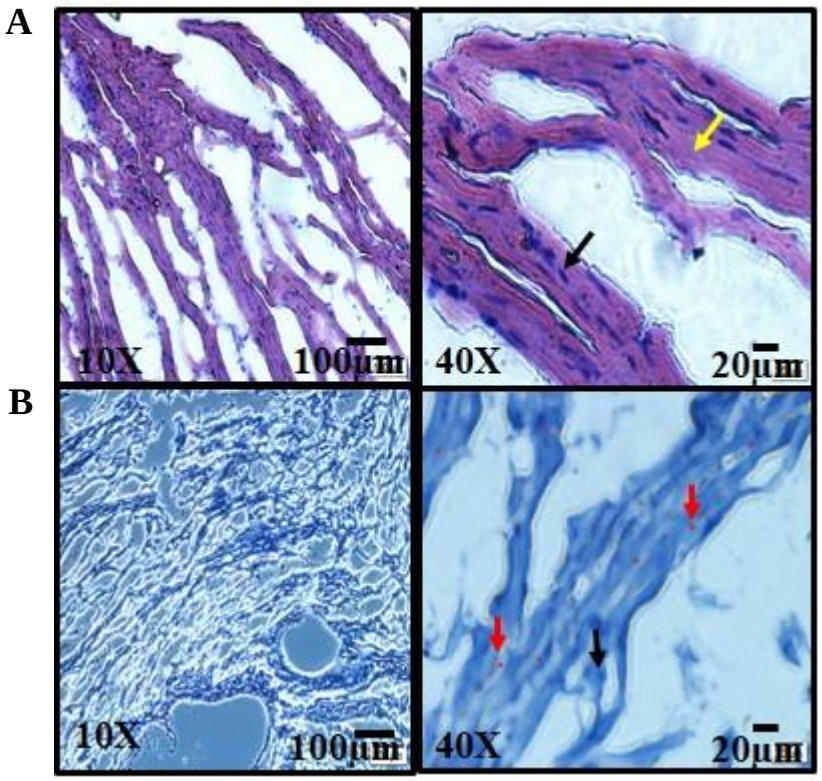

Figure 3.2 Histological section of heart tissues of rat model under HFDSham

(A) H&E stain of nuclei appear as blue (black arrow) and the cytoplasm and cell membrane emerge as red-pink colour (yellow arrow). (B) Under oil red O stain, the heart tissues of HFDSham the nuclei become blue (black arrow) and lipid droplets are stained in red colour (red arrow). The scale bar represents 100µm at X10 magnification and 20µm at X40 magnification.

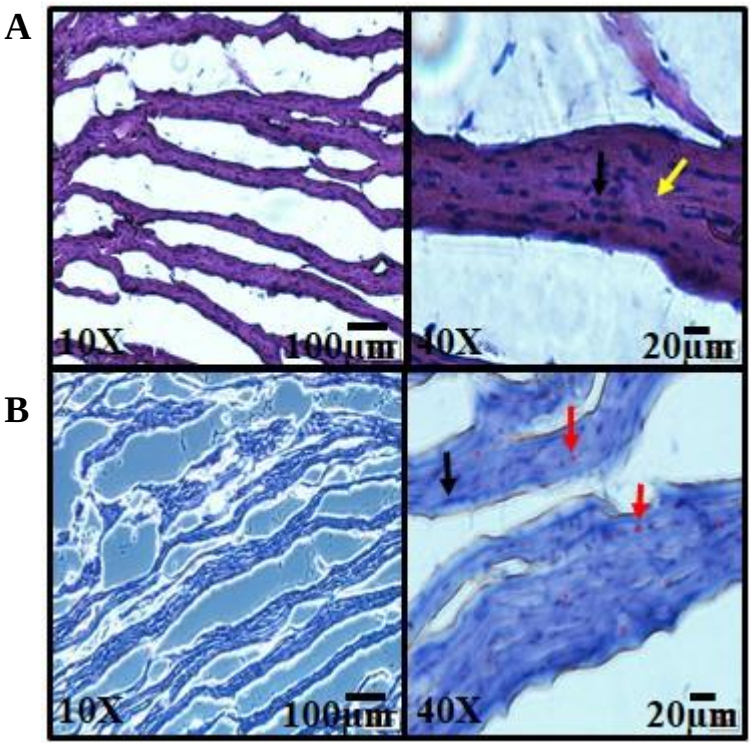

Figure 3.3 Histological section of heart tissues of rat model under WDAC

(A) H&E stain of nuclei appear as blue (black arrow) and the cytoplasm and cell membrane emerge as red-pink colour (yellow arrow). (B) Under oil red O stain, the heart tissues of WDAC the nuclei become blue (black arrow) and lipid droplets are stained in red (red arrow). The scale bar represents 100µm at X10 magnification and 20µm at X40 magnification.

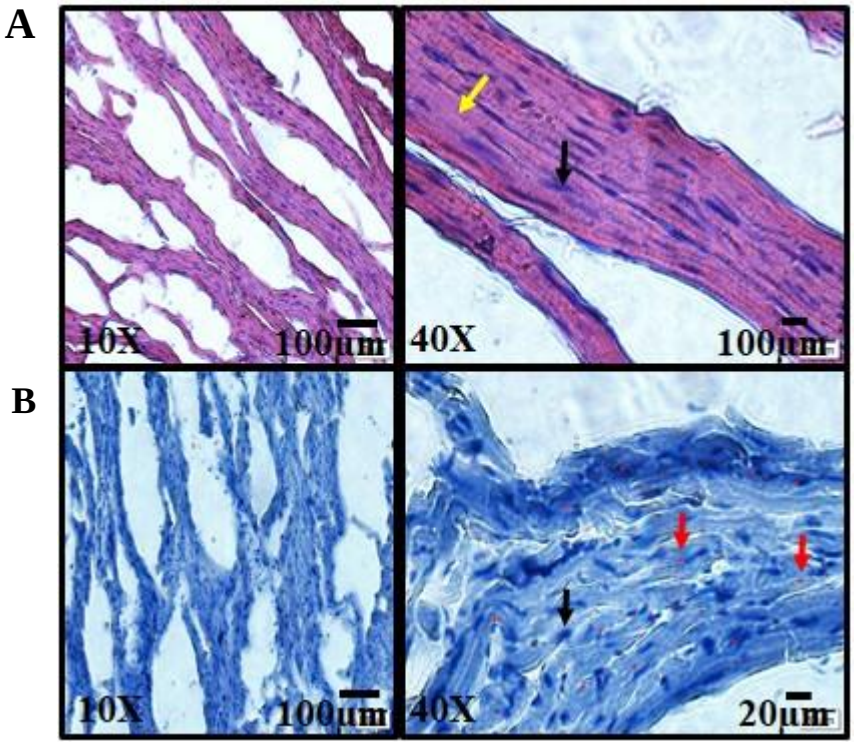

Figure 3.4 Histological section of heart tissues of rat model under WDSham

(A) H&E stain of nuclei appear as blue (black arrow) and the cytoplasm and cell membrane emerge as red-pink colour (yellow arrow). (B) Under oil red O stain, the heart tissues of WDSham the nuclei become blue (black arrow) and lipid droplets are staied in red (red arrow). The scale bar represents 100µm at X10 magnification and 20µm at X40 magnification.

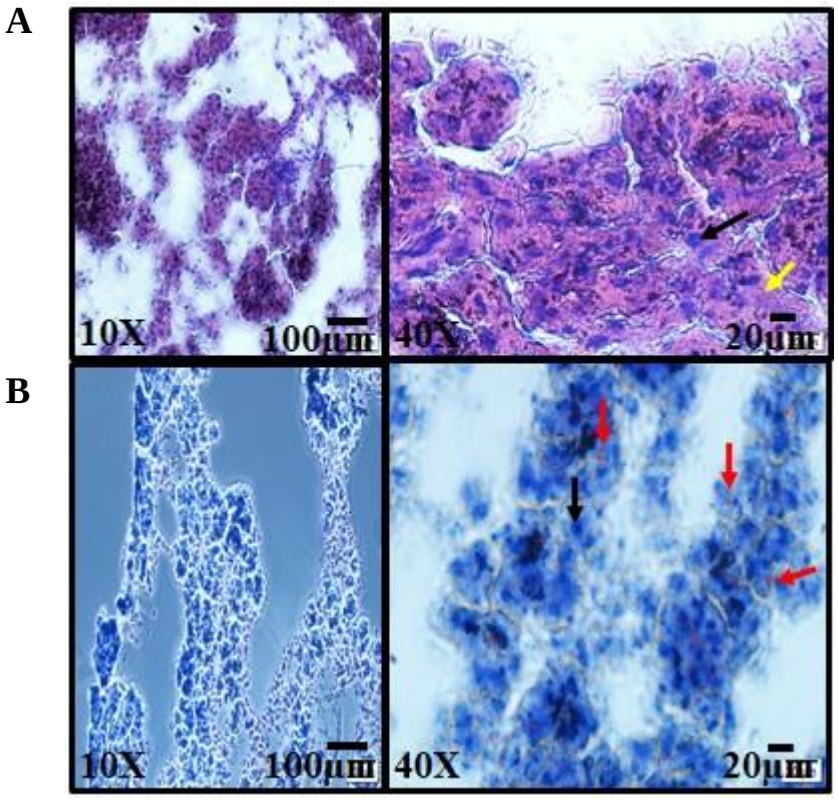

Figure 3.5 Histological section of liver tissues of rat model under HFDAC

(A) H&E stain of nuclei appear as blue (black arrow) and the cytoplasm and cell membrane emerge as red-pink colour (yellow arrow). (B) Under oil red O stain, the liver tissues of HFDAC the nuclei become blue (black arrow) and lipid droplets are stained in red (red arrow). The scale bar represents 100µm at X10 magnification and 20µm at X40 magnification.

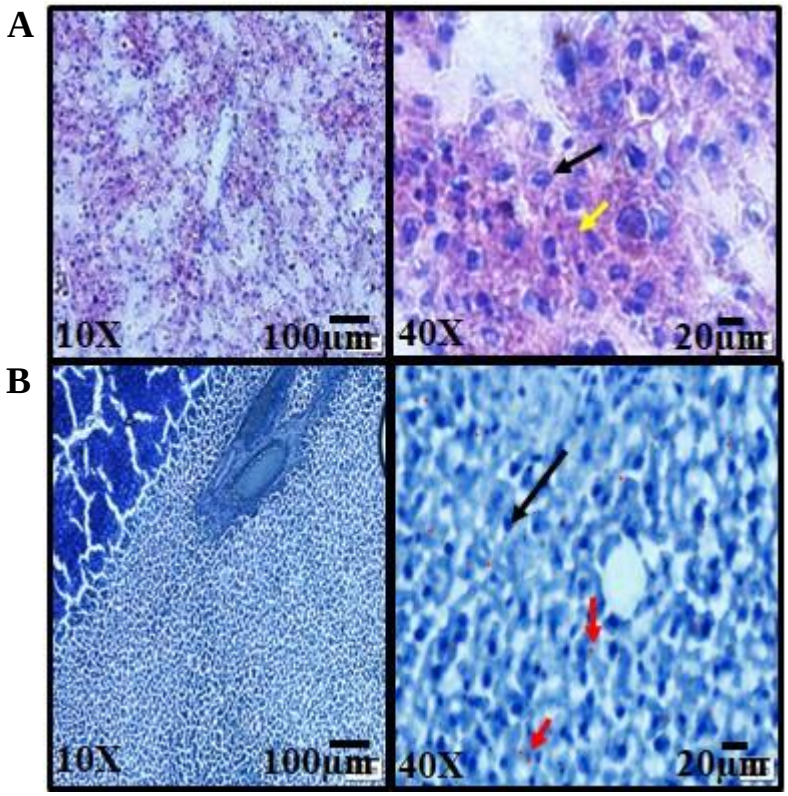

Figure 3.6 Histological section of liver tissues of rat model under HFDSham

(A) H&E stain of nuclei appear as blue (black arrow) and the cytoplasm and cell membrane emerge as red-pink colour (yellow arrow). (B) Under oil red O stain, the liver tissues of HFDSham the nuclei become blue (black arrow) and lipid droplets are stained in red (red arrow). The scale bar represents 100µm at X10 magnification and 20µm at X40 magnification.

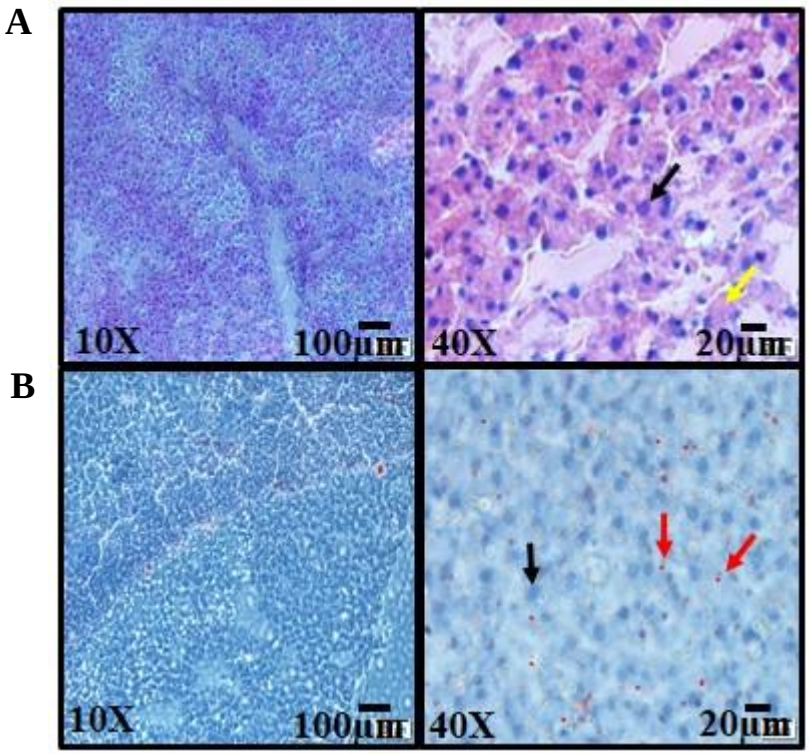

Figure 3.7 Histological section of liver tissues of rat model under WDAC

(A) H&E stain of nuclei appear as blue (black arrow) and the cytoplasm and cell membrane emerge as red-pink colour (yellow arrow). (B) Under oil red O stain, the liver tissues of WDAC the nuclei become blue (black arrow) and lipid droplets are stained in red (red arrow). The scale bar represents 100µm at X10 magnification and 20µm at X40 magnification.

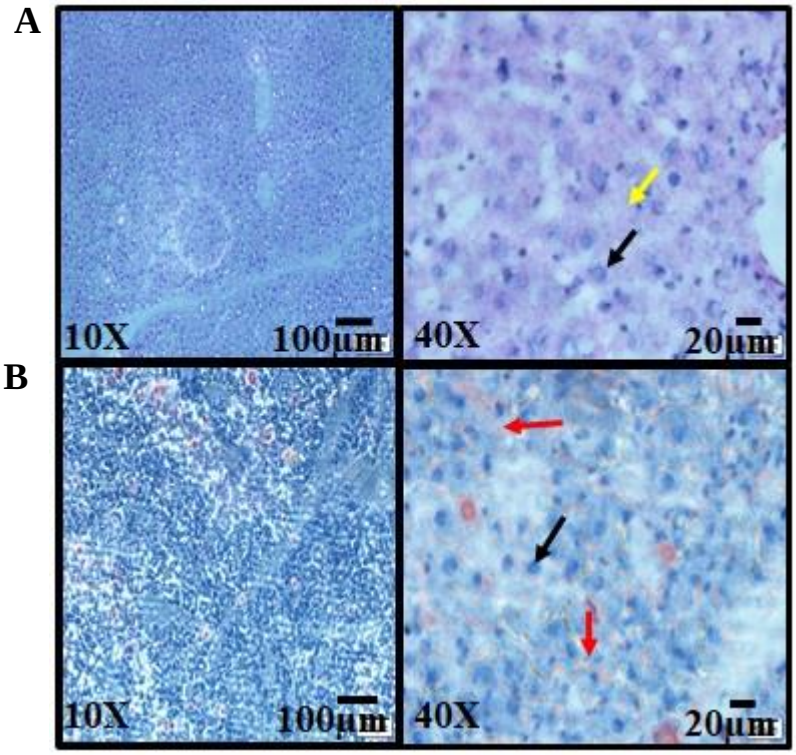

Figure 3.8 Histological section of liver tissues of rat model under WDSham

(A) H&E stain of nuclei appear as blue (black arrow) and the cytoplasm and cell membrane emerge as red-pink colour (yellow arrow). (B) Under oil red O stain, the liver tissues of WDSham the nuclei become blue (black arrow) and lipid droplets are stained in red (red arrow). The scale bar represents 100µm at X10 magnification and 20µm at X40 magnification.

The histological sections of rat liver tissues under H&E nuclei appeared as blue coloured whereas cell membrane and cytoplasm emerged as a red-pink colour in HFAC (Figure 3.5A), HFSham (Figure3.6A), WDAC (Figure 3.7A) and WDSham (Figure 3.8A). The H&E stain results of liver tissues suggested that there were no pathological changes in both dietary and surgical conditions of rat models. Under Oil red O staining, microscopic images suggested that the lipids were accumulated in the form of lipid droplets in the liver tissues of rat models; HFAC (Figure3.5B), HFSham (figure3.6B), WDAC (Figure3.7B) and WDSham (Figure3.8B).

3.5 Discussion

LDs are noticeable features of cardiac myocytes and hepatocytes.[39-42] LDs play a critically important role in coronary artery disease. The accumulation of cholesterol esters within LDs are one of the leading causes of formation of atherosclerotic plaque formation. [43, 44] The lipid composition of LDs influences the signalling and metabolism mechanisms, which ultimately hampers the liver function and promotes liver diseases.[42] An emerging hypothesis is that over-accumulation of lipids in the LDs causes lipotoxicity and this may trigger metabolic diseases.[45, 46]Many studies in animal models have provided mechanisms by which lipid accumulation is associated with cardiac and hepatic dysfunctions.[47-49] However, it is not clear which types of dietary fats accumulation in LDs cause cardiac and hepatic diseases.

The main aim of this study was to investigate the dietary effects of lipids accumulation in the rat heart and liver tissues. The heart and liver tissues were obtained from WD and HF diets model rats after nine weeks of feeding using Sham and AC surgery methods (described in Chapter 2). WD and HF diets have been linked with weight gain, increased

adiposity, cardiac and hepatic diseases.[49-52] The WD and HF diets contain fats 45% and 65%, respectively from different sources such as soybean oil, coconut oil, lard and vegetable shortening.[49] Lard and vegetable shortening contain rich saturated fatty acids and monounsaturated fatty acids causing metabolic changes effectively in heart and liver.[49, 52, 53]

The microscopic images under Oil Red O stain of heart from HFD (Figure 3.1B-3.2B) and WD (Figure 3.3B-3.4B) groups and liver from HFD (Figure 3.5B-3.6B) and WD (Figure 3.7B-3.8B) showed red structure in the cytoplasm evidencing lipid accumulation as lipid droplets. Howener, there was no significant difference in the lipid density of staining from either Sham or AC WD/HF groups. These observations are consistent with the results of Crescenzo *et al*. (2014), where rats were fed WD and HF diet. These results clearly demonstrated that the effects of dietary fat fed to adult rats, in the proportions of the WD, are similar to those induced by the HF diet. [54, 55]

In conclusion, the experimental diets, WD and HF, showed that there were no significant changes in lipid density levels in heart as well as liver tissues in either Sham and AC surgical conditions. These microscopic images suggest that the lipid compositions and their accumulation in LDs under WD and HF diets may be similar. However, it requires further investigations to understand the lipid compositions of WD and HF diets and their metabolic effects on the heart and liver.

3.6 References

1. R. Altmann, *Die Elementarorganismen und ihre Beziehungen zu den Zellen*, Veit & comp, Leipzig, 1890.
2. E. Wilson, *The Cell in Development and Inheritance* Macmillan, New York, 1896.
3. Q. Gao and J. M. Goodman, *Frontiers in cell and developmental biology*, 2015, **3**, 49.
4. R. Bartz, W. H. Li, B. Venables, J. K. Zehmer, M. R. Roth, R. Welti, R. G. Anderson, P. Liu and K. D. Chapman, *Journal of lipid research*, 2007, **48**, 837-847.
5. S. Xu, X. Zhang and P. Liu, *Biochimica et biophysica acta*, 2017, DOI: 10.1016/j.bbadis.2017.07.019.
6. K. Bersuker and J. A. Olzmann, *Biochimica et biophysica acta*, 2017, **1862**, 1166-1177.
7. V. Choudhary, N. Ojha, A. Golden and W. A. Prinz, *The Journal of cell biology*, 2015, **211**, 261-271.
8. N. Jacquier, V. Choudhary, M. Mari, A. Toulmay, F. Reggiori and R. Schneiter, *Journal of cell science*, 2011, **124**, 2424-2437.
9. A. Kassan, A. Herms, A. Fernandez-Vidal, M. Bosch, N. L. Schieber, B. J. Reddy, A. Fajardo, M. Gelabert-Baldrich, F. Tebar, C. Enrich, S. P. Gross, R. G. Parton and A. Pol, *The Journal of cell biology*, 2013, **203**, 985-1001.
10. D. J. Murphy and J. Vance, *Trends in biochemical sciences*, 1999, **24**, 109-115.
11. M. J. Robenek, N. J. Severs, K. Schlattmann, G. Plenz, K. P. Zimmer, D. Troyer and H. Robenek, *FASEB journal: official publication of the Federation of American Societies for Experimental Biology*, 2004, **18**, 866-868.
12. H. L. Ploegh, *Nature*, 2007, **448**, 435-438.

13. V. Choudhary, N. Jacquier and R. Schneiter, *Communicative & integrative biology*, 2011, **4**, 781-784.

14. S. Cases, S. J. Smith, Y. W. Zheng, H. M. Myers, S. R. Lear, E. Sande, S. Novak, C. Collins, C. B. Welch, A. J. Lusis, S. K. Erickson and R. V. Farese, Jr., *Proceedings of the National Academy of Sciences of the United States of America*, 1998, **95**, 13018-13023.

15. S. Cases, S. J. Stone, P. Zhou, E. Yen, B. Tow, K. D. Lardizabal, T. Voelker and R. V. Farese, Jr., *The Journal of biological chemistry*, 2001, **276**, 38870-38876.

16. K. D. Lardizabal, J. T. Mai, N. W. Wagner, A. Wyrick, T. Voelker and D. J. Hawkins, *The Journal of biological chemistry*, 2001, **276**, 38862-38869.

17. C. L. Yen, S. J. Stone, S. Koliwad, C. Harris and R. V. Farese, Jr., *Journal of lipid research*, 2008, **49**, 2283-2301.

18. D. A. Gross, C. Zhan and D. L. Silver, *Proceedings of the National Academy of Sciences of the United States of America*, 2011, **108**, 19581-19586.

19. A. V. Bulankina, A. Deggerich, D. Wenzel, K. Mutenda, J. G. Wittmann, M. G. Rudolph, K. N. Burger and S. Honing, *The Journal of cell biology*, 2009, **185**, 641-655.

20. F. Wilfling, J. T. Haas, T. C. Walther and R. V. Farese, Jr., *Current opinion in cell biology*, 2014, **29**, 39-45.

21. V. T. Salo, I. Belevich, S. Li, L. Karhinen, H. Vihinen, C. Vigouroux, J. Magre, C. Thiele, M. Holtta-Vuori, E. Jokitalo and E. Ikonen, *The EMBO journal*, 2016, **35**, 2699-2716.

22. H. Wang, M. Becuwe, B. E. Housden, C. Chitraju, A. J. Porras, M. M. Graham, X. N. Liu, A. R. Thiam, D. B. Savage, A. K. Agarwal, A. Garg, M. J. Olarte, Q. Lin, F. Frohlich, H. K. Hannibal-Bach, S. Upadhyayula, N. Perrimon, T. Kirchhausen, C. S. Ejsing, T. C. Walther and R. V. Farese, *eLife*, 2016, **5**.

23. A. Grippa, L. Buxo, G. Mora, C. Funaya, F. Z. Idrissi, F. Mancuso, R. Gomez, J. Muntanya, E. Sabido and P. Carvalho, *The Journal of cell biology*, 2015, **211**, 829-844.

24. F. Wilfling, H. Wang, J. T. Haas, N. Krahmer, T. J. Gould, A. Uchida, J. X. Cheng, M. Graham, R. Christiano, F. Frohlich, X. Liu, K. K. Buhman, R. A. Coleman, J. Bewersdorf, R. V. Farese, Jr. and T. C. Walther, *Developmental cell*, 2013, **24**, 384-399.

25. F. Wilfling, A. R. Thiam, M. J. Olarte, J. Wang, R. Beck, T. J. Gould, E. S. Allgeyer, F. Pincet, J. Bewersdorf, R. V. Farese, Jr. and T. C. Walther, *eLife*, 2014, **3**, e01607.

26. N. Kory, R. V. Farese, Jr. and T. C. Walther, *Trends in cell biology*, 2016, **26**, 535-546.

27. I. J. Goldberg, C. M. Trent and P. C. Schulze, *Cell metabolism*, 2012, **15**, 805-812.

28. T. Osumi and K. Kuramoto, *Experimental cell research*, 2016, **340**, 198-204.

29. L. Liu, X. Shi, K. G. Bharadwaj, S. Ikeda, H. Yamashita, H. Yagyu, J. E. Schaffer, Y. H. Yu and I. J. Goldberg, *The Journal of biological chemistry*, 2009, **284**, 36312-36323.

30. S. Tiwari and S. A. Siddiqi, *Arteriosclerosis, thrombosis, and vascular biology*, 2012, **32**, 1079-1086.

31. R. A. Coleman and D. G. Mashek, *Chemical reviews*, 2011, **111**, 6359-6386.

32. R. Singh, S. Kaushik, Y. Wang, Y. Xiang, I. Novak, M. Komatsu, K. Tanaka, A. M. Cuervo and M. J. Czaja, *Nature*, 2009, **458**, 1131-1135.

33. B. Schroeder, R. J. Schulze, S. G. Weller, A. C. Sletten, C. A. Casey and M. A. McNiven, *Hepatology (Baltimore, Md.)*, 2015, **61**, 1896-1907.

34. N. L. Gluchowski, M. Becuwe, T. C. Walther and R. V. Farese, Jr., *Nature reviews. Gastroenterology & hepatology*, 2017, **14**, 343-355.

35. Y. Ikura and S. H. Caldwell, *International journal of clinical and experimental pathology*, 2015, **8**, 8699-8708.

36. M. J. Andres-Manzano, V. Andres and B. Dorado, *Methods Mol Biol*, 2015, **1339**, 85-99.

37. C. Masserdotti, U. Bonfanti, D. De Lorenzi and N. Ottolini, *Veterinary clinical pathology*, 2006, **35**, 37-41.

38. A. H. Fischer, K. A. Jacobson, J. Rose and R. Zeller, *CSH Protoc*, 2008, **2008**, pdb prot4986.

39. S. Sharma, J. V. Adrogue, L. Golfman, I. Uray, J. Lemm, K. Youker, G. P. Noon, O. H. Frazier and H. Taegtmeyer, *FASEB journal: official publication of the Federation of American Societies for Experimental Biology*, 2004, **18**, 1692-1700.

40. C. Christoffersen, E. Bollano, M. L. Lindegaard, E. D. Bartels, J. P. Goetze, C. B. Andersen and L. B. Nielsen, *Endocrinology*, 2003, **144**, 3483-3490.

41. H. Wang, A. D. Quiroga and R. Lehner, *Methods Cell Biol*, 2013, **116**, 107-127.

42. D. G. Mashek, S. A. Khan, A. Sathyanarayan, J. M. Ploeger and M. P. Franklin, *Hepatology (Baltimore, Md.)*, 2015, **62**, 964-967.

43. R. P. Choudhury, J. M. Lee and D. R. Greaves, *Nature clinical practice. Cardiovascular medicine*, 2005, **2**, 309-315.

44. G. Larigauderie, C. Cuaz-Perolin, A. B. Younes, C. Furman, C. Lasselin, C. Copin, M. Jaye, J. C. Fruchart and M. Rouis, *FEBS J*, 2006, **273**, 3498-3510.

45. J. M. Weinberg, *Kidney Int*, 2006, **70**, 1560-1566.

46. J. Kusunoki, A. Kanatani and D. E. Moller, *Endocrine*, 2006, **29**, 91-100.

47. H. Bugger and E. D. Abel, *Cardiovasc Res*, 2010, **88**, 229-240.

48. A. R. Wende and E. D. Abel, *Biochimica et biophysica acta*, 2010, **1801**, 311-319.

49. L. Ramalho, M. N. da Jornada, L. C. Antunes and M. P. Hidalgo, *Nutr Diabetes*, 2017, **7**, e245.

50. R. A. Stewart, L. Wallentin, J. Benatar, N. Danchin, E. Hagstrom, C. Held, S. Husted, E. Lonn, A. Stebbins, K. Chiswell, O. Vedin, D. Watson and H. D. White, *European heart journal*, 2016, **37**, 1993-2001.

51. P. Mirmiran, Z. Amirhamidi, H. S. Ejtahed, Z. Bahadoran and F. Azizi, *Iran J Public Health*, 2017, **46**, 1007-1017.

52. H. M. Dashti, T. C. Mathew, T. Hussein, S. K. Asfar, A. Behbahani, M. A. Khoursheed, H. M. Al-Sayer, Y. Y. Bo-Abbas and N. S. Al-Zaid, *Exp Clin Cardiol*, 2004, **9**, 200-205.

53. E. D. Abel, *Nat Med*, 2011, **17**, 1045-1046.

54. R. Crescenzo, F. Bianco, P. Coppola, A. Mazzoli, M. Tussellino, R. Carotenuto, G. Liverini and S. Iossa, *Exp Physiol*, 2014, **99**, 1203-1213.

55. J. Kunes, *Exp Physiol*, 2014, **99**, 1180-1181.

Chapter 4

Effect of fatty diet on lipid composition in heart and liver tissues

4.1 Introduction

Problems associated with being overweight and obese have increased over the past few decades.[1-3] Being overweight is one of the primary risk factors for metabolic diseases, such as fatty liver disease and cardiovascular disease. This results in major health problems in society.[4, 5] The mechanisms linking fatty diet to lipid metabolism occurring in hepatic and cardiac diseases are not completely understood.[1, 3, 4] Recently established lipidomics methods show that the lipidome is extremely complex.[6] Therefore, it is important to know which lipid metabolites contribute to disease progression. The objective of this study was to define changes in cardiac and hepatic lipid composition caused by fatty diets and then model heart and liver disease to identify changes associated with disease progression. The aim is to identify lipid biomarkers associated with a fatty diet that may be relevant in pathophysiology, diagnosis, and therapy.

Adipose tissues (fatty connective tissues) have a significant role in nutrient homeostasis, including calorie storage and a reservoir of free fatty acids when hungry.[1] The new attention given to dietary fat has transpired as a result of the many diseases related to dietary fat intake, such as heart attack, stroke and plaque formation.[7] Many studies suggest that lipid accumulation in the liver causes several hepatic diseases.[8-13] It is established that the liver plays a key role in various aspects of lipid metabolism within many types of lipids.[14-17] Numerous transformed lipid types comprise lipid groups that are biologically dynamic and disturb signaling pathways of insulin, cell injury, lipogenesis, and pathways of cellular repair.[18]

4.1.1 Magic angle spinning solid state NMR

Magic-angle spinning (MAS) ^{1}H NMR spectroscopy is one of the best techniques for examining the metabolic composition of whole tissues of any organ. This technique is capable of analysing the lipid metabolites without damaging the tissues, at a resolution approaching that of lipid extracts and liquid state.[7-10] Hence, it has been used extensively to study metabolic changes in diseased cells and tissues.[19-21]

In solution NMR, the liquid molecules tumble rapidly in isotropic motions (Figure 4.1A) resulting in averaging out the orientation of nuclear magnetic interactions, detecting only the isotropic component. Thus, the spectra of solution NMR appear as sharp peaks. In contrast, the solid-phase samples do not undergo unrestricted isotropic molecular motions. Hence the NMR spectra shows broad lines. These broad line spectra are known as “powder patterns” (Figure 4.1C). In other words, the frequency and intensity profiles reflect the orientation-dependent (Figure 4.1B) interactions between molecules in the sample.[22] In a solid powder sample molecules have all possible orientations. More precisely the broadness of the NMR spectrum of solid samples or powder is due to the chemical shift of each molecule being different.[23]

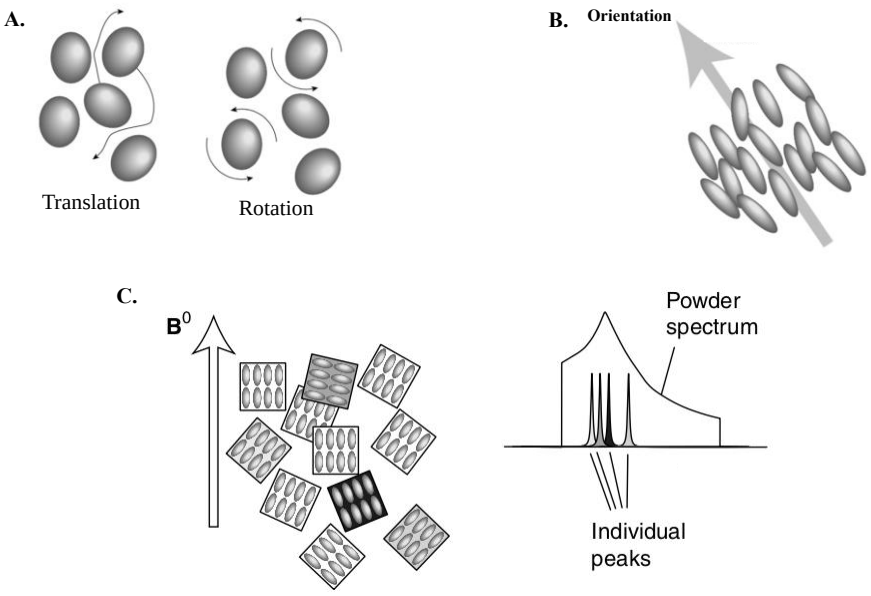

Figure 4.1 Schematic diagram of isotropic and anisotropic molecular motion and powder pattern spectrum[23]

(A) Liquid molecules possess both translational and rotational motion in all directions and due to fast tumbling between molecules generate sharp peaks of NMR spectrum. (B) Solid molecules do not possess rotational and translational motion but they arrange compactly in an orientation- dependent manner. (C) The broad pattern comes from the superposition of many sharp peaks with different frequencies, each one coming from each molecule with a different orientation.[24, 25]

In solid powder samples there is chemical shift anisotropy and dipolar couplings are high. Therefore, solid molecules generate broad NMR spectral line widths [23-26] (Figure 4.2Da). This issue was finally resolved by I. J. Lowe and E. R. Andrew. They packed the solid sample into a rotor (made up of zirconia or silicon nitride), capped (Figure 4.2C) and then placed at an angle 54.74° relative to the external magnetic field and spun at high speed (Figure 4.2B). Spinning the sample suppresses the anisotropic dipolar interactions of solid nuclei and placing the sample at 54.74° to the external magnetic field generates average orientation around the x, y and z planes [23-26] as shown in figure 4.2A. This average orientation angle (54.74°) is commonly known as the magic angle. At this magic angle, the anisotropic nature of solid samples produces NMR sidebands (Figure 4.2Db) and

these bands gradually disappear after spinning the sample at high speed (500 Hz to 67 kHz, depending upon experiment types). Finally, the NMR spectrum resides into thin lines at the isotropic shifts and produces a high-resolution spectrum of solid sample [26] as shown in figure 4.2Dc.

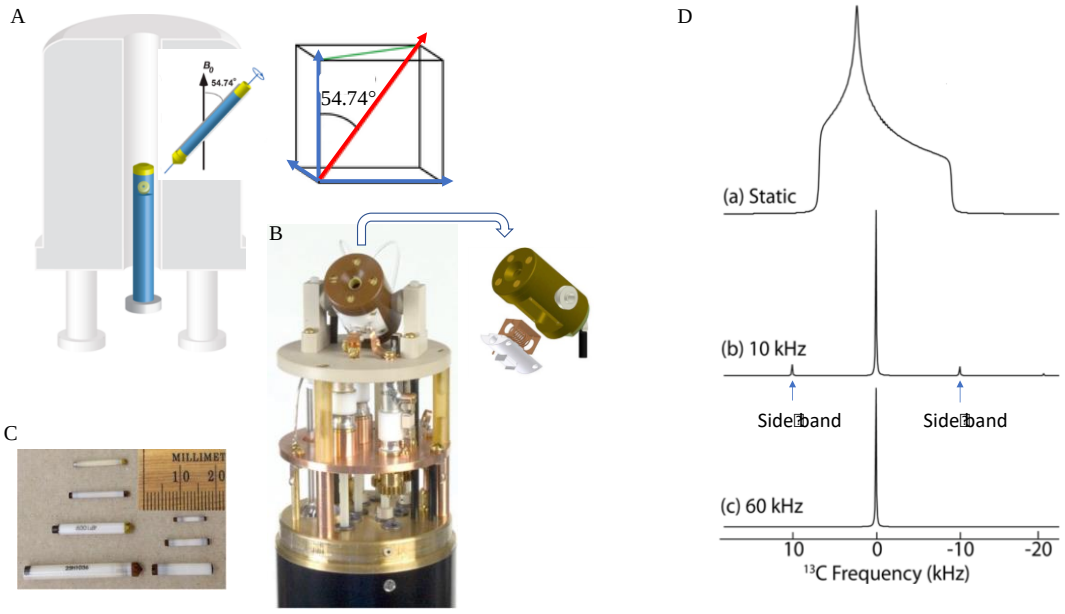

Figure 4.2 Schematic representation of MAS NMR.

(A) The sample is placed into an NMR probe at the "magic" angle of 54.74° (B) Magic angle spinning probe (C) Rotor with caps (D(a)) Broad powder pattern ^{13}C NMR of a static sample (D(b)) spinning sidebands appear at low spinning speed (10kHz) (D(c)),side bands disappear at high spinning speed (60kHz) and are averaged out into an isotropic peak.[26]

4.2 Aims

To investigate the changes in lipid compositions under as a result of specific diets in rat heart and liver tissues using solid state ^{1}H NMR. The NMR massive data will be analysed by PCA software to obtain a clear view in variables effecting the data. This will show the effect of lipids composition from different diets on rat hearts and liver tissues.

4.3 Materials and methods

Adult male Sprague Dawely rats (220-250 gm, Charles River Inc.,Kent, UK) were maintained on diets containing 61.6% fat and 20.3% sucrose (high-fat diet, HFD); or 45% fat and 15% sucrose (Western diet, WD), 48 hours post-surgery, as described in Chapter 2 section 2.1, generating four experimental groups:

- High-fat diet + Sham (HFDSham).
- Western diet + Sham (WDSham).
- High-fat diet + Aortic Constriction (HFDAC).
- Western diet + Aortic Constriction (WDAC).

After nine weeks, animals were anaesthetised, hearts and livers were harvested, rinsed, freeze-clamped and processed as described in chapter 2 section 2.1.

The ^{1}H HR-MAS NMR experiments on intact heart and liver tissue of the left lobe excised from rats were performed on a Bruker Avance II spectrometer operating at a frequency of 500.1025 MHz (^{1}H). The adult male Sprague Dawley rats were subjected to aortic constriction (AC; induced cardiac hypertrophy and heart failure) or Sham (placebo) surgical methods. Then the rats were fed either Western or high fat diet for nine weeks (detailed explanation in Chapter 2 section 2.1). ^{1}H MAS NMR experiments were performed on a Bruker 500 MHz (11.7 tesla) and a 4.0 mm MAS probe from Bruker was

used. About 30-40 mg heart or liver tissue was packed between Kellogg-fluoropolymer (Kel-F)/polychlorotrifluoroethylene plugs to prevent fluid leakage in the zirconium oxide 4mm diameter MAS rotor from Bruker. The sample spinning rate used was about 8 kHz at 278K. A standard Topspin ZgPr pulse sequence was used for the measurement with a single pulse excitation and 0.5 s low power pre-saturation at the H_2O peak position for H_2O suppression. The acquisition time was 1 sec and the recycle delay time was 1 sec, resulting in a total length of the pulse sequence of about 2.5 sec. Each spectrum was acquired with a total of 256 accumulations in about 10 min 30 sec. A detailed explanation is discussed in Chapter 2 section 2.2.4.

The data from solid state NMR spectra were analysed by PCA statistical tool described in Chapter 2 section 2.2.6.

4.4 Results

4.4.1 ^{1}H MAS SS NMR spectra of rat heart and liver tissue

The spectra were referenced to the lipid CH_3 at 0.9ppm in each spectrum and peaks were assigned based on prior published results. [27-33]

The ^{1}H MAS NMR spectra of intact heart tissues (Figure 4.3) and the intensities of peak 3 (Lipids/triglyceride $(CH_2)_n$) and peak 22 (triglyceride –CH-O-COR) were different among all four experiment groups (WDAC, WDSham, HFDAC and HFDSham). The intensities of peak 23 (Lipids -CH=CH-) were weak in HFDAC samples. The peak 20 (α-Glucose) was visible in the spectra of WDAC, HFDSham and HFDAC samples. The intensity of peak 19 (Esterified cholesterol 3-CHOH) was found only in HFD samples. The peak 6 (Leucine) was not found in WDSham samples. The peak 5 (Lipids CH_2CH_2CO) was appeared only in WD samples. The peak 1 (Lipids/Triglyceride CH_3), 4 (Alanin β-CH_3), 7 (Lipids CH=CH-CH_2), 8 (Lipids CH_2-CH_2-CO), 9 (Glutamate CH_2), 10 (Lipids CH=CH-CH_2),11(Creatine),12 (Choline/Phosphocholine/Phosphothanolamine/ Glycerophosphocholin) , 13 (Glucose/Taurine –CH_2NH_2), 14 (Phosphocholine), 15 (Alanine), 16 (Creatine) and 17 (Triglyceride –CH-O-COR) were found with the same intensities in all samples.

^{1}H MAS NMR spectra of intact liver tissues (Figure 4.4) and the intensities of peaks **8** (Choline/Phosphocholine), **9** (Taurine), **10** (Cholesterol 3-CHOH), **11** (Phosphocholine NCH_3), **12** (Glucose/glycogen), **16** (β-Glucose C_1H), and **21** (Glycogen) were higher in WD samples than HFD samples. The intensities of peaks **1** (Cholesterol/esters -CH_3), **2** (Lipids/Triglyceride CH_3), **3** (Lipids $(CH_2)_n$), **4** (Lipids β-CH_2), **5** (Lipids -CH_2–CH=), **6** (Lipids α-CH_2), **7** (Lipids =CH- CH_2–CH=), **13** (Cholin CH_2(OH)), **14** (Phosphocholine

PO_3CH_2), **15** (Triglyceride), 1**9** (α-Glucose C_1H) and **20** (Lipids –CH=CH) were appeared the same in all group samples.

The spectra suggest that lipids and other components (proteins and carbohydrates etc.) in the heart and liver tissues were almost similar. However, there are variations in some metabolites peak intensities - in heart samples the lipid groups, such as (i) -CH=CH- at 5.32ppm were weak in tissues of HFD samples under aortic constriction condition, (ii) $CH_2)_n$ at 1.27-1.38ppm and –CH-O-COR at 5.25-5.28ppm were asymmetrical among WD and HFD samples obtained either from aortic constriction or placebo surgical methods, (iii) -CHOH at 4.75ppm appeared only in aortic constriction or placebo HFD heart tissue samples and (iv) CH_2CH_2CO at 1.62ppm was found in WD aortic constriction or placebo samples. The non-lipid metabolites peak intensities of heart tissues, such as leucine at 1.75ppm and α-glucose at 4.85ppm were not found in the WD samples under placebo surgical condition. In liver samples, the peak intensities of lipid groups at 3.21-3.3ppm choline/phosphocholine, at 3.53ppm -CHOH and at 3.6ppm NCH_3 were higher in WD than HFD samples under both aortic constriction and placebo surgical conditions. The peak intensities of non-lipid groups of liver samples at 3.42ppm taurine, 3.7-3.95ppm glucose/glycogen, 4.65ppm β-glucose C1H, and 5.41glycogen were also higher in WD than HFD samples under both aortic constriction and placebo conditions. These findings reveal that these significant variations in some metabolites may be related to dietary fat composition and surgery methods.

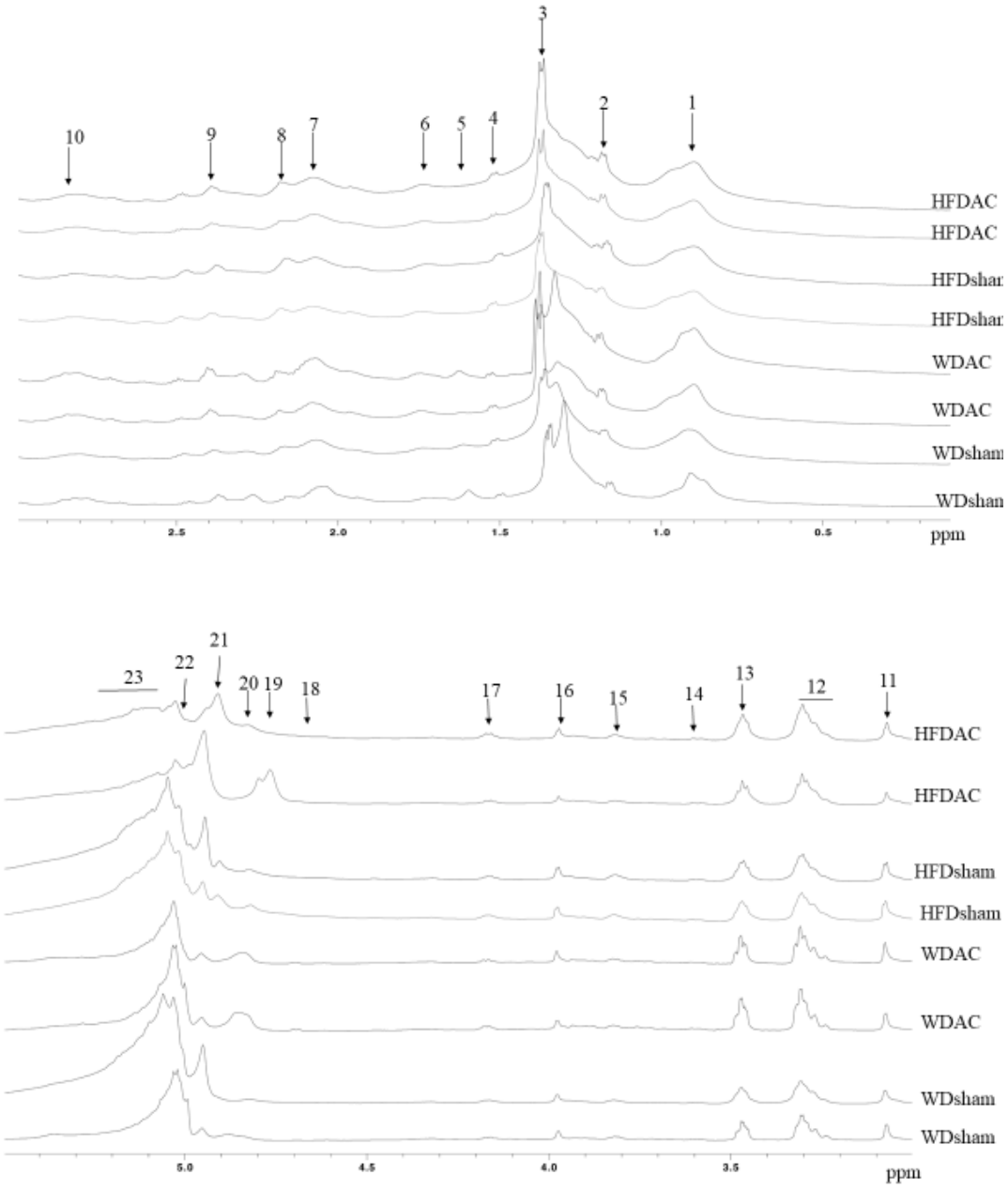

Figure 4.3 ^{1}H MAS SS NMR spectra of rat heart tissue

Where 1 (0.9ppm) Lipids/Triglyceride CH_3; 2 (1.18ppm) Unassingned peak; 3 (1.27-1.38ppm) Lipids/Triglyceride $(CH_2)_n$; 4 (1.52ppm) Alanin β-CH_3; 5 (1.62ppm) Lipids CH_2CH_2CO; 6 (1.75ppm) Leucine; 7 (2.08 ppm) Lipids CH=CH-CH_2; 8 (2.20ppm) Lipids CH_2-CH_2-CO; 9 (2.38ppm) Glutamate CH_2; 10 (2.82ppm) Lipids CH=CH-CH_2; 11(3.07ppm)Creatine;12(3.21-3.27ppm) Choline/Phosphocholine/Phosphothanolamine/Glycerophosphocholin;13(3.42ppm) Glucose/Taurine –CH_2NH_2; 14 (3.60ppm) Phosphocholine; 15 (3.79ppm) Alanine; 16 (3.95ppm) Creatine; 17 (4.15ppm)Triglyceride –CH-O-COR; 18 (4.65ppm) β-Glucose; 19 (4.75ppm) Esterified cholesterol 3-CHOH; 20 (4.85ppm) α-Glucose; 21 (4.9ppm) Unassigned peak; 22 (5.03ppm) α-Glucose C1H; 22 (5.25-5.28ppm) Triglyceride –CH-O-COR; 23 (5.32ppm) Lipids -CH=CH-.

Table 4.1 List of metabolite peak assignments in the heart tissues

Metabolite	^{1}H chemical shifts
Lipids /Triglyceride CH_3	0.9ppm
Lipids/Triglyceride $(CH_2)_n$	1.27- 1.38ppm
Alanin β-CH_3	1.52ppm
Lipids CH_2CH_2CO	1.62ppm
Leucine	1.75ppm
Lipids CH=CH-CH_2	2.08 ppm
Lipids CH_2-CH_2-CO	2.20ppm
Glutamate CH_2	2.38ppm
Lipids CH=CH-CH_2	2.82ppm
Creatine	3.07ppm
Choline/Phosphocholine/Phosphothanolamine/Glycerophosphocholin	3.21-3.27ppm
Glucose/Taurine –CH_2NH_2	3.42ppm
Phosphocholine	3.60ppm
Alanine	3.79ppm
Creatine	3.95ppm
Triglyceride –CH-O-COR	4.15ppm
β-Glucose	4.65ppm
Esterified cholesterol 3-CHOH	4.75ppm
α-Glucose	4.85ppm
α-GlucoseC1H	5.03ppm
Triglyceride –CH-O-COR	5.25-5.28ppm
Lipids -CH=CH-	5.32ppm
Glycogen	5.41ppm

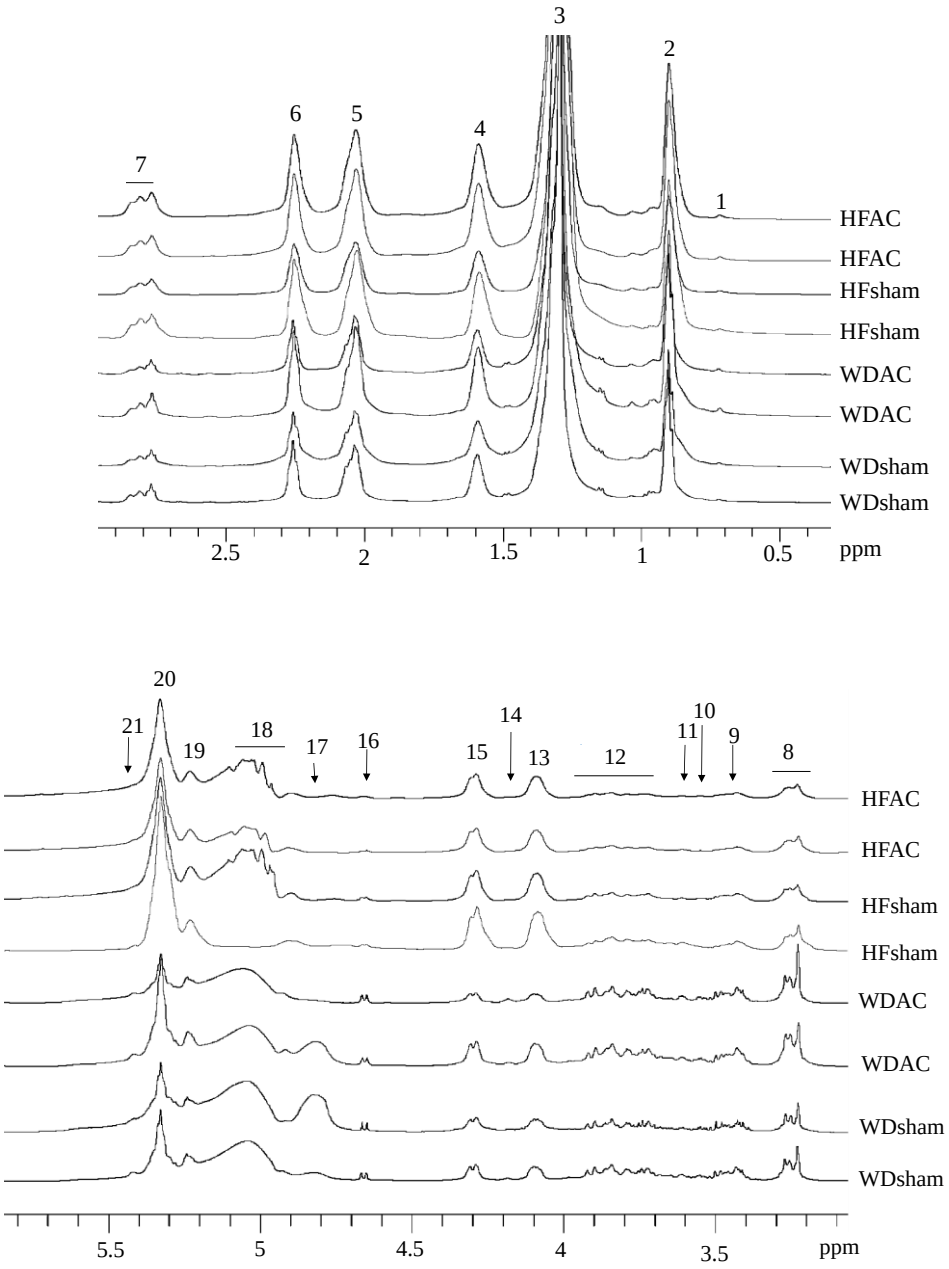

Figure 4.4 ^{1}H MAS SS NMR spectra of intact rat liver tissue.

Where 1 (0.72ppm) Cholesterol/esters -CH_3; 2 (0.9ppm) Lipids/Triglyceride CH_3; 3 (1.29ppm) Lipids $(CH_2)_n$; 4 (1.59 ppm) Lipids β-CH_2; 5 (2.03ppm) Lipids -CH_2–CH=; 6 (2.25 ppm) Lipids α-CH_2; 7 (2.78-2.83 ppm) Lipids =CH-CH_2–CH=; 8 (3.21 -3.3ppm) Choline/Phosphocholine; 9 (3.42ppm) Taurine; 10 (3.53ppm) Cholesterol 3-CHOH; 11 (3.6ppm) Phosphocholine NCH_3; 12 (3.7-3.95ppm) Glucose/glycogen; 13 (4.09ppm) Cholin CH_2(OH); 14 (4.18ppm) Phosphocholine PO_3CH_2; 15 (4.3ppm) Triglyceride; 16 (4.65ppm) β-Glucose C1H; 17 (4.8ppm) Unassigned peak; 18 (4.95-5.19ppm) Unassigned peak; 19 (5.23ppm) α-Glucose C1H; 20 (5.32ppm) Lipids –CH=CH; 21 (5.41ppm) Glycogen.

Table 4.2 List of metabolite peak assignments in the liver tissues

Metabolite	^{1}H chemical shifts
Cholesterol/esters -CH_3	0.72ppm
Lipids/Triglyceride CH_3	0.9ppm
Lipids $(CH_2)_n$	1.29ppm
Lipids β-CH_2	1.59ppm
Lipids -CH_2–CH=	2.03ppm
Lipids α-CH_2	2.25ppm
Lipids = CH-CH_2–CH=	2.78-2.83ppm
Choline/Phosphocholine	3.21 -3.3ppm
Taurine	3.42ppm
Cholesterol 3-CHOH	3.53ppm
Phosphocholine NCH_3	3.6ppm
Glucose/glycogen	3.7-3.95ppm
Cholin CH_2(OH)	4.09ppm
Phosphocholine PO_3CH_2	4.18ppm
Triglyceride	4.3ppm
β-Glucose C1H	4.65ppm
α-Glucose C1H	5.23 ppm
Lipids –CH=CH	5.32ppm
Glycogen	5.41ppm

4.4.2 PCA analysis of ^{1}H MAS SS NMR spectra of intact rat heart and liver tissues

The data from ^{1}H MAS SS NMR spectra of intact rat heart and liver tissues were examined using a multivariate statistical analysis (MVA) approach. Principal components analysis (PCA) is one such MVA method that reduces the data into a small number of variables called principal components (PCs), describing most of the variation in the spectral data. This analysis produces a scores scatter plot (Figures 4.5.1 and 4.6.1) and a loadings scatter plot (Figures 4.5.2and 4.6.2) that show which spectral variable contributes to each PC producing better separation of sample types. The corresponding loadings plots are shown (Figure 4.5.2 and 4.6.2) that best discriminate between samples. The absolute size of the peaks on the loading plots show the data points related to the principal component that can correctly identify the most variable component of the samples. Displaying the ^{1}H NMR spectra of the data variables (Figures 4.5.3 and 4.6.3) is essential. Tracing the variable value from the spectra clearly demonstrates the metabolite peaks (Figure4.5.3 and 4.6.3). This metabolite is then identified from the known ^{1}H chemical shifts of each component in Tables 4.1 and 4.2.

The scores PC1, PC2 are variables derived from the NMR peaks and summarizing the variables. The observation scores of PC1, PC2 are completely independent of each other. PC1 explains the largest variation of the data, followed by PC2. The scatter plot of PC1 vs PC2 displays how the observations are situated with respect to each other. Observations near each other are similar, which means less variation and observation far away from each other are dissimilar, having more variation.

The PCA analysis of heart tissues suggests that there are three different patterns of group between WD and HFD samples (Figure 4.5). In one group, there are four WD samples (WDAC8, WDAC2, WDSham3 and WDSham7). Here, WDSham samples are clearly separated from WDAC samples situated in the IV quadrant. This group suggests that the variation is the highest among other samples and there is also a significant variation between the Sham and AC surgery method conditions in the WD samples of this group. The second group is the cluster of HFD samples. The samples of this group are close to each other and non-overlapping, situated in all quadrants near to the zero point or near to the centre. This cluster shows less variation among the samples of this group and no separation between Sham and AC HFD samples. The third group is a mixture of WD and HFD samples clustering very close to each other or overlapping, situated in the second quadrant. The third group suggests that there is no variation and separation among the samples of this cluster.

The loading scatter plot of heart tissues (Figure 4.6), PC1 on the X axis suggests that variable points 1008-1012 have strong impact, because these variable points are far away from the centre at the zero point of PC1 on the X-axis. The variable point 1010 shows strong effect on the data, causing the highest variation among PC1. In the PC2 on the Y axis, the variable points 1041,1042,1043 and 1013 are far away from the centre at the zero value of PC2 on the Y-axis, causing strong variation impact among PC2. The variable point 1041 shows the strongest variation among PC2 variables because it is far away from other variables on PC2 on the Y-axis. The variable points 1008-1013 correspond to lipids -CH=CH- at (5.32ppm), whereas variable points 1041,1042,1043 correspond to triglyceride –CH-O-COR at (5.25-5.28ppm) of ^{1}H MAS SS NMR (Figure 4.7).

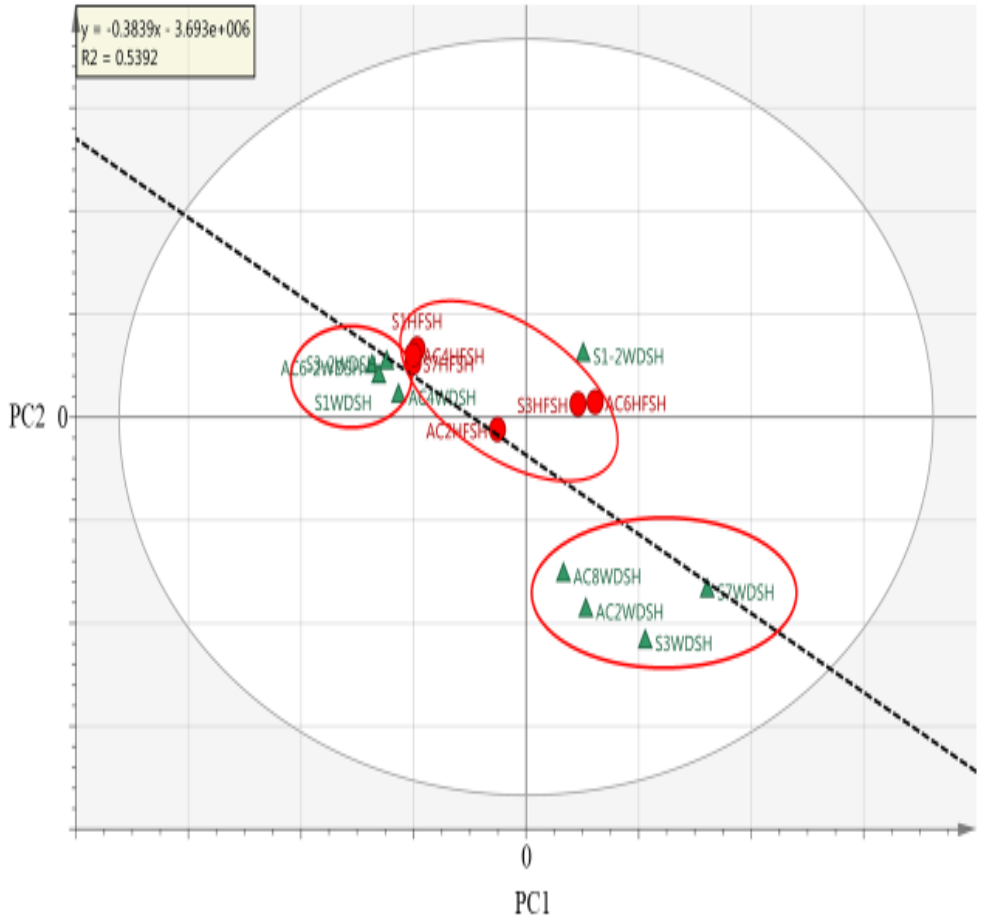

Figure 4.5 Score scatter plot of 1H MAS SS NMR spectra of rat heart tissues.

Where green triangles are WD and red circles are HFD. ACWD: Aortic constriction Western diet; SWD: Sham Western diet; ACHFD: Aortic constriction high fat diet; SHFD: Sham high fat diet. The graph is plotted against PC1 and PC2 which represent the score variation in the object direction.

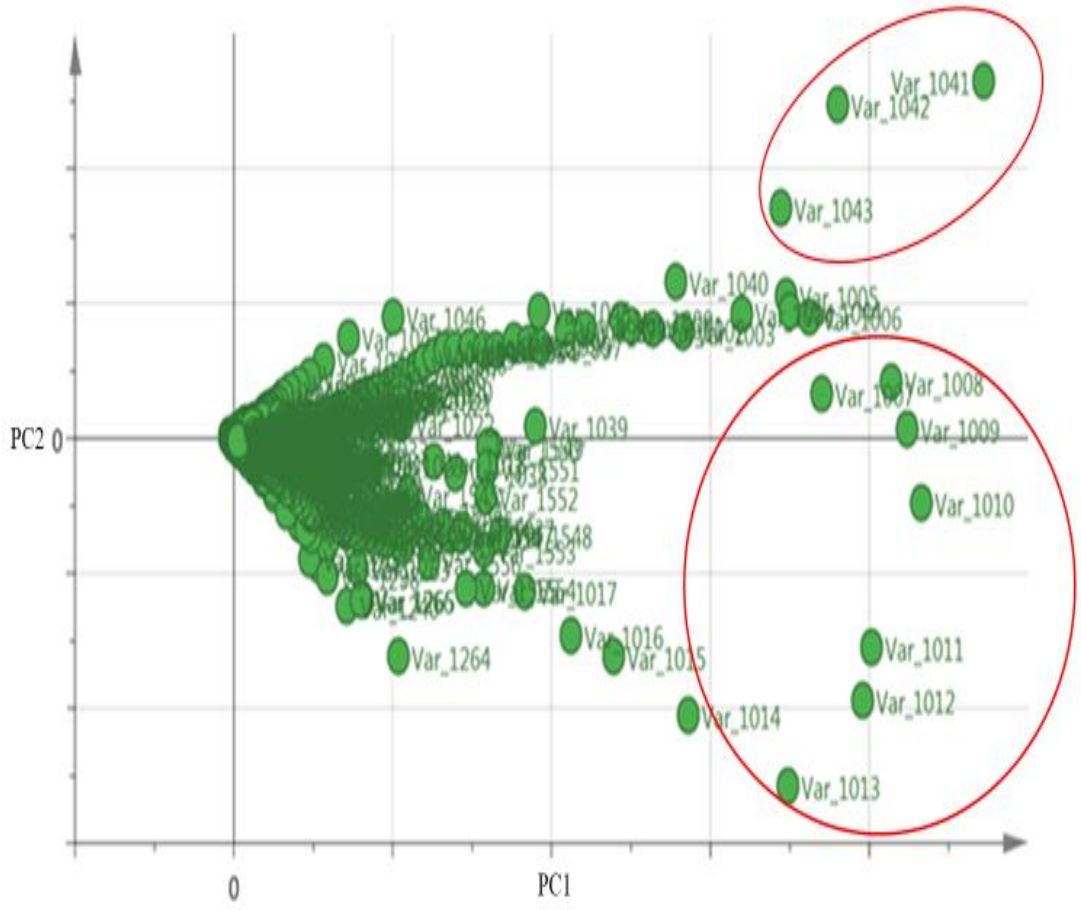

Figure 4.6 Loadings scatter plots of PC1 and PC2 component variables of heart tissues.

Each point is a variable that represents the ^{1}H MAS SS NMR peak intensity from rat heart tissue samples, where, Var: variable point.

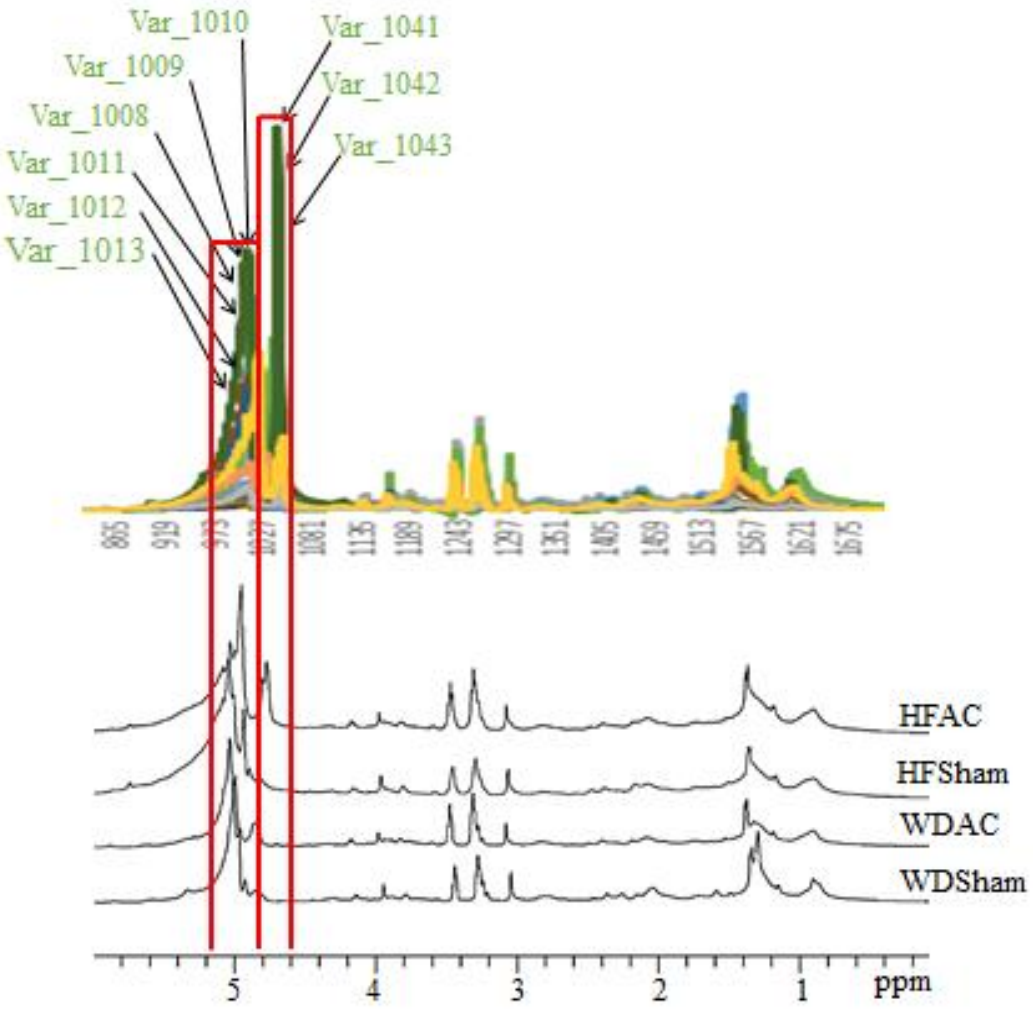

Figure 4.7 ^{1}H MAS SS NMR spectrum of heart tissues corresponding to the variables PCA analysis.

Where variable points 1008-1013 correspond to lipids -CH=CH- at (5.32ppm) and variable points 1041,1042,1043 correspond to triglyceride –CH-O-COR at (5.25-5.28ppm) and ^{1}H MAS SS NMR spectra of rat heart tissues. Red boxes represent the variables and their corresponding chemical shifts.

The PCA analysis of liver tissues suggests that the score scatter plot divides the WD and HFD samples into almost two halves (Figure 4.8). Below the regression line the scores are from WDAC samples, suggesting the variation is the highest among the other samples and significantly separating the WD and HFD samples. The cluster of HFD scores is close to the WDSham scores. Some scores of HFD overlap with WDSham scores and some HFD scores are also non-overlapping. Overlapping scores between HFD and WDSham indicate no variations among the samples, whereas non-overlapping scores suggest significant variation. HFD scores are non-overlapping and clearly separated, suggesting variations among HFD samples.

The loading scatter plot of liver tissues (Figure 4.9), PC1 on the X axis suggests that variable plots 1549, 1550, 1551 and 1552 show strong impact, because these variable points are far away from the centre or zero point on the X axis. However, the variable points from 1545 to 1557 are present between PC1 and PC2 and these variable points are the same as variable points between 1549 to 1552. The variable points from 1545 to 1557 correspond to lipids $(CH_2)_n$ at (1.29ppm) of ^1H MAS SS NMR (Figure 4.10). However, in the PC2 on Y axis the variable points 1608,1416,1415 and 1417 are far away and thus cause strong impact in PC2. The variable point 1608 corresponds to lipids/triglyceride CH_3 at 0.9ppm and variable points 1416,1415 and 1417 correspond to lipids α-CH_2 at 2.25ppm of ^1H MAS SS NMR (Figure 4.10).

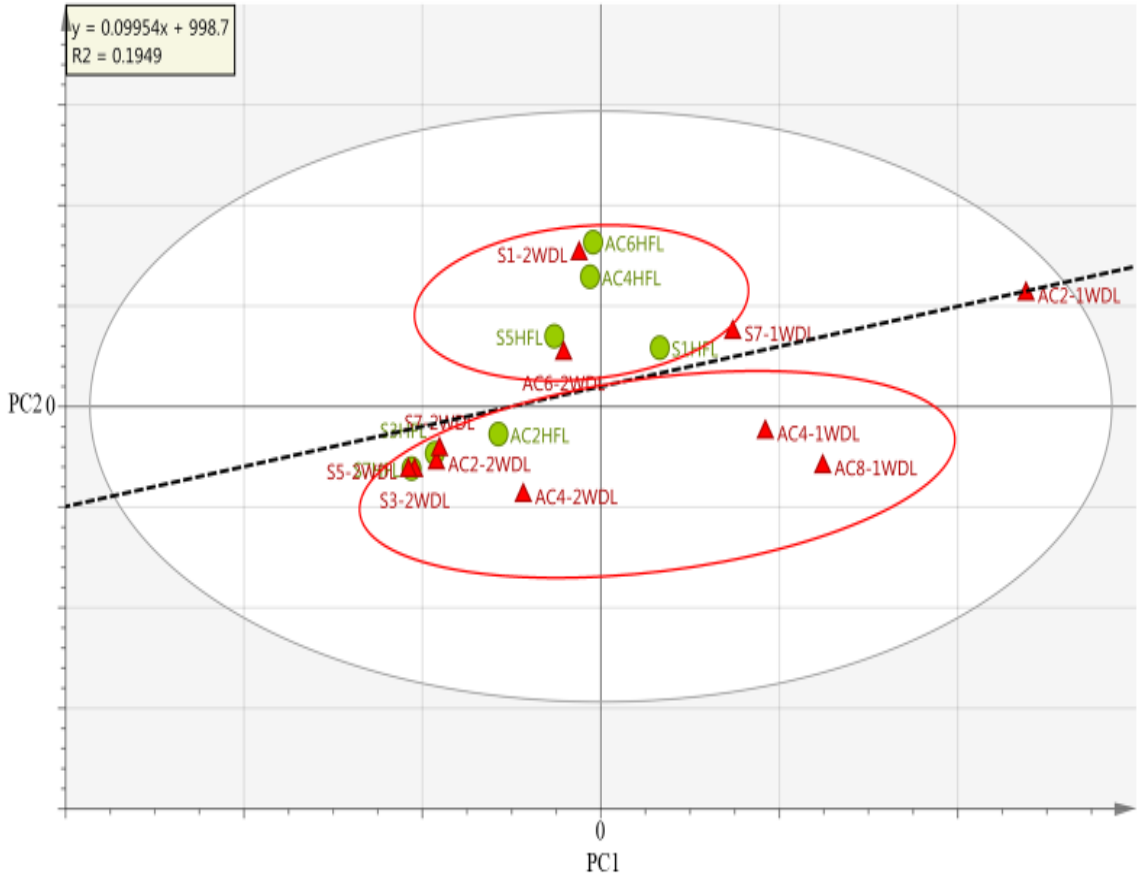

Figure 4.8 Score scatter plot of ^{1}H MAS SS NMR spectra of rat liver tissues

Where, red triangles are WD and green circles are HFD. ACWD: Aortic constriction Western diet; SWD: Sham Western diet; ACHFD: Aortic constriction high fat diet; SHFD: Sham high fat diet. The graph is plotted against PC1 and PC2 which represent the score variation in the object direction.

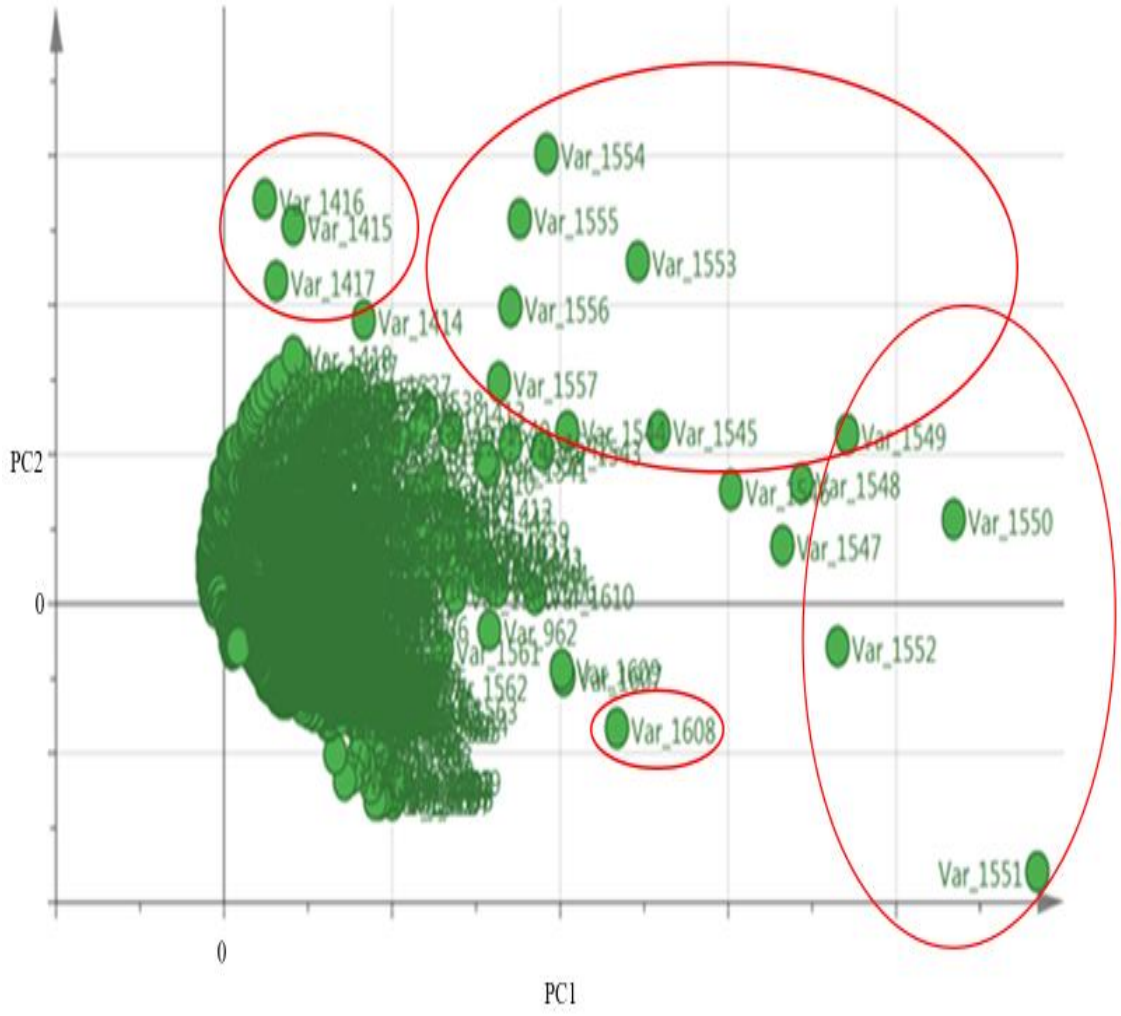

Figure 4.9 Loadings scatter plots of PC1 and PC2 component variables of liver tissues.

Each point is a variable that represents the ^{1}H MAS SS NMR peak intensity from rat liver tissue samples, where, Var: variable point.

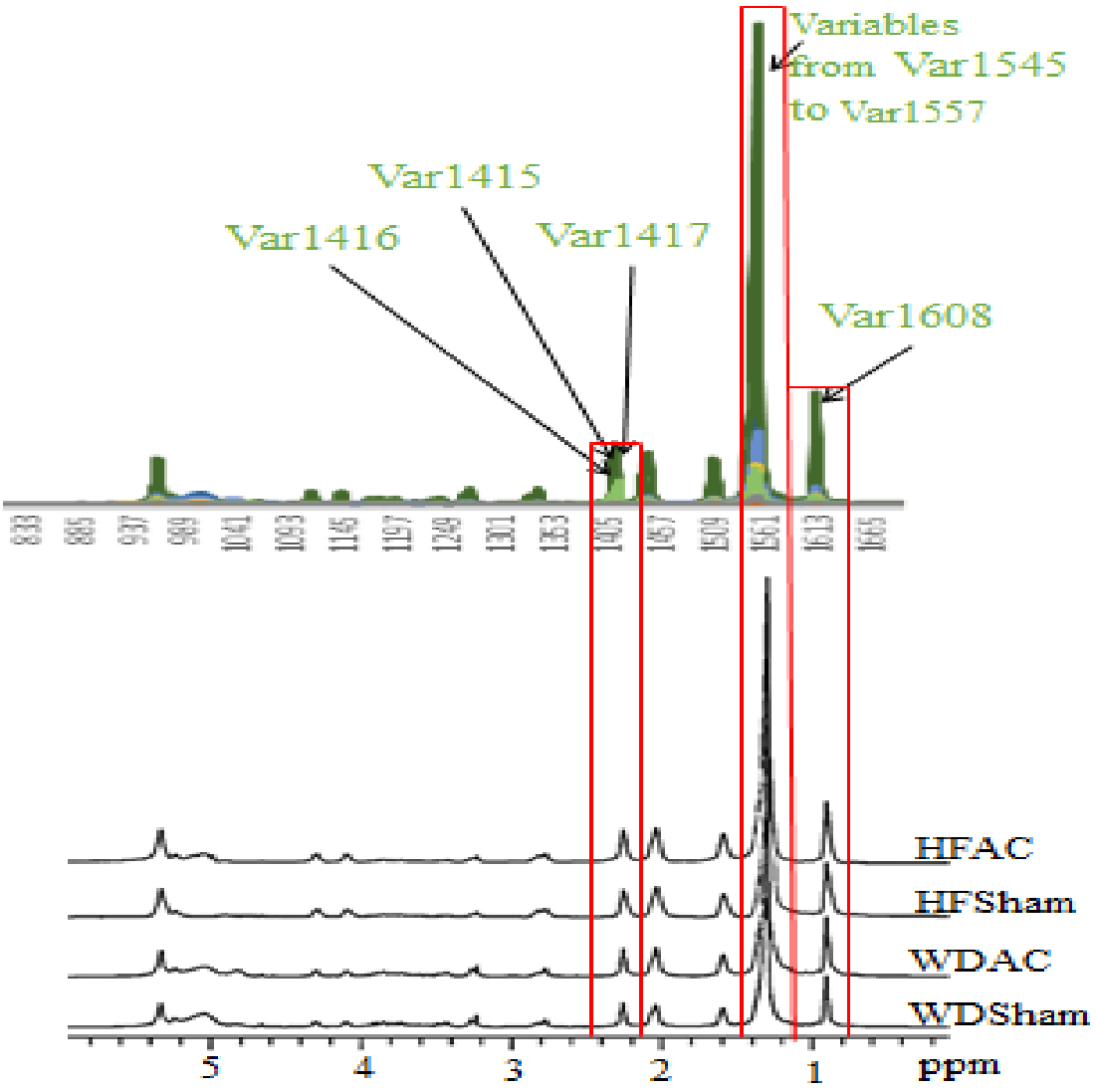

Figure 4.10 ^{1}H MAS SS NMR spectrum of liver tissues corresponding to the variables PCA analysis.

Where variable point 1608 corresponds to lipids/triglyceride CH_3 at 0.9ppm, variable points 1545-1557 correspond to lipids $(CH_2)_n$ at 1.29ppm and variable points 1415-1417 correspond to lipids α-CH_2 at 2.25ppm and ^{1}H MAS SS NMR spectra of rat liver tissues. Red boxes represent the variables and their corresponding chemical shifts.

4.5 Discussion

Metabolites, including lipid profile, are one of the strong biology tools for diagnosing and evaluating the efficacy of a therapy in an early stage of diseases.[34, 35] Fat depots within and surrounding the heart primarily supply fatty acid (FA) deposits.[36] In normal physiological heart condition, fats are the main source of fuel, accounting for 70% of oxidative adenosine triphosphate (ATP) production.[37] However, the excessive accumulation of fats has been related to myocardial damage, inflammation, and heart disease. Evidence suggests that high-fat diets promote an elevation of triglycerides and fatty acids, leading to myocardial dysfunction and lipotoxic cardiomyopathy.[38-40] Increased lipid oxidation is related to reactive oxygen species (ROS) causing metabolic abnormalities in heart. The "lipid hypothesis"[41] states the link between high dietary fat contents, mainly saturated fatty acids (SFA), and TG promoting heart and liver diseases.[41-44] Consequently, dietary fat, particularly intake of SFA, has been constantly demonized.[45] Ever since, reduced consumption of SFA has been promoted in the regular diet to reduce the risk of heart and liver diseases.[45] The intimate connection between cardiac inflammation and fat metabolism causing dyslipidemia in Western and developed societies, especially elevated level of triglycerides, small dense low-density lipoprotein and dysfunctional high-density lipoprotein, is influenced by high dietary fats.[46] The low intake of saturated fat together with high consumption of polyunsaturated and monounsaturated fat is linked with low risk of CVD studied in many populations.[47] The liver is one of the important organs to regulate dietary nutrients, such as fats and carbohydrates.[46] The deposition of intrahepatic fat may contribute to metabolic hepatic diseases. [46]The excess fats are stored in the liver as TGs via secretion or oxidation pathways. The retention of TGs in liver tissues are the precondition for the development of fatty liver diseases.[48]

Among various pathological features of cardiac and liver diseases, the content and composition of lipids deserve special consideration.[46-48] Dietary lipids intake and their composition may be driving forces in the transition to cause toxicity in the heart and liver. Numerous lipidomics profiling investigations highlighted the existence of lipid signature to promote heart and liver disorders.[46-48] However, it is not clear which types of dietary lipids/fats are the real cause to disturb the metabolism or physiology of heart and liver tissues.[46-48]

The main aim of this study was to investigate the molecular lipid profiles of different diet using heart and liver tissues from rat models of WD and HFD under MAS NMR and PCA. MAS is a well-known method for achieving high resolution ^{1}H-NMR spectrum of metabolites of the intact biological tissues without losing tissue architecture and without the need of extraction.[49-51] Therefore, it is used to obtain HR spectra of heterogeneous biological samples for determining the metabolic profile of the studied system under the considered conditions, such as cancer, dietary effects on diseases etc.[49-52] Subsequently the metabolic changes are evaluated by using PCA of data obtained from MS-NMR spectra and systematically evaluating the variations in metabolites from a distribution pattern.[32, 52] The PCA is a statistical method used to detect interrelationships between the different variables by data a prediction scheme that manages sample grouping with selection and dimensionality reduction.[53] In PCA, the direction of length and the angles between the connecting line variables and centroids signify the connection between variables and principal component axes; the longer the line, the higher the variance.[54]

The rats were fed either Western or high fat diet for nine weeks. The aortic constriction (AC; induced cardiac hypertrophy and heart failure) and Sham (placebo) surgical

methods were used before feeding (described in section 2.1.1). About 30-40mg of heart and liver tissues were used for each experiment.

Table 4.3 Assignment of heart tissue metabolites in WDSham, WDAC, HFSham, HFAC and PCA variables

Metabolites	WDSham	WDAC	HFDSham	HFDAC	PCA Variables
Lipids /Triglyceride CH_3 (0.9ppm)	√	√	√	√	X
Lipids/Triglyceride $(CH_2)_n$ (1.27-1.38ppm)	√	√	√	√	X
Alanin β-CH_3 (1.52ppm)	√	√	√	√	X
Lipids CH_2CH_2CO (1.62ppm)	√	√	X	X	X
Leucine (1.75ppm)	√	√	√	√	X
Lipids CH=CH-CH_2 (2.08ppm)	√	√	√	√	X
Lipids CH_2-CH_2-CO (2.20ppm)	√	√	√	√	X
Glutamate CH_2 (2.38ppm)	√	√	√	√	X
Lipids CH=CH-CH_2 (2.82ppm)	√	√	√	√	X
Creatine (3.07ppm)	√	√	√	√	X
Choline/Phosphocholine/PT/GPC (3.21-3.27ppm)	√	√	√	√	X
Glucose/Taurine –CH_2NH_2 (3.42ppm)	√	√	√	√	X
Phosphocholine (3.60ppm)	√	√	√	√	X
Alanine (3.79ppm)	√	√	√	√	X
Creatine (3.95ppm)	√	√	√	√	X
Triglyceride –CH-O-COR (4.15ppm)	√	√	√	√	X
β-Glucose (4.65ppm)	√	√	√	√	X
Esterified cholesterol 3-CHOH (4.75ppm)	X	X	√	√	X
α-Glucose (4.85ppm)	√	√	√	√	X
α-GlucoseC1H (5.03ppm)	√	√	√	√	X
Triglyceride –CH-O-COR(5.25-5.28ppm)	√	√	√	√	√
Lipids -CH=CH- (5.32ppm)	√	√	√	√	√
Glycogen (5.41ppm)	√	√	√	√	X

The high-resolution proton MAS NMR spectra of intact heart tissues were dominated by resonances associated with metabolites (Table 4.3), especially lipid groups such as lipids/triglyceride $(CH_2)_n$ at 1.27-1.38ppm and triglyceride –CH-O-COR at 5.25-5.28ppm (Figure 4.3). These peak intensities differed among WDAC, WDSham, HFDAC and HFDSham groups. The lipid group -CH=CH- at 5.32ppm intensity was weaker in

HFDAC than HFDSham and WD samples. The Esterified cholesterol -CHOH at 4.75ppm was found only in HFD samples (Figure 4.3). The lipid group CH_2CH_2CO at 1.62ppm only appeared in WD samples. The lipid groups CH_3 at 0.9ppm, $CH=CH-CH_2$ at 2.08ppm, CH_2-CH_2-CO at 2.20ppm, $CH=CH-CH_2$ at 2.82ppm, choline/phosphocholine/phosphothanolamine/glycerophosphocholin at 3.21-3.27ppm, phosphocholine at 3.60ppm and triglyceride –CH-O-COR at 5.25-5.28ppm were found with the same intensities in all samples (Figure 4.3). PCA data suggest that the variable points 1008-1013 correspond to unsaturated lipids -CH=CH- at 5.32ppm and variable points 1041-1043 correspond to triglyceride –CH-O-COR at 5.25-5.28ppm of ^1H MAS SS NMR (Figure 4.7).

Dayton *et al.* conducted a dietary experiment on 846 men with an average age of 65 years with 30% CVD by replacing saturated fat with high polyunsaturated linoleic acid in one group. They found that serum cholesterol was reduced by 13% in the polyunsaturated group but there was no significant difference between the two groups in terms of myocardial infraction.[55] Leren performed the Oslo diet-heart study. In this experiment, he randomly selected 412 men having myocardial infraction. In one group, he gave the usual high saturated fat diet. The other group's diet was changed from high saturated fat to low saturated fat with high polyunsaturated vegetable oils. He found that the mortality rate was less in the low saturated fat with high polyunsaturated diet group.[56] Houtsmuller *et al* selected 51-51 persons in two groups of newly diagnosed diabetes mellitus. They gave to one group high saturated fat diet and in the other group, high saturated fat was replaced with a high polyunsaturated fats and low saturated fats diet. They monitored CVD by electrocardiography and found that CVD was diagnosed in 24 of 51 in the high saturated fat diet group. In the polyunsaturated and low saturated fat diet group, CVD was

found in 8 of 51, suggesting that a polyunsaturated fat and low saturated fat diet reduced the risk of CVD.[57]

Burgmaier *et al*. reported that obese Zucker rats significantly decreased in cardiac power and increased triglyceride (TG) accumulation after feeding WD for 7 days. They found that these changes were not seen in control-diet rats, in which FA oxidation was upregulated after seven days of high-calorie diet. They also found mismatch between FA uptake and oxidation led to myocardial TG accumulation and left ventricular (LV) dysfunction at seven days of WD.[58] Ouwens *et al.* found rats that were fed HFD for 8 weeks exhibited increased TG accumulation and decreased LV fractional shortening.[59] Chen *el al.*reported that dietary long-chain SFA encouraged cardiac dysfunction, without triggering substantial changes in blood pressure, blood glucose and insulin resistance in mice. They also suggested that the excess individual SFA may compromise myocardial function by mechanisms independent of the majority of metabolic disorders.[60] Listenberger *et al.* used a cellular lipid metabolism model and suggested that unsaturated fatty acids protect against lipotoxicity via elevation of triglyceride accumulation.[61] Zhou *et al.* used obese Zucker diabetic fatty rats as a model to determine the metabolic abnormalities that cause lipotoxicity on myocardial cells. They found that accumulation of TG was rapid in the heart because of under expression of fatty acid oxidative enzymes. They suggested that fat-laden hearts promote lipoapoptosis followed by cardiac dysfunction.[62]

The lipid compositions of WD and HFD was investigated on heart tissues in this chapter. These data suggest that there are no significant differences in the lipid compositions of WD and HFD either in cardiac stress (AC) or normal (sham) condition surgical methods (Figure 4.3). However, PCA data of this study suggest that unsaturated lipids and TG

compositions show variation in all experimental groups (Figure 4.5-4.7). These findings support the suggestions of previous studies that the composition of unsaturated lipids and TG may influence the lipid metabolism along with saturated fats on heart tissues. The non-lipid metabolites such as leucine and α-glucose are found in HFD groups in both cardiac stress (AC) or normal (Sham) surgical conditions. However, these non-lipid metabolites are not recorded as variable groups under PCA. However, it is needed to understand the role of leucine and α-glucose in the metabolism of heart and related diseases during HFD conditions. In this study, the esterified cholesterol was only found in HFD samples of proton MAS NMR spectra. It has been proposed that esterified cholesterol may be associated to antiatherogenics. However, animal and epidemiologic studies suggest that esterified cholesterol has not been linked to antiatherogenic. However, there is a need to further investigate the role of esterified cholesterol of HFD and lipid profiling of cardiac metabolism.

Proton MAS NMR spectra of intact liver tissue metabolites (Table 4.4) suggest that the peak intensities with lipid groups, such as choline/phosphocholine at 3.21-3.3ppm, cholesterol 3-CHOH at 3.53ppm and phosphocholine NCH_3 at 3.6ppm and the peak intensities of non-lipid groups, such as taurine at 3.42ppm, glucose/glycogen at 3.7-3.95ppm, β-glucose C1H at 4.65ppm and glycogen at 5.41ppm are higher in WD than HFD samples (Figure 4.4). Moreover, the PCA data suggest that the variable points 1545-1557 correspond to polyunsaturated lipids $(CH_2)_n$ at 1.29ppm, variable point 1608 corresponds to lipids/triglyceride CH_3 at 0.9ppm and variable points 1416,1415 and 1417 correspond to lipids α-CH_2 at 2.25ppm of ^{1}H MAS SS NMR (Figure 4.10).

Table 4.4 Assignment of liver tissue metabolites in WDSham, WDAC, HFSham, HFAC and PCA variables

Metabolites	WDSham	WDAC	HFDSham	HFDAC	PCA Variables
Cholesterol/esters -CH_3 (0.72ppm)	√	√	√	√	X
Lipids/Triglyceride CH_3 (0.90ppm)	√	√	√	√	√
Lipids $(CH_2)_n$ (1.29ppm)	√	√	√	√	√
Lipids β-CH_2 (1.59ppm)	√	√	√	√	X
Lipids -CH_2–CH= (2.03ppm)	√	√	√	√	X
Lipids α-CH_2 (2.25ppm)	√	√	√	√	√
Lipids = CH-CH_2–CH= (2.78-2.83ppm)	√	√	√	√	X
Choline/Phosphocholine (3.21-3.30ppm)	√	√	√	√	X
Taurine (3.42ppm)	√	√	√	√	X
Cholesterol 3-CHOH (3.53ppm)	√	√	√	√	X
Phosphocholine NCH_3 (3.60ppm)	√	√	√	√	X
Glucose/glycogen (3.70-3.95ppm)	√	√	√	√	X
Cholin CH_2(OH) (4.09ppm)	√	√	√	√	X
Phosphocholine PO_3CH_2 (4.18ppm)	√	√	√	√	X
Triglyceride (4.30ppm)	√	√	√	√	X
β-Glucose C1H (4.65ppm)	√	√	√	√	X
α-Glucose C1H (5.23ppm)	√	√	√	√	X
Lipids –CH=CH (5.32ppm)	√	√	√	√	X
Glycogen (5.41ppm)	√	√	√	√	X

The association between dietary fat consumption and liver fat compositions have been investigated. Koch *et al.* examined the connection between dietary fats and liver fat contents measured by magnetic resonance imaging (MRI) in 354 adults. They observed that consumption of fats was not linked with liver fats, whilst alcohol was associated with hepatic fats.[63] In contrast, Mollard *et al.* suggested that dietary fat may be the determinant of hepatic steatosis and significantly associated with hepatic TG using magnetic resonance spectroscopy in 74 overweight adolescents.[64] Kuk *et al.* investigated the association between acute (1 day) or habitual (10 day) dietary fat intake and liver fat using

computed tomography in 42 abdominally-obese men. They found that there was no link between liver fat and acute dietary fat intake, but a positive association was found between liver fat and habitual fat consumption.[65] Rosqvist *et al.* investigated the effect of excess feeding of SFA or polyunsaturated fatty acids (PUFA) on liver fat accumulation in healthy adults for seven weeks using MRI. They found that SFA increased liver fat to a greater extent than PUFA.[66]

The data of PCA of proton MAS NMR from liver tissues after nine weeks feeding WD and HFD of this study suggest that the variations in mono- or polyunsaturated and TG in both dietary conditions (Figure 4.8 - 4.10). TG and unsaturated lipid compositions may influence the lipid metabolism in the liver. These findings support the previous studies showing that TG and UFA may play an important role in lipid metabolism in the liver. However, these data did not identify the most variable SFA groups in all experimental conditions and here these findings contradict previous studies showing that SFA has a greater influence than UFA on the liver.

In conclusion, lipid compositions associated with dietary sources relies on the detection of key dietary factors that influence the lipidomics profile in the heart and liver causing toxicity and diseases. The dietary fats intake may affect its composition, such as TG, and saturated fatty acids in the metabolism of liver and heart physiology. The variables in TG and unsaturated lipids of WD and HFD conditions suggest that they may play an important role in lipid metabolism and propagation of diseases, which may need further investigation and validation.

4.6 References

1. E. D. Rosen and B. M. Spiegelman, *Cell*, 2014, **156**, 20-44.
2. S. N. Bhupathiraju and F. B. Hu, *Circulation research*, 2016, **118**, 1723-1735.
3. C. L. Ogden, M. D. Carroll, L. R. Curtin, M. A. McDowell, C. J. Tabak and K. M. Flegal, *Jama*, 2006, **295**, 1549-1555.
4. C. Buechler, J. Wanninger and M. Neumeier, *World journal of gastroenterology*, 2011, **17**, 2801-2811.
5. S. Yusuf, S. Hawken, S. Ounpuu, T. Dans, A. Avezum, F. Lanas, M. McQueen, A. Budaj, P. Pais, J. Varigos and L. Lisheng, *Lancet (London, England)*, 2004, **364**, 937-952.
6. O. Quehenberger, A. M. Armando, A. H. Brown, S. B. Milne, D. S. Myers, A. H. Merrill, S. Bandyopadhyay, K. N. Jones, S. Kelly, R. L. Shaner, C. M. Sullards, E. Wang, R. C. Murphy, R. M. Barkley, T. J. Leiker, C. R. Raetz, Z. Guan, G. M. Laird, D. A. Six, D. W. Russell, J. G. McDonald, S. Subramaniam, E. Fahy and E. A. Dennis, *Journal of lipid research*, 2010, **51**, 3299-3305.
7. A. M. Lundberg and G. K. Hansson, *Clinical immunology (Orlando, Fla.)*, 2010, **134**, 5-24.
8. Y. Wei, D. Wang, F. Topczewski and M. J. Pagliassotti, *American journal of physiology. Endocrinology and metabolism*, 2006, **291**, E275-281.
9. H. Malhi, S. F. Bronk, N. W. Werneburg and G. J. Gores, *The Journal of biological chemistry*, 2006, **281**, 12093-12101.
10. Z. Z. Li, M. Berk, T. M. McIntyre and A. E. Feldstein, *The Journal of biological chemistry*, 2009, **284**, 5637-5644.
11. V. Nehra, P. Angulo, A. L. Buchman and K. D. Lindor, *Digestive diseases and sciences*, 2001, **46**, 2347-2352.

12. C. L. Gentile and M. J. Pagliassotti, *The Journal of nutritional biochemistry*, 2008, **19**, 567-576.

13. A. K. Leamy, R. A. Egnatchik and J. D. Young, *Progress in lipid research*, 2013, **52**, 165-174.

14. B. A. Neuschwander-Tetri, *Hepatology (Baltimore, Md.)*, 2010, **52**, 774-788.

15. A. Grzelczyk and E. Gendaszewska-Darmach, *Biochimie*, 2013, **95**, 667-679.

16. M. Pagadala, T. Kasumov, A. J. McCullough, N. N. Zein and J. P. Kirwan, *Trends in endocrinology and metabolism: TEM*, 2012, **23**, 365-371.

17. P. Puri, R. A. Baillie, M. M. Wiest, F. Mirshahi, J. Choudhury, O. Cheung, C. Sargeant, M. J. Contos and A. J. Sanyal, *Hepatology (Baltimore, Md.)*, 2007, **46**, 1081-1090.

18. A. J. Sanyal and T. Pacana, *Transactions of the American Clinical and Climatological Association*, 2015, **126**, 271-288.

19. L. C. Wright, G. L. May, M. Dyne and C. E. Mountford, *FEBS letters*, 1986, **203**, 164-168.

20. J. Z. Hu, *Metabolomics: open access*, 2016, **6**, 1000e147.

21. K. Shet, S. M. Siddiqui, H. Yoshihara, J. Kurhanewicz, M. Ries and X. Li, *NMR in biomedicine*, 2012, **25**, 538-544.

22. U. Haeberlen, *High Resolution NMR in Solids Selective Averaging*, Academic Press, Newyork, USA, 1976.

23. M. H. Levitt, *Spin dynamics Basics of Nuclear Magnetic Resonance*, John Wiley & sons Ltd., West Sussex, England, 2001.

24. A. L. Skinner and J. S. Laurence, *Journal of pharmaceutical sciences*, 2008, **97**, 4670-4695.

25. P. Schanda and M. Ernst, *Prog Nucl Magn Reson Spectrosc*, 2016, **96**, 1-46.

26. T. Polenova, R. Gupta and A. Goldbourt, *Anal Chem*, 2015, **87**, 5458-5469.

27. Y. Wang, M. E. Bollard, H. Keun, H. Antti, O. Beckonert, T. M. Ebbels, J. C. Lindon, E. Holmes, H. Tang and J. K. Nicholson, *Analytical biochemistry*, 2003, **323**, 26-32.

28. M. E. Bollard, S. Garrod, E. Holmes, J. C. Lindon, E. Humpfer, M. Spraul and J. K. Nicholson, *Magnetic resonance in medicine*, 2000, **44**, 201-207.

29. F. P. Martin, M. E. Dumas, Y. Wang, C. Legido-Quigley, I. K. Yap, H. Tang, S. Zirah, G. M. Murphy, O. Cloarec, J. C. Lindon, N. Sprenger, L. B. Fay, S. Kochhar, P. van Bladeren, E. Holmes and J. K. Nicholson, *Mol Syst Biol*, 2007, **3**, 112.

30. H. Zhang, L. Ding, X. Fang, Z. Shi, Y. Zhang, H. Chen, X. Yan and J. Dai, *PLoS One*, 2011, **6**, e20862.

31. F. P. Martin, Y. Wang, N. Sprenger, E. Holmes, J. C. Lindon, S. Kochhar and J. K. Nicholson, *J Proteome Res*, 2007, **6**, 1471-1481.

32. J. Feng, N. G. Isern, S. D. Burton and J. Z. Hu, *Metabolites*, 2013, **3**, 1011-1035.

33. M. E. Bollard, A. J. Murray, K. Clarke, J. K. Nicholson and J. L. Griffin, *FEBS letters*, 2003, **553**, 73-78.

34. O. Beckonert, M. Coen, H. C. Keun, Y. Wang, T. M. Ebbels, E. Holmes, J. C. Lindon and J. K. Nicholson, *Nat Protoc*, 2010, **5**, 1019-1032.

35. E. Holmes, J. K. Nicholson, A. W. Nicholls, J. C. Lindon, S. C. Connor, S. Polley and J. Connelly, *Chemometrics and Intelligent Laboratory Systems*, 1998, **44**, 245-255.

36. J. Lommi, M. Kupari and H. Yki-Jarvinen, *The American journal of cardiology*, 1998, **81**, 45-50.

37. T. S. Park, H. Yamashita, W. S. Blaner and I. J. Goldberg, *Current opinion in lipidology*, 2007, **18**, 277-282.

38. F. Giacco and M. Brownlee, *Circulation research*, 2010, **107**, 1058-1070.

39. J. Buchanan, P. K. Mazumder, P. Hu, G. Chakrabarti, M. W. Roberts, U. J. Yun, R. C. Cooksey, S. E. Litwin and E. D. Abel, *Endocrinology*, 2005, **146**, 5341-5349.

40. S. Boudina and E. D. Abel, *Circulation*, 2007, **115**, 3213-3223.

41. A. Keys, *Journal of the Mount Sinai Hospital, New York*, 1953, **20**, 118-139.

42. H. Yki-Jarvinen, *Digestive diseases (Basel, Switzerland)*, 2010, **28**, 203-209.

43. W. C. Willett, *Journal of internal medicine*, 2012, **272**, 13-24.

44. F. Diraison and M. Beylot, *The American journal of physiology*, 1998, **274**, E321-327.

45. S. M. Grundy, D. Bilheimer, H. Blackburn, W. V. Brown, P. O. Kwiterovich, Jr., F. Mattson, G. Schonfeld and W. H. Weidman, *Circulation*, 1982, **65**, 839A-854A.

46. S. A. Parry and L. Hodson, *Journal of investigative medicine : the official publication of the American Federation for Clinical Research*, 2017, **65**, 1102-1115.

47. F. M. Sacks, A. H. Lichtenstein, J. H. Y. Wu, L. J. Appel, M. A. Creager, P. M. Kris-Etherton, M. Miller, E. B. Rimm, L. L. Rudel, J. G. Robinson, N. J. Stone, L. V. Van Horn and A. American Heart, *Circulation*, 2017, **136**, e1-e23.

48. C. J. Green and L. Hodson, *Nutrients*, 2014, **6**, 5018-5033.

49. M. N. Triba, A. Starzec, N. Bouchemal, E. Guenin, G. Y. Perret and L. Le Moyec, *NMR in biomedicine*, 2010, **23**, 1009-1016.

50. P. Guitera, P. Bourgeat, J. R. Stretch, R. A. Scolyer, S. Ourselin, C. Lean, J. F. Thompson and R. Bourne, *Melanoma research*, 2010, **20**, 311-317.

51. W. Li, R. Slominski and A. T. Slominski, *Analytical biochemistry*, 2009, **386**, 282-284.

52. C. Corsaro, D. Mallamace, S. Vasi, V. Ferrantelli, G. Dugo and N. Cicero, *Journal of Analytical Methods in Chemistry*, 2015, **2015**.

53. G. McCombie, G. Medina-Gomez, C. J. Lelliott, A. Vidal-Puig and J. L. Griffin, *Metabolites*, 2012, **2**, 366-381.

54. C. P. Klingenberg, *Development Genes and Evolution*, 2016, **226**, 113-137.

55. S. Dayton, M. L. Pearce, H. Goldman, A. Harnish, D. Plotkin, M. Shickman, M. Winfield, A. Zager and W. Dixon, *Lancet (London, England)*, 1968, **2**, 1060-1062.

56. P. Leren, *Circulation*, 1970, **42**, 935-942.

57. A. J. Houtsmuller, J. van Hal-Ferwerda, K. J. Zahn and H. E. Henkes, *Progress in lipid research*, 1981, **20**, 377-386.

58. M. Burgmaier, S. Sen, F. Philip, C. R. Wilson, C. C. Miller, 3rd, M. E. Young and H. Taegtmeyer, *Obesity (Silver Spring, Md.)*, 2010, **18**, 1895-1901.

59. D. M. Ouwens, M. Diamant, M. Fodor, D. D. J. Habets, M. Pelsers, M. El Hasnaoui, Z. C. Dang, C. E. van den Brom, R. Vlasblom, A. Rietdijk, C. Boer, S. L. M. Coort, J. F. C. Glatz and J. Luiken, *Diabetologia*, 2007, **50**, 1938-1948.

60. B. Chen, Y. Huang, D. Zheng, R. Ni and M. A. Bernards, *Nutrients*, 2018, **10**.

61. L. L. Listenberger, X. Han, S. E. Lewis, S. Cases, R. V. Farese, Jr., D. S. Ory and J. E. Schaffer, *Proc Natl Acad Sci U S A*, 2003, **100**, 3077-3082.

62. Y. T. Zhou, P. Grayburn, A. Karim, M. Shimabukuro, M. Higa, D. Baetens, L. Orci and R. H. Unger, *Proc Natl Acad Sci U S A*, 2000, **97**, 1784-1789.

63. M. Koch, J. Borggrefe, J. Barbaresko, G. Groth, G. Jacobs, S. Siegert, W. Lieb, M. J. Muller, A. Bosy-Westphal, M. Heller and U. Nothlings, *The American journal of clinical nutrition*, 2014, **99**, 369-377.

64. R. C. Mollard, M. Senechal, A. C. MacIntosh, J. Hay, B. A. Wicklow, K. D. Wittmeier, E. A. Sellers, H. J. Dean, L. Ryner, L. Berard and J. M. McGavock, *The American journal of clinical nutrition*, 2014, **99**, 804-812.

65. J. L. Kuk, L. E. Davidson, R. Hudson, K. Kilpatrick, K. Bacskai and R. Ross, *Applied physiology, nutrition, and metabolism = Physiologie appliquee, nutrition et metabolisme*, 2008, **33**, 239-245.

66. F. Rosqvist, D. Iggman, J. Kullberg, J. Cedernaes, H. E. Johansson, A. Larsson, L. Johansson, H. Ahlstrom, P. Arner, I. Dahlman and U. Riserus, *Diabetes*, 2014, **63**, 2356-2368.

Chapter 5

WD and HFD lipid profiling of lipids extracted from heart and liver

5.1 Introduction

The metabolome is a group of small molecules or metabolites of an entire physiological system.[1, 2] The metabolites are exogenous - dietary, or drug related and endogenous - chemical substrates, intermediates and their final products that are synthesised or produced in the biological system. Metabolites comprise lipids, carbohydrates, amino acids, peptides, nucleotides and organic acids.[3, 4] In this study, the main objective was to examine the effect of lipid metabolites from dietary fats extracted from rat's heart and liver tissues.

Fats or lipids are generally deposited on subcutaneous and visceral fat tissues. However, excess fats can accumulate in non-adipose tissues such as hepatocytes (liver tissues) and cardiomyocytes (heart tissues).[5-8] Deposition of excess fats is one of the hallmarks of obesity. Visceral obesity is associated with high mortality rate.[9] However, obesity may also promote hypertension, insulin resistance syndrome including diabetes, increased risk of cardiovascular diseases (CVD) and non-alcoholic fatty liver diseases.[10] The surplus fat is generally ectopic fat coming from dietary sources.[11] The Western diet and high fat diet contain an excessive percentage of saturated fats, which is identified as a risk factor of pathological conditions for cardiovascular disease, hepatic disorders and dyslipidaemia in both humans and mice.[12-15] To investigate the effect of dietary fats on heart and liver - lipid compositions, WD and HF diet were fed to rats for nine weeks before lipid extraction from heart and liver tissues.

The abnormal accumulation and excessive deposition of fats/lipids within cardiomyocytes or hepatocytes mainly involve triglycerides, saturated and unsaturated lipids although other lipid metabolites such as free fatty acids, cholesterol, and phospholipids also exist.[16-19] Free fatty acids are one of the main substrates to form

triglycerides that induce oxidative stress and provoke generation of reactive oxygen species (ROS) causing cellular apoptosis or toxicity.[16-19]

Lipidomics is the use of analytical methods together with chemometrics for the study of lipid profile.[20] Chemometrics is the combination of statistical and computational applications to analyse the data obtained from the spectra of analytical experiments.[21] Proton nuclear magnetic resonance (^{1}H NMR) is one of the useful analytical methods in probing for lipid profile.[22]

5.1.1 Proton ^{1}H NMR

^{1}H NMR spectroscopy is a useful method to take advantage of the magnetic properties of protons to acquire structural information. The strong magnetic field of NMR and electromagnetic radiation as radiofrequency (rf) pulses are applied to excite the protons of samples.[23] When the excited protons relax and achieve the equilibrium state, energy is collected in the form of an oscillating electromagnetic signal, commonly known as free induction decay (FID). This signal (intensity versus time) is normally Fourier Transformed to generate a spectrum of intensity versus frequency.[23] The protons of the different molecules show different chemical shift with a specific pattern of peaks giving information about both the chemical shift and the intensities of those peaks.[23] A detail explanation of the principles of NMR is provided in Chapter 1 section 1.6.1.

5.2 Aims

To investigate the lipidomics changes induced by western diet fat and high fat feeding in the rat using ^{1}H NMR. Lipids were extracted from rat heart and liver tissues. Multivariate

statistics, via a PCA tool was used to analyse the NMR spectra chromatograms produced by lipidomics analyses to obtain a clear view of the variables affecting the data.

5.3 Materials and methods

Adult male Sprague Dawely rats (220-250 gm, Charles River Inc.,Kent, UK) were maintained on diets containing 61.6% fat and 20.3% sucrose (high-fat diet, HFD); or 45% fat and 15% sucrose (Western diet, WD), 48 hours post-surgery, as described in Chapter 2 section 2.1, generating four experimental groups:

- High-fat diet + Sham (HFDSham).
- Western diet + Sham (WDSham).
- High-fat diet + Aortic Constriction (HFDAC).
- Western diet + Aortic Constriction (WDAC).

After nine weeks, animals were anaesthetised, and hearts and livers were harvested, rinsed, freeze-clamped and processed as described in Chapter 2 section 2.1. The ^{1}H NMR experiments on lipids extracted from heart and liver tissues from rats were performed on a Bruker Avance II spectrometer operating at a frequency of 500.1025 MHz (^{1}H) detail explanation in Chapter 2 section 2.2.3. for Proton NMR lipid profiling experiments, the lipid soluble metabolites were reconstituted in 600 µl of $CDCl_3$ (0.03% v/v TMS). About 500 µl of the prepared sample was loaded into a standard 5 mm NMR tube. A standard Topspin Zg pulse sequence was used for the measurement with a single pulse excitation using 256 scans at 288K. The acquisition time was 1s and the recycle delay time was 1s, resulting in a total experimental time of about 17 mins. The data from NMR spectra were analysed by the PCA statistical tool described in Chapter 2 section 2.2.6.

5.4 Results

5.4.1 ^{1}H NMR spectra of lipid metabolites extracted from rat heart and liver tissue

The spectra were referenced to TMS at 0.0ppm in each spectrum and peaks were assigned according to prior published results.[24-27]

The ^{1}H NMR spectra of lipids extracted from heart tissues (Figure 5.3) and the intensity of peak **7** (FA β-CH_2) were only observed in HF samples. The peak **16** (PC and SM CH_2 -N^+ $(CH_3)_3$) was found in WDSham and HFSham samples. The peak **20** (PC and SM -O-CH_2-CH_2-$N^+(CH_3)_3$) was appeared in WDAC and HFSham samples. Peaks **1** (Chol-18 -CH_3), **2** (FA ω-CH_3), **3** (Chol-21 -CH_3) and FA omega3 -CH_3, **4** (Chol-19 -CH_3), **5** (FA $(CH_2)_n$), **6** (FA CH_2CH_2CO), **8** (unassigned), **9** (FA CH-CH=), **10** (FA -CO-CH_2-CH_2-), **11** (FA α and β -CH_2), **12** (FA -CH=CH-CH_2-CH=CH-), **13** (FA (CH=CH-CH_2-CH=CH)$_n$), **14** (Phosphatidylethanolamine (PE) -CH_2-NH_2), **15** (Phosphatidylcholine(PC) and Sphingomyelin(SM) $N^+(CH_3)_3$, **17** (unassigned), **18** (Glycerophospholipid backbone -CH_2, **19** (Glycerol (TG) C1H, C3H), **21** (Glyceryl-C1H(TG/PC/PE)), **22** (Glycerophosphocholine (GPC) -CH_2), **23** (Glycerol (TG) -CH), **24** (Glycerol (PC/PE) -CH) and **25** (FA -CH=CH- and Chol-6 -CH_3) were found with the same intensities in all samples.

^{1}H MAS NMR spectra of extracted lipids from liver tissues (Figure 5.4) and the intensity of peak **16** (Glycerophosphocholine (GPC) -CH_2) were higher in WD samples than HF samples. The intensities of peaks **1** (Chol–18 -CH_3), **2** (FA ω-CH_3/ Cho-26&27 -CH_3), **3** (Chol-19 -CH_3), **4** (FA $(CH_2)_n$), **5** (FA CO-CH_2 -CH_2), **6** (unassigned), **7** (FA CH-CH=), **8** (FA CO-CH_2), **9** (FA CH=CH-CH_2-CH=CH- and (CH=CH-CH_2-CH=CH)$_n$), **10**

(Phosphatidylethanolamine (PE) -CH_2-NH_2), **11** (Cholin –$N^+(CH_3)_3$), **12** (unassigned), **13** (Glycerophosphospholipid backbone -CH_2), **14** (TG glycerol C1H), **15** (Glyceryl-C1H (TG/PC/PE)), **17** (Glycerol(TG) –CH), **18** (Glycerol(PC/PE) C2H and **19** (FA CH=CH / Chol-6 -CH_3 appeared the same in all group samples.

The spectra suggest that lipid components extracted from heart and liver tissues were similar. However, there were variations in some lipid peak intensities - in the samples of heart lipid groups, such as β-CH_2 of FA at 1.67ppm appears either in aortic constriction or placebo HFD samples and CH_2-N^+ $(CH_3)_3$ of PC and SM at 3.65ppm were not found in either WD or HFD aortic constriction samples. In liver samples, the peak intensities of the lipid group -CH_2 of GPC at 4.38ppm were higher in WD than HFD samples under both aortic constriction and placebo surgical conditions. These findings indicate that these significant variations in some lipid compositions may be related to either dietary fat compositions or surgical methods.

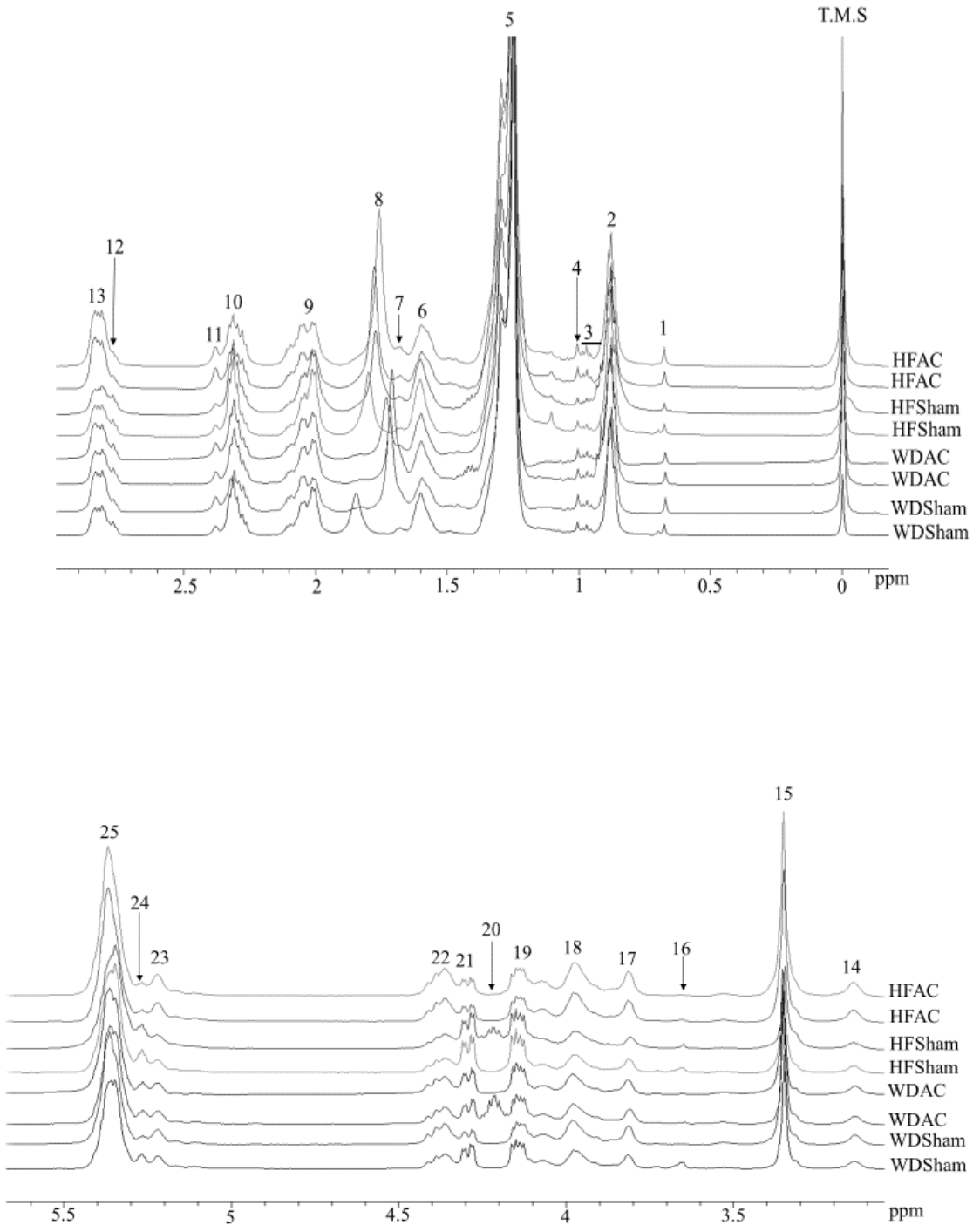

Figure 5.1 ^{1}H NMR spectra of lipid extractions from rat heart tissues.

Where 1 (0.70ppm) Cholesterol (Chol-18) -CH_3; 2 (0.88ppm) Fatty acids (FA) ω-CH_3; 3 (0.9 - 0.96ppm Chol-21 -CH_3) and FA omega3 -CH_3; 4 (1.00ppm) Chol-19 -CH_3; 5 (1.30ppm) FA $(CH_2)_n$; 6 (1.59ppm) FA CH_2CH_2CO; 7 (1.67ppm) FA β-CH_2; 8 (1.84ppm) Unassigned; 9 (2.04ppm) FA CH-CH=; 10 (2.30ppm) FA -CO-CH_2-CH_2-; 11 (2.38ppm) FA α and β -CH_2; 12 (2.75ppm) FA -CH=CH-CH_2-CH=CH- ; 13 (2.80ppm) FA $(CH=CH-CH_2-CH=CH)_n$; 14 (3.11ppm) Phosphatidylethanolamine (PE) -CH_2-NH_2; 15 (3.35ppm) Phosphatidylcholine(PC) and Sphingomyelin(SM) $N^+(CH_3)_3$; 16 (3.65ppm) PC and SM CH_2-N^+ $(CH_3)_3$; 17 (3.8ppm) unassigned; 18 (3.98 ppm) Glycerophospholipid backbone -CH_2; 19 (4.16ppm) Glycerol (TG) C1H, C3H; 20 (4.24ppm) PC and SM -O-CH_2-CH_2-$N^+(CH_3)_3$; 21 (4.32ppm) Glyceryl-C1H(TG/PC/PE); 22 (4.38 ppm) Glycerophosphocholine (GPC) -CH_2; 23 (5.22ppm) Glycerol (TG) -CH; 24(5.28ppm) Glycerol (PC/PE) -CH; 25 (5.36ppm) FA -CH=CH- and Chol-6 -CH_3.

Table 5.1 List of lipid group peak assignments in the lipid extracted from heart

Lipid groups	^{1}H chemical shifts
Cholesterol (Chol-18) -CH_3	0.70ppm
Fatty acids (FA) ω-CH_3	0.88ppm
Chol-21 -CH_3	0.9- 0.95ppm
FA omega3 -CH_3	0.96 ppm
Chol-19 -CH_3	1.00ppm
FA $(CH_2)_n$	1.30ppm
FA CH_2CH_2CO	1.59ppm
FA β-CH_2	1.67ppm
FA CH-CH=	2.04 ppm
FA -CO-CH_2-CH_2-	2.30ppm
FA α and β -CH_2	2.38ppm
FA -CH=CH-CH_2-CH=CH-	2.75ppm
FA $(CH=CH-CH_2-CH=CH)_n$	2.80ppm
Phosphatidylethanolamine (PE) -CH_2-NH_2	3.11ppm
Phosphatidylcholine (PC) and Sphingomyelin (SM) $N^+(CH_3)_3$	3.35ppm
PC and SM CH_2 -N^+ $(CH_3)_3$	3.65ppm
Glycerophospholipid backbone -CH_2	3.97ppm
Glycerol (TG) C1H, C3H	4.16ppm
PC and SM -O-CH_2 -CH_2 -N^+ $(CH_3)_3$	4.24ppm
Glyceryl-C1H(TG/PC/PE)	4.32ppm
Glycerophosphocholine (GPC) -CH_2	4.38ppm
Glycerol (TG) -CH	5.22ppm
Glycerol (PC/PE) -CH	5.28ppm
FA -CH=CH- and Chol-6 -CH_3	5.36ppm

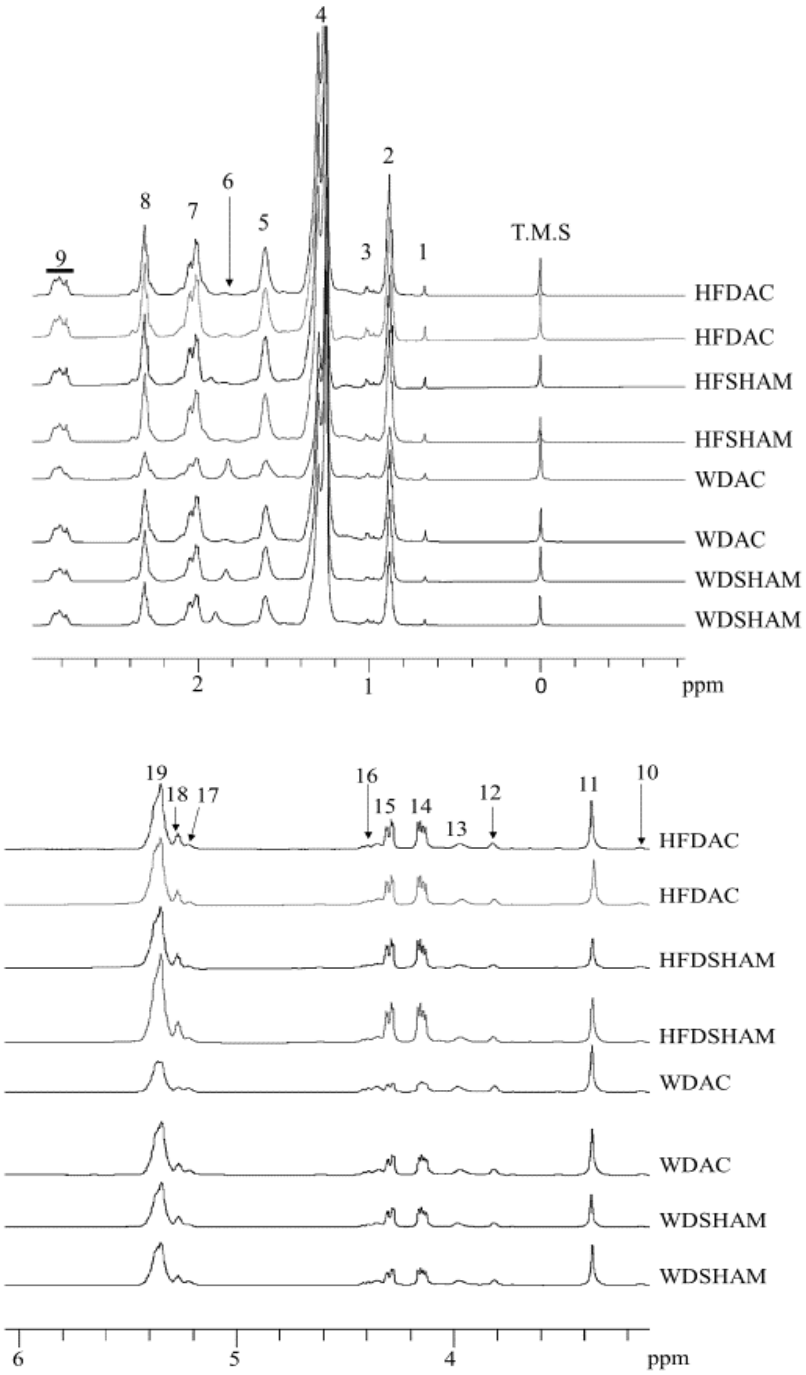

Figure 5.2 ^{1}H NMR spectra of lipid extractions from rat liver tissues.

Where 1 (0.69ppm) Cholesterol(Chol–18) -CH_3; 2 (0.88ppm) Fatty acids (FA) ω-CH_3/ Cho-26&27 -CH_3; 3 (1.00ppm) Chol-19 -CH_3; 4 (1.30ppm) FA $(CH_2)_n$; 5 (1.59ppm) FA CO-CH_2 -CH_2; 6 (1.8ppm) Unassigned; 7 (2.04ppm) FA CH-CH=; 8 (2.30ppm) FA CO-CH_2; 9 (2.75 -2.80ppm) FA CH=CH-CH_2-CH=CH- and $(CH=CH-CH_2-CH=CH)_n$; 10 (3.14ppm) Phosphatidylethanolamine (PE) -CH_2-NH_2; 11 (3.37ppm) Cholin –$N^+(CH_3)_3$; 12 (3.8ppm) Unassigned; 13 (3.98ppm) Glycerophosphospholipid backbone -CH_2; 14 (4.16ppm) TG glycerol C1H; 15 (4.32ppm) Glyceryl-C1H (TG/PC/PE); 16 (4.38ppm) Glycerophosphocholine (GPC) -CH_2; 17 (5.22ppm) Glycerol(TG) –CH; 18(5.27ppm) Glycerol(PC/PE) C2H; 19 (5.35ppm) FA CH=CH and Chol-6 -CH.

Table 5.2 List of lipid group peak assignments in the lipid extracted from liver

Lipid groups	^{1}H chemical shifts
Cholesterol (Chol–18) -CH_3	0.69ppm
Fatty acids (FA) ω-CH_3/ Cho-26&27 -CH_3	0.88ppm
Chol-19 -CH_3	1.00ppm
FA $(CH_2)_n$	1.30ppm
FA CO-CH_2 -CH_2	1.59ppm
FA CH-CH=	2.04ppm
FA CO-CH_2	2.30ppm
FA CH=CH-CH_2-CH=CH-	2.75ppm
FA (CH=CH-CH_2-CH=CH)n	2.80ppm
Phosphatidylethanolamine (PE) -CH_2-NH_2	3.10ppm
Cholin –$N^+(CH_3)_3$	3.37ppm
Glycerophosphospholipid backbone -CH_2	3.97ppm
TG glycerol C1H	4.16ppm
Glyceryl-C1H (TG/PC/PE)	4.32ppm
Glycerophosphocholine (GPC) -CH_2	4.38ppm
Glycerol(TG) –CH	5.22ppm
Glycerol(PC/PE) C2H	5.27ppm
FA CH=CH and Chol-6 -CH_3	5.37ppm

5.4.2 PCA analysis of ^{1}H spectra of lipid metabolites extracted from rat heart and liver

The data from ^{1}H NMR spectra of lipids extracted from rat heart and liver tissues were examined using a multivariate statistical analysis (MVA) approach. Principal components analysis (PCA) is one such MVA method that reduces the data into a small number of variables called principal components (PCs), describing most of the variation in the spectral data. This analysis produces a scores scatter plot (Figures 5.3 and 5.6) and a loadings scatter plot (Figures 5.4 and 5.7) that show which spectral variable contributes to each PC producing better separation of sample types. The corresponding loadings plots are shown (Figure 5.4 and 5.7) that best discriminate between samples. The absolute size of the peaks on the loading plots shows the data point is related to the principal component that can correctly identify the most variable component of the samples. Displaying the ^{1}H NMR spectra of the data variables (Figures 5.5 and 5.8) is essential. Tracing the variable value from the spectra demonstrates the metabolite peaks (Figure5.5 and 5.8). The lipid metabolites are then identified from the known ^{1}H chemical shifts of each component in Tables 5.1 and 5.2.

The scores PC1, PC2 are variables derived from the NMR peaks and summarizing the variables. The observation scores of PC1, PC2 are completely independent of each other. PC1 explains the largest variation of the data, followed by PC2. The scatter plot of PC1 vs PC2 displays how the observations are situated with respect to each other. Observations near each other are similar, which means less variation and observation far away from each other are dissimilar, having more variation.

The PCA analysis of lipids from heart tissues suggest that the score scatter plot shows two different patterns of group between WD and HF samples (Figure 5.3). In one group, there are HF samples and some WDSham samples above the regression line. This group suggests that the variation is the highest among the samples and there is also a significant difference between Sham and AC surgery method of WD samples of this group. The second group is the cluster of WD samples below the regression line. The samples of this group are close to each other and overlapping situating near to the zero point or near to the centre. This cluster shows less variation among the samples of this group but no separation between Sham and AC WD samples.

In loading scatter plot of heart lipids (Figure 5.4), PC1 on the X axis suggests that variable points 1858-1890 have strong impact, because these variable points are far away from the centre at the zero point of PC1 on X-axis. The variable points 1884 and 1885 show strong effect on the data causing the highest variation among PC1, whereas in the PC2 on the Y axis the variable points 2015-2030 are far away from the centre at zero value of PC2 on the Y-axis causing strong variation impact among PC2. The variable point 2015 shows the strongest variation among the PC2 variables because it is far away from other variables of PC2 on the Y-axis. The variable points 2015-20130 correspond to fatty acids (FA) ω-CH_3 at 0.88ppm, whereas the variable points 1858- 1890 correspond to FA $(CH_2)_n$ at 1.30ppm of ^1H NMR (Figure 5.5).

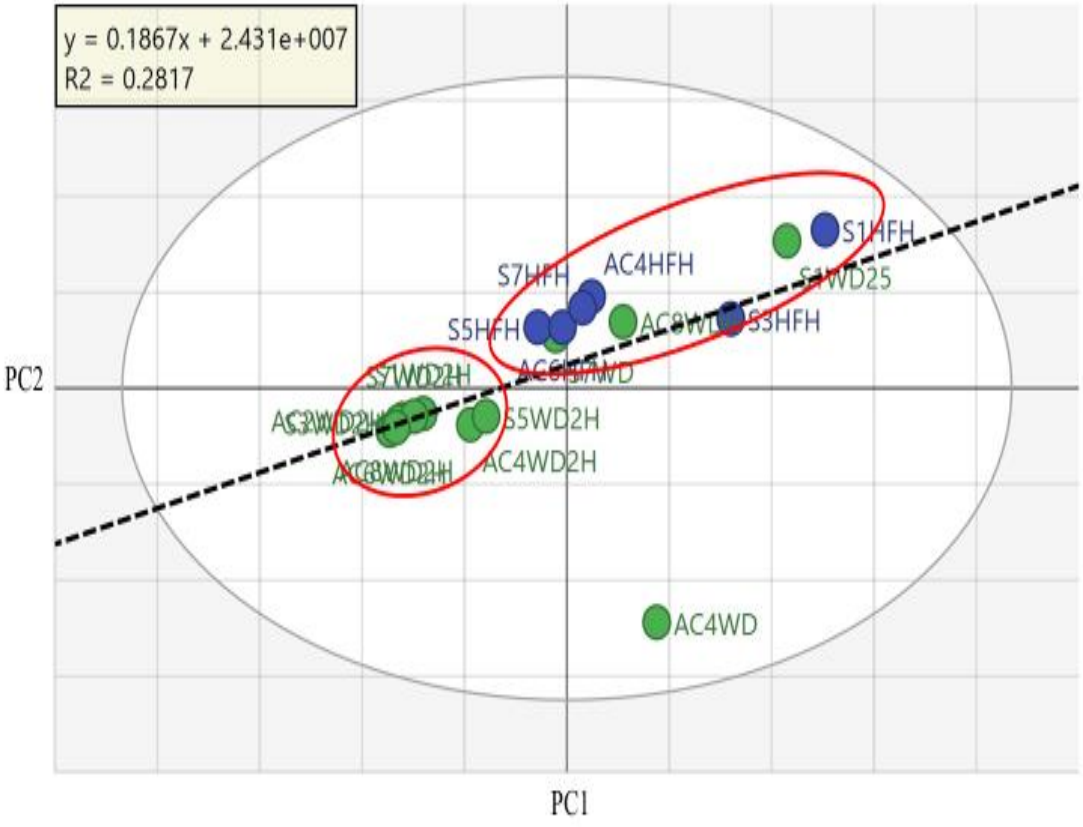

Figure 5.3 Score scatter plot of 1H NMR spectra of lipids extracted from rat heart tissues.

Where green circles are WD and blue circles are HFD. ACWD: Aortic constriction Western diet; SWD: Sham Western diet; ACHFD: Aortic constriction high fat diet; SHFD: Sham high fat diet. The graph is plotted against PC1 and PC2 which represent the score variation in the object direction.

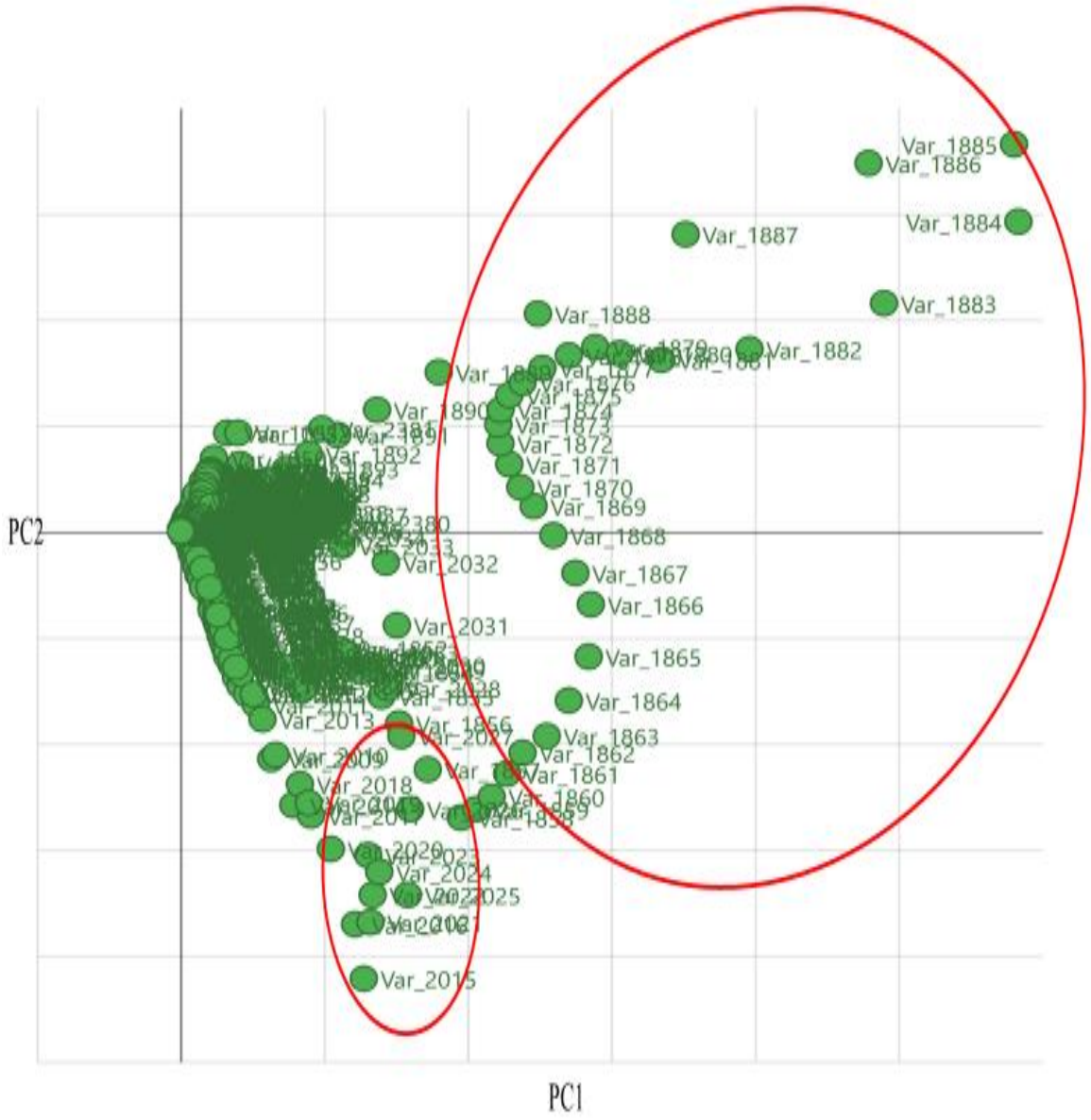

Figure 5.4 Loadings scatter plots of PC1 and PC2 component variables of lipids from heart.

Each point is a variable that presents the ^{1}H NMR peak intensity of lipids from rat heart samples. Where, Var: variable point.

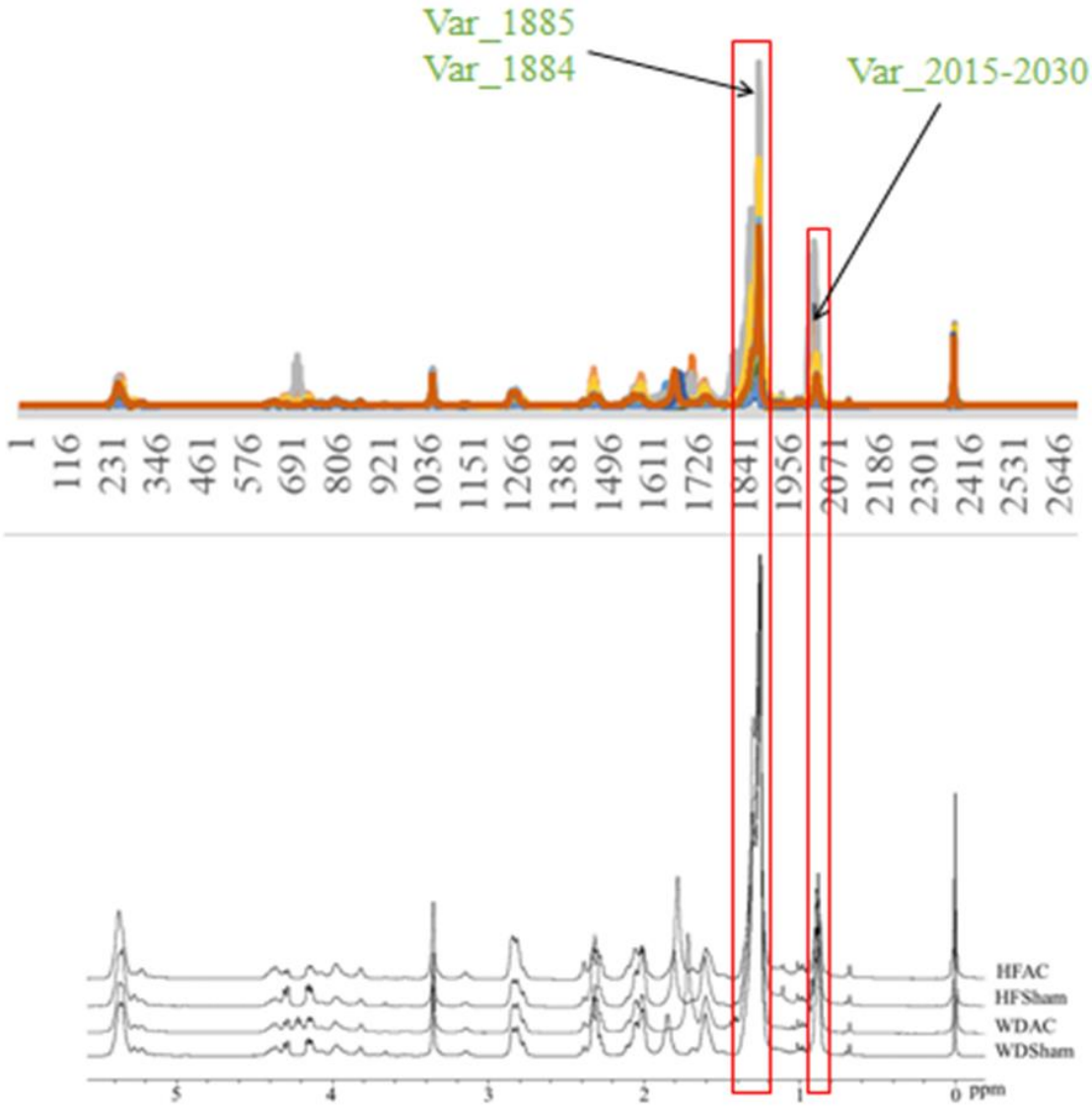

Figure 5.5 ^{1}H NMR spectrum of heart lipids corresponding to the lipid variables PCA analysis.

Where 2015-20130 correspond to fatty acids (FA) ω-CH_3 at 0.88ppm, whereas variable points 1858- 1890 correspond to FA $(CH_2)_n$ at 1.30ppm of ^{1}H NMR. ^{1}H NMR spectra of lipids extract from rat heart tissues. Red boxes represent the variables and their corresponding chemical shifts.

In PCA analysis of lipids from liver tissues, the score scatter plot divides the WD and HF samples into three groups (Figure 5.6). The WD samples are separated significantly from HF samples. The cluster of HF scores are non-overlapping and clear separation is observed between HFSham and HFAC samples. There are two group clusters of WD samples. In these WD groups, the Sham and AC samples are separated and do not overlap with each other.

In loading scatter plot of lipids from liver tissues (Figure 5.7), PC1 on the X axis suggests that variable poits 1886 and 1887 show strong impact, because these variable points are far away from the centre or zero point on the X axis. However, the variable points from 1881 to 1884 and variable point from 1889 to 1891 are present between PC1 and PC2 and these variable points are the same as variable points between 1881 to 1891. In the PC2 on the Y axis the variable points 1883 and 1889 are far away and thus cause strong impact on PC2. The variable points from 1881 to 1891correspond to FA $(CH_2)_n$ at 1.30ppm of ^1H NMR (Figure 5.8).

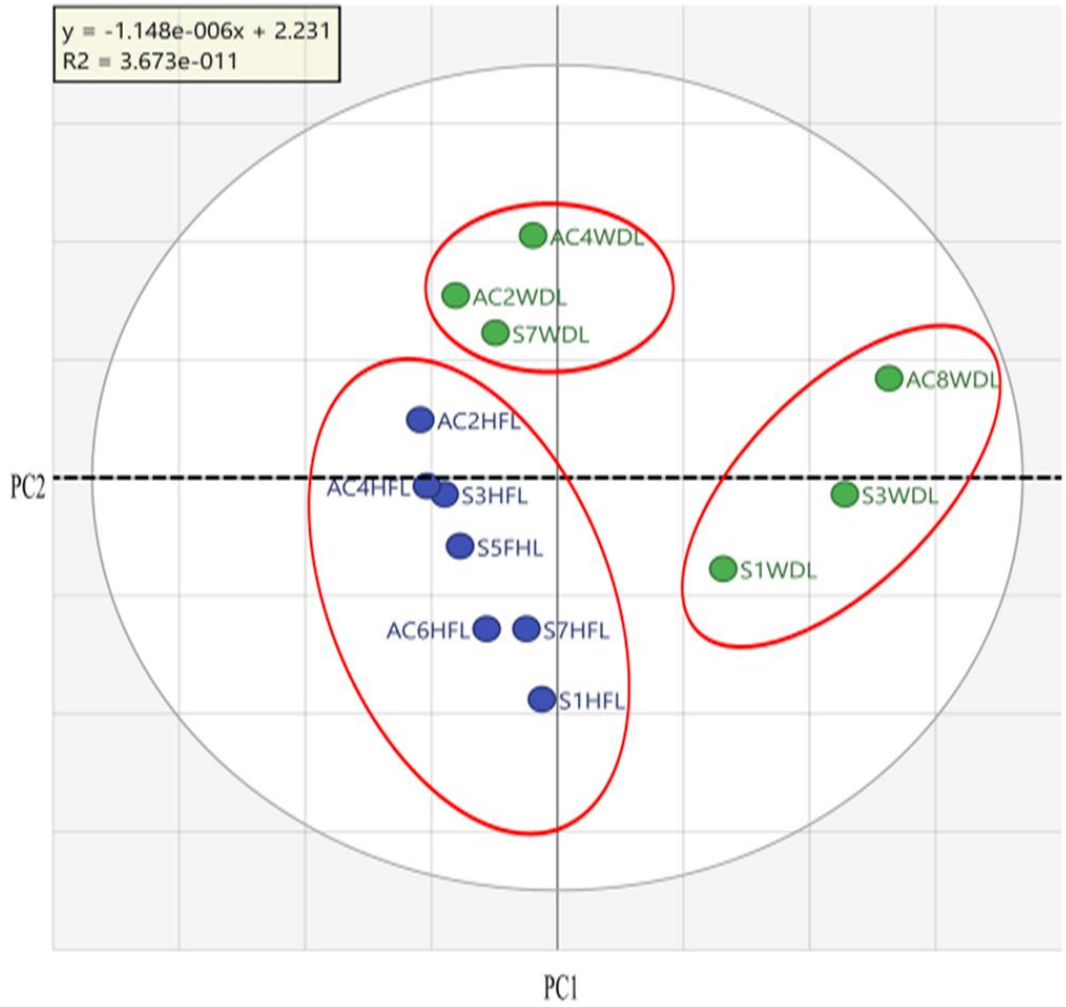

Figure 5.6 Score scatter plot of ^{1}H NMR spectra of lipids extracted from rat liver tissues.

Where green circles are WD and blue circles are HFD. ACWD: Aortic constriction Western diet; SWD: Sham Western diet; ACHFD: Aortic constriction high fat diet; SHFD: Sham high fat diet. The graph is plotted against PC1 and PC2 which represent the score variation in the object direction.

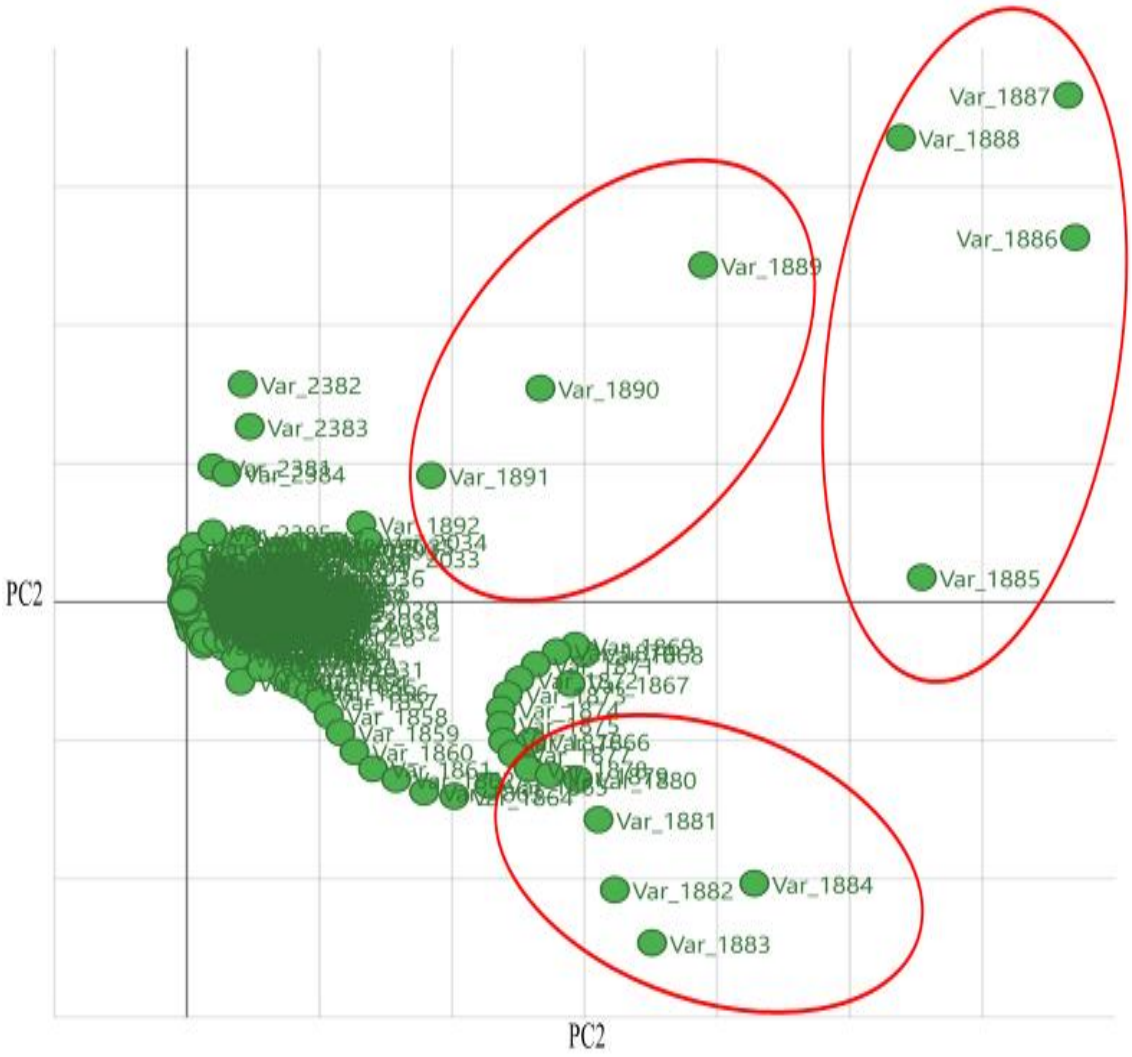

Figure 5.7 Loadings scatter plots of PC1 and PC2 component variables.

Each point is a variable that represents the ^{1}H NMR peak intensity of lipids from rat liver samples, where, Var: variable point.

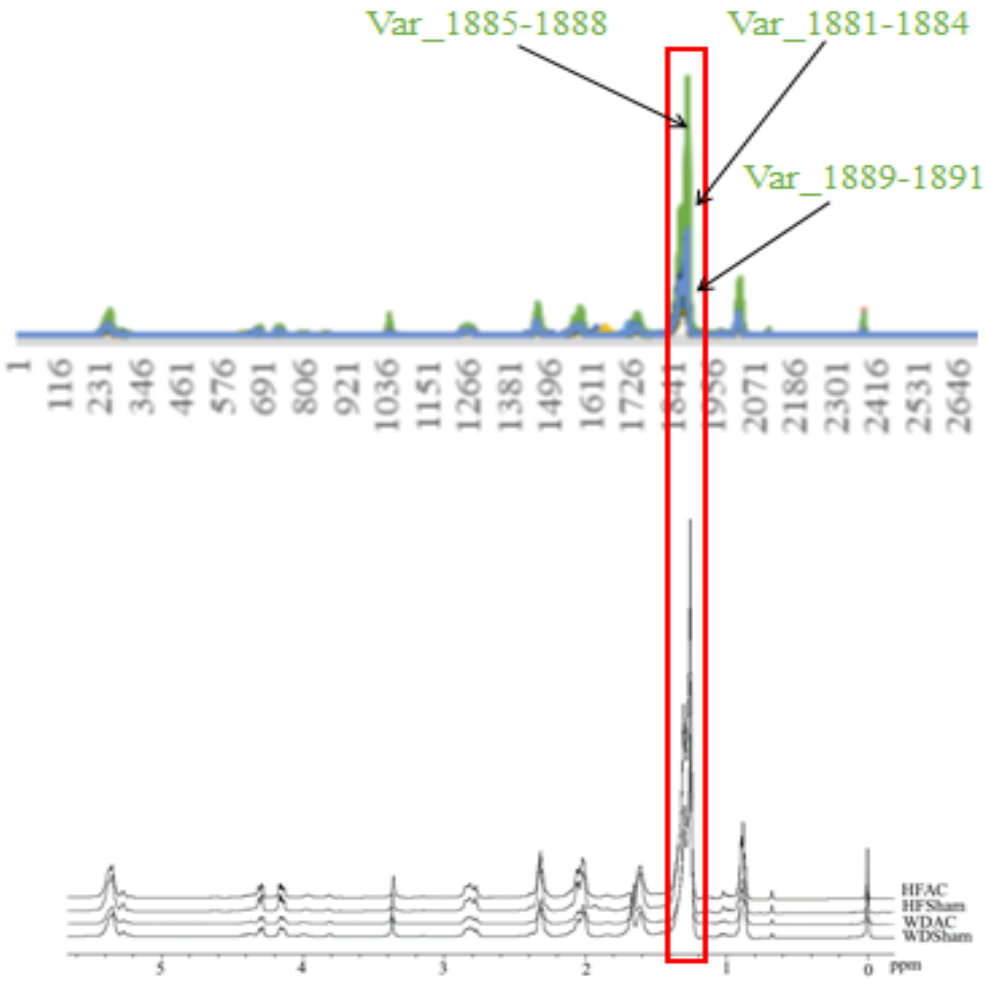

Figure 5.8 ^{1}H NMR spectrum of liver lipids corresponding to the lipid variables PCA analysis.

Where variable points 1881- 1891 correspond to FA $(CH_2)_n$ at 1.30ppm of ^{1}H NMR. ^{1}H NMR spectra of lipids extract from rat liver tissues. Red boxes represent the variables and their corresponding chemical shifts.

5.5 Discussion

Metabolomics has been emerging as an important tool to detect the novel biomarkers of dietary intake in recent times.[28-30] Lipidomics is a subset of metabolomics dealing with lipid profiles.[31, 32] It helps to quantify lipid compositions in biological matrixes.[33] The lipidomics technologies provide a deep understanding of heart and liver pathophysiological processes to identify potential lipid biomarkers in order to develop clinical applications.[34-36] The main aim of this study was to investigate the molecular lipid profiles of different diets (WD and HFD) extracted from heart and liver tissues analysed by proton NMR and PCA. Proton nuclear magnetic resonance (^{1}H NMR) spectroscopy is an ideal instrument for lipid analysis which helps to generate lipid molecular profiling.[34, 35, 37] It is a quick, reproducible, noninvasive, and nondestructive tool that needs minimal volume of sample, giving thorough information of lipid molecular structure.[38-40] The lipid abnormalities associated to diseases are closely reflected on the ^{1}H NMR lipid finger print.[41] Thus, the proton NMR-based lipid approach is an effective technique for the identification of lipid biomarkers of a dietary pattern and associated disease state.[41] Brindle *et al*. first used 600 MHz ^{1}H NMR to analyse total serum lipid related to severe coronary heart disease.[42] Further, Kirschenlohr *et al.* used 400 MHz NMR spectra for plasma samples and suggested that CVD is influenced by cholesterol.[43] In both early studies, the ^{1}H NMR analysis was based on the regions mainly assigned to the key lipid groups.[42, 43] However, in recent time the explanation of the NMR-generated composite lipid data has been simplified by the use of multivariate statistical analysis, such as PCA that provide a prevailing platform to understand the lipid profile of different dietary patterns and related diseases.[44]

The rats were fed either Western or high fat diet for nine weeks. The aortic constriction (AC; induced cardiac hypertrophy and heart failure) and Sham (placebo) surgical methods were used before feeding (described in section 2.1.1). About 300mg of heart and liver tissues were used to extract lipids for each experiment. The ^{1}H NMR spectra of lipids from the heart suggest that the lipid groups (Table 5.1) β-CH_2 at 1.67ppm of FA was only observed in HF samples (HFSham and HFAC), CH_2-$N^{+}(CH_3)_3$ at 3.65ppm of PC and SM was found in WDSham and HFSham samples and -O-CH_2-CH_2-N+$(CH_3)_3$ at 4.24ppm of PC and SM appeared in WDAC and HFSham samples (Figure 5.1). PCA data suggest that the variable points 2015-20130 correspond to FA methyl group (ω-CH_3) at 0.88ppm, whereas variable points 1858- 1890 correspond to the FA polyunsaturated group $(CH_2)_n$ at 1.30ppm of ^{1}H NMR (Figure 5.5).

Berthiaume *et al.* used Wistar rats - intervention of 8 weeks standard diet or high saturated fat diet under electrocardiography, genomic expression and pressure-volume catheter.[45] They reported that high fat feeding rats recovered myocardial function during rest or non-physiological stress condition.[45] However, during physiological stress, they found heart failure or LV dysfunction was mild to moderate.[45] Further, they examined whether HFD fed to rats for eight weeks post-infarction raised the metabolic physiological changes in the heart.[46] They found a cardioprotective effect of HFD when fed after myocardial infarction (MI) as compared to standard or control diet cohorts, despite the lipotoxic effects of elevating FA.[46] Using ^{31}P NMR, they observed that Langendorff perfused hearts had no differences in phosphocreatine to ATP ratios, suggesting no overt energy deficit in MI HFD groups.[46]

O'Donnell *et al*. used Sprague-Dowley rats and followed Sham surgical method.[47] Under ^{13}C NMR, they observed that HF from endogenous fatty acids remained negligible during inotropic challenges and contributions from palmitate dropped by 18%.[47] The lowering of palmitate was balanced by increasing glucose and glycogen oxidation. They concluded that endogenous FA oxidation induced heart failure and that endogenous fat oxidation does not offset the exogenous fat oxidation of a failing heart.[47]

Table 5.3 Assignment of heart lipid groups in WDSham, WDAC, HFSham, HFAC and PCA variables

Lipid groups	WDSham	WDAC	HFSham	HFAC	PCA variables
Cholesterol (Chol-18) -CH_3 (0.70ppm)	√	√	√	√	X
FA ω-CH_3 (0.88ppm)	√	√	√	√	√
Chol-21 -CH_3 (0.9-0.95ppm)	√	√	√	√	X
FA omega3 -CH_3 (0.96ppm)	√	√	√	√	X
Chol-19 -CH_3 (1.00ppm)	√	√	√	√	X
FA $(CH_2)_n$ (1.30ppm)	√	√	√	√	√
FA CH_2CH_2CO (1.59ppm)	√	√	√	√	X
FA β-CH_2 (1.67ppm)	X	X	√	√	X
FA CH-CH= (2.04ppm)	√	√	√	√	X
FA -CO-CH_2-CH_2- (2.30ppm)	√	√	√	√	X
FA α and β -CH_2 (2.38ppm)	√	√	√	√	X
FA -CH=CH-CH_2-CH=CH- (2.75ppm)	√	√	√	√	X
FA $(CH=CH-CH_2-CH=CH)_n$ (2.80ppm)	√	√	√	√	X
PE -CH_2-NH_2 (3.11ppm)	√	√	√	√	X
PC and SM $N^+(CH_3)_3$ (3.35ppm)	√	√	√	√	X
PC and SM CH_2 -$N^+(CH_3)_3$ (3.65ppm)	√	X	√	X	X
Glycerophospholipid backbone -CH_2 (3.97ppm)	√	√	√	√	X
Glycerol (TG) C1H, C3H (4.16ppm)	√	√	√	√	X
PC/SM -O-CH_2-CH_2-$N^+(CH_3)_3$ (4.24ppm)	X	√	√	X	X
Glyceryl-C1H(TG/PC/PE) (4.32ppm)	√	√	√	√	X
Glycerophosphocholine (GPC) -CH_2 (4.38ppm)	√	√	√	√	X
Glycerol (TG) -CH (5.22ppm)	√	√	√	√	X
Glycerol (PC/PE) -CH (5.28ppm)	√	√	√	√	X
FA -CH=CH- and Chol-6 -CH_3 (5.36ppm)	√	√	√	√	X

It is well known that intramyocardial TG yield is reduced in failing hearts, restraining the rich source of long-chain fatty acids for mitochondrial β-oxidation. Lahey *et al.* studied dietary long-chain fatty acids, palmitate and oleate for TG dynamics and peroxisome proliferator-activated receptor-α activation in Sham and AC rat hearts.[48] Using ^{13}C NMR they reported that palmitate contribution into TG stores was less in the AC heart as compared to the Sham.[48] However, oleate restored TG enhancement in AC hearts. They suggested that oleate rescues lipid metabolism in the failing heart or else it is reduced in the presence of palmitate.[48] Further, Akki *et al.* reported that WD induced dysregulation of FA metabolism that was significantly greater in cardiac hypertrophy as compared to standard diet (SD) condition using Sprague–Dawley AC rats under ^{13}C NMR.[49] Butler *et al.* found that WD induced significant metabolic remodelling in the heart as compared to SD and HFD using diet-induced rat model under AC surgical condition.[50]

However, in this study, lipids from heart showing FA β-unsaturated groups were only observed in HFD groups, either in aortic constriction (to mimic of the cardiac stress) or Sham (normal or control cardiac condition) surgical methods under proton NMR spectra. PCA data revealed that the FA methyl group and polyunsaturated group were more variable in both WD or HFD groups. Therefore, these data suggest that FA may play an important role in the lipid dynamics and metabolism in the heart and related diseases. However, the data from NMR and PCA of this study contradict the other findings by Berthiaume *et al.*[45, 46], Lahey *et al.*[48] and O'Donnell *et al.*[47] suggesting that saturated high fats or TG cause cardiac diseases. Further, there is a needed to understand the link between unsaturated FA and cardiac diseases.

Table 5.4 Assignment of liver lipid groups in WDSham, WDAC, HFSham, HFAC and PCA variables

Lipid group	WDsham	WDAC	HFDSham	HFDAC	PCA Variables
Chol–18 -CH_3 (0.69ppm)	√	√	√	√	X
FA ω-CH_3/ Cho-26&27 -CH_3 (0.88ppm)	√	√	√	√	X
Chol-19 -CH_3 (1.00ppm)	√	√	√	√	X
FA $(CH_2)_n$ (1.30ppm)	√	√	√	√	√
FA CO-CH_2 -CH_2 (1.59ppm)	√	√	√	√	X
FA CH-CH= (2.04ppm)	√	√	√	√	X
FA CO-CH_2 (2.30ppm)	√	√	√	√	X
FA CH=CH-CH_2-CH=CH- (2.75ppm)	√	√	√	√	X
FA$(CH=CH-CH_2-CH=CH)_n$ (2.80ppm)	√	√	√	√	X
PE -CH_2-NH_2 (3.10ppm)	√	√	√	√	X
Cholin –$N^+(CH_3)_3$ (3.37ppm)	√	√	√	√	X
Glycerophosphospholipid backbone -CH_2 (3.97ppm)	√	√	√	√	X
TG glycerol C1H (4.16ppm)	√	√	√	√	X
Glyceryl-C1H(TG/PC/PE) (4.32ppm)	√	√	√	√	X
GPC -CH_2 (4.38ppm)	√	√	√	√	X
Glycerol(TG) –CH (5.22ppm)	√	√	√	√	X
Glycerol(PC/PE) C2H (5.27ppm)	√	√	√	√	X
FA CH=CH & Chol-6 -CH_3 (5.37ppm)	√	√	√	√	X

The ^{1}H NMR spectra of lipids from liver showed that in the lipid groups (Table 5.2) such as -CH_2 at 4.38ppm of GPC, the peak intensity was higher in WD samples than HF

samples (Figure 5.2). PCA data suggest that the variable points from 1881 to 1891correspond to FA polyunsaturated groups at 1.30ppm of ^{1}H NMR (Figure 5.8).

Sobrecases *et al.* reported that SFA diet increased liver fat more than fructose, suggesting that surplus SFA is more toxic to liver fat accumulation than extra added sugars.[51] Van der Meer *et al*. observed a significant increase in liver fat accumulation in three days of over eating of a high-fat diet using ^{1}H NMR.[52] They also reported that short-term intake of HFD and high energy diet increased the plasma TG and non-esterified fatty acid concentrations and hepatic TG.[52] Further using MRI Rosqvist *et al* suggested that SFA caused an elevation of liver fat accumulation as compared with PUFA.[53] Wei *et al* reported that SFA disturbed the homeostasis of ER inducing apoptosis in liver cells using immunoassay.[54]

In this study, the lipids from liver of proton NMR spectra showed the peak intensities of lipid group -CH_2 of GPC at 4.38ppm were higher in WD than HFD samples. Otherwise there was no significant difference in proton NMR spectra between WD and HFD groups either in cardiac stress (AC) or normal (Sham) surgical conditions. PCA data revealed that polyunsaturated FA were more variable in both WD and HFD groups. However, these data contradict previous findings by Sobrecases *et al*.,[51] van der Meer *et al*.,[52] Rosqvist *et al.*[53] and Wei *et al.*[54] who suggested that the SFA group is the most influential lipid group in disturbing the lipid metabolism in the liver and associated diseases. Further, it may be necessary to understand the role of unsaturated FA in the lipid dynamics and metabolism in the liver or related diseases.

In conclusion, lipid compositions may be important in the lipid dynamics of the heart and liver and related abnormalities. The data suggest that the variations in unsaturated FA

lipid groups of WD and HFD conditions may influence the heart and liver lipid profiles and related diseases. The unsaturated FA group may be used as a biomarker to understand the link between diets, WD or HFD and lipid profiling or the heart and liver.

5.6 References

1. L. D. Roberts, A. L. Souza, R. E. Gerszten and C. B. Clish, *Curr Protoc Mol Biol*, 2012, **Chapter 30**, Unit 30 32 31-24.
2. B. Peng, H. Li and X. X. Peng, *Protein & cell*, 2015, **6**, 628-637.
3. C. Herder, M. Karakas and W. Koenig, *Clinical pharmacology and therapeutics*, 2011, **90**, 52-66.
4. E. P. Rhee and R. E. Gerszten, *Clinical chemistry*, 2012, **58**, 139-147.
5. A. E. Field, E. H. Coakley, A. Must, J. L. Spadano, N. Laird, W. H. Dietz, E. Rimm and G. A. Colditz, *Archives of internal medicine*, 2001, **161**, 1581-1586.
6. P. W. Wilson, R. B. D'Agostino, L. Sullivan, H. Parise and W. B. Kannel, *Archives of internal medicine*, 2002, **162**, 1867-1872.
7. S. G. Sheth, F. D. Gordon and S. Chopra, *Annals of internal medicine*, 1997, **126**, 137-145.
8. I. R. Wanless and J. S. Lentz, *Hepatology (Baltimore, Md.)*, 1990, **12**, 1106-1110.
9. J. L. Kuk, P. T. Katzmarzyk, M. Z. Nichaman, T. S. Church, S. N. Blair and R. Ross, *Obesity (Silver Spring, Md.)*, 2006, **14**, 336-341.
10. J. Szendroedi and M. Roden, *Current opinion in lipidology*, 2009, **20**, 50-56.
11. N. A. van Herpen and V. B. Schrauwen-Hinderling, *Physiology & behavior*, 2008, **94**, 231-241.
12. R. Harmancey, C. R. Wilson, N. R. Wright and H. Taegtmeyer, *J Lipid Res*, 2010, **51**, 1380-1393.
13. P. Silva Figueiredo, A. Carla Inada, G. Marcelino, C. Maiara Lopes Cardozo, K. de Cassia Freitas, R. de Cassia Avellaneda Guimaraes, A. Pereira de Castro, V. Aragao do Nascimento and P. Aiko Hiane, *Nutrients*, 2017, **9**, E1158.
14. A. Must and N. M. McKeown, in *Endotext*, eds. L. J. De Groot, G. Chrousos, K. Dungan, K. R. Feingold, A. Grossman, J. M. Hershman, C. Koch, M. Korbonits,

R. McLachlan, M. New, J. Purnell, R. Rebar, F. Singer and A. Vinik, South Dartmouth (MA), 2000. www.endotext.org.

15. K. H. Williams, N. A. Shackel, M. D. Gorrell, S. V. McLennan and S. M. Twigg, *Endocr Rev*, 2013, **34**, 84-129.

16. C. A. Matteoni, Z. M. Younossi, T. Gramlich, N. Boparai, Y. C. Liu and A. J. McCullough, *Gastroenterology*, 1999, **116**, 1413-1419.

17. P. Angulo, J. C. Keach, K. P. Batts and K. D. Lindor, *Hepatology (Baltimore, Md.)*, 1999, **30**, 1356-1362.

18. T. Gramlich, D. E. Kleiner, A. J. McCullough, C. A. Matteoni, N. Boparai and Z. M. Younossi, *Human pathology*, 2004, **35**, 196-199.

19. S. B. Reeder, I. Cruite, G. Hamilton and C. B. Sirlin, *Journal of magnetic resonance imaging: JMRI*, 2011, **34**, 729-749.

20. C. Zeng, B. Wen, G. Hou, L. Lei, Z. Mei, X. Jia, X. Chen, W. Zhu, J. Li, Y. Kuang, W. Zeng, J. Su, S. Liu, C. Peng and X. Chen, *GigaScience*, 2017, **6**, 1-11.

21. G. Steiner, *Anal Bioanal Chem*, 2017, **409**, 5615-5616.

22. E. Rodriguez-Garcia, J. Ruiz-Nava, S. Santamaria-Fernandez, J. C. Fernandez-Garcia, A. Vargas-Candela, R. Yahyaoui, F. J. Tinahones, M. R. Bernal-Lopez and R. Gomez-Huelgas, *Medicine*, 2017, **96**, e7040.

23. J. H. Bothwell and J. L. Griffin, *Biological reviews of the Cambridge Philosophical Society*, 2011, **86**, 493-510.

24. J. Feng, N. G. Isern, S. D. Burton and J. Z. Hu, *Metabolites*, 2013, **3**, 1011-1035.

25. A. Papathanasiou, C. Kostara, M. T. Cung, K. Seferiadis, M. Elisaf, E. Bairaktari and I. A. Goudevenos, *Hellenic journal of cardiology : HJC = Hellenike kardiologike epitheorese*, 2008, **49**, 72-78.

26. F. P. Martin, M. E. Dumas, Y. Wang, C. Legido-Quigley, I. K. Yap, H. Tang, S. Zirah, G. M. Murphy, O. Cloarec, J. C. Lindon, N. Sprenger, L. B. Fay, S.

Kochhar, P. van Bladeren, E. Holmes and J. K. Nicholson, *Molecular systems biology*, 2007, **3**, 112.

27. H. Zhang, L. Ding, X. Fang, Z. Shi, Y. Zhang, H. Chen, X. Yan and J. Dai, *PloS one*, 2011, **6**, e20862.

28. M. Jenab, N. Slimani, M. Bictash, P. Ferrari and S. A. Bingham, *Human genetics*, 2009, **125**, 507-525.

29. A. O'Gorman, H. Gibbons and L. Brennan, *Computational and structural biotechnology journal*, 2013, **4**, e201301004.

30. V. E. Hedrick, A. M. Dietrich, P. A. Estabrooks, J. Savla, E. Serrano and B. M. Davy, *Nutrition journal*, 2012, **11**, 109.

31. M. R. Wenk, *Nature reviews. Drug discovery*, 2005, **4**, 594-610.

32. M. Oresic, *Nutrition, metabolism, and cardiovascular diseases : NMCD*, 2009, **19**, 816-824.

33. W. J. Griffiths, M. Ogundare, C. M. Williams and Y. Wang, *J Inherit Metab Dis*, 2011, **34**, 583-592.

34. A. Giovane, A. Balestrieri and C. Napoli, *J Cell Biochem*, 2008, **105**, 648-654.

35. K. Ekroos, M. Janis, K. Tarasov, R. Hurme and R. Laaksonen, *Curr Atheroscler Rep*, 2010, **12**, 273-281.

36. K. Scupakova, Z. Soons, G. Ertaylan, K. A. Pierzchalski, G. B. Eijkel, S. R. Ellis, J. W. Greve, A. Driessen, J. Verheij, T. de Kok, S. W. M. Olde Damink, S. S. Rensen and R. M. A. Heeren, *Analytical chemistry*, 2018, DOI: 10.1021/acs.analchem.7b05215.

37. C. E. Kostara, A. Papathanasiou, M. T. Cung, M. S. Elisaf, J. Goudevenos and E. T. Bairaktari, *J Proteome Res*, 2010, **9**, 897-911.

38. J. K. Nicholson and I. D. Wilson, *Prog Nucl Magn Reson Spectrosc*, 1989, **21**, 449-501.

39. M. Casu, G. J. Anderson, G. Choi and W. A. Gibbons, *Magn.Reson.Chem.*, 1991, **29**, 594-602.

40. M. R. Tosi, A. Trinchero, A. Poerio and V. Tugnoli, *Ital J Biochem*, 2003, **52**, 141-144.

41. R. S. Rosenson, *Curr Atheroscler Rep*, 2010, **12**, 184-186.

42. J. T. Brindle, H. Antti, E. Holmes, G. Tranter, J. K. Nicholson, H. W. Bethell, S. Clarke, P. M. Schofield, E. McKilligin, D. E. Mosedale and D. J. Grainger, *Nature medicine*, 2002, **8**, 1439-1444.

43. H. L. Kirschenlohr, J. L. Griffin, S. C. Clarke, R. Rhydwen, A. A. Grace, P. M. Schofield, K. M. Brindle and J. C. Metcalfe, *Nature medicine*, 2006, **12**, 705-710.

44. J. C. Lindon, E. Holmes and J. K. Nicholson, *Expert Rev Mol Diagn*, 2004, **4**, 189-199.

45. J. M. Berthiaume, M. S. Bray, T. A. McElfresh, X. Chen, S. Azam, M. E. Young, B. D. Hoit and M. P. Chandler, *Am J Physiol Heart Circ Physiol*, 2010, **299**, H410-421.

46. J. M. Berthiaume, M. E. Young, X. Chen, T. A. McElfresh, X. Yu and M. P. Chandler, *J Mol Cell Cardiol*, 2012, **53**, 125-133.

47. J. M. O'Donnell, A. D. Fields, N. Sorokina and E. D. Lewandowski, *J Mol Cell Cardiol*, 2008, **44**, 315-322.

48. R. Lahey, X. Wang, A. N. Carley and E. D. Lewandowski, *Circulation*, 2014, **130**, 1790-1799.

49. A. Akki and A. M. Seymour, *Cardiovascular research*, 2009, **81**, 610-617.

50. T. J. Butler, D. Ashford and A. M. Seymour, *Nutrition, metabolism, and cardiovascular diseases : NMCD*, 2017, **27**, 991-998.

51. H. Sobrecases, K. A. Le, M. Bortolotti, P. Schneiter, M. Ith, R. Kreis, C. Boesch and L. Tappy, *Diabetes Metab*, 2010, **36**, 244-246.

52. R. W. van der Meer, S. Hammer, H. J. Lamb, M. Frolich, M. Diamant, L. J. Rijzewijk, A. de Roos, J. A. Romijn and J. W. Smit, *The Journal of clinical endocrinology and metabolism*, 2008, **93**, 2702-2708.

53. F. Rosqvist, D. Iggman, J. Kullberg, J. Cedernaes, H. E. Johansson, A. Larsson, L. Johansson, H. Ahlstrom, P. Arner, I. Dahlman and U. Riserus, *Diabetes*, 2014, **63**, 2356-2368.

54. Y. Wei, D. Wang, F. Topczewski and M. J. Pagliassotti, *Am J Physiol Endocrinol Metab*, 2006, **291**, E275-281.

Chapter 6

Summary

The aim of this project was to investigate the lipid profiling of WD and HFD and their effect on rat's heart and liver using liquid and solid state ^{1}H NMR. The massive NMR data were analysed by PCA software to understand the most effective variables of the lipid compositions. Rats were assigned to either Western diet (WD) or high fat diet (HFD). Rats were maintained for nine weeks post-surgery (Sham and AC) in a 12:12 hour light-dark cycle and provided with food and water. Lipid samples collected from heart and liver tissues were analysed by ^{1}H NMR liquid state and intact tissues were analysed by ^{1}H NMR solid state. The data gained from peak intensity was analysed by the PCA statistical tool.

The experimental conditions were grouped into four categories: WDSham, WDAC, HFDSham and HFDAC. To establish the presence of lipids in the heart and liver tissues, H&E and Oil Red O stain were used. The microscopic images suggested that the lipids were accumulated in the form of LDs. The density of LDs was significantly similar under WD and HFD groups in both heart and liver tissues.

The MAS SS NMR of intact heart and liver tissues spectra showed the similar compositions of metabolites including lipid compositions under all experimental groups. However, PCA data suggested lipid metabolites showed greater variation than carbohydrates and proteins. The most variable lipid were TG and unsaturated lipids, in all dietary conditions, although previous studies suggest that SFA and TG influence the lipid metabolism more than USFA in the heart.

Further lipids extracted from heart and liver tissues were examined under proton NMR. The spectra were not significantly different among experimental dietary groups. However, PCA data suggested that the unsaturated FA groups were the most variable in

WD and HFD groups. Both tissues and extracted lipid samples suggested that unsaturated lipid groups were variable. The unsaturated lipid group may be recognised as a biomarker to examine the effect of dietary fats on the pathophysiological conditions or lipid metabolism of heart and liver and related diseases.

Appendix

The following steps of SIMCA14.1 were used for PCA analysis: -

Step 1: Firstly, imported the normalised NMR spectral data on a new created project sheet in SIMCA. Then the second column set to a Secondary Observation ID. The columns are set to Y-axis. The Primary Variable ID defined for the first row as shown in figure below and then picked Primary Variable ID. This first row is corresponding to the chemical shift regions in the NMR-spectra.

A.

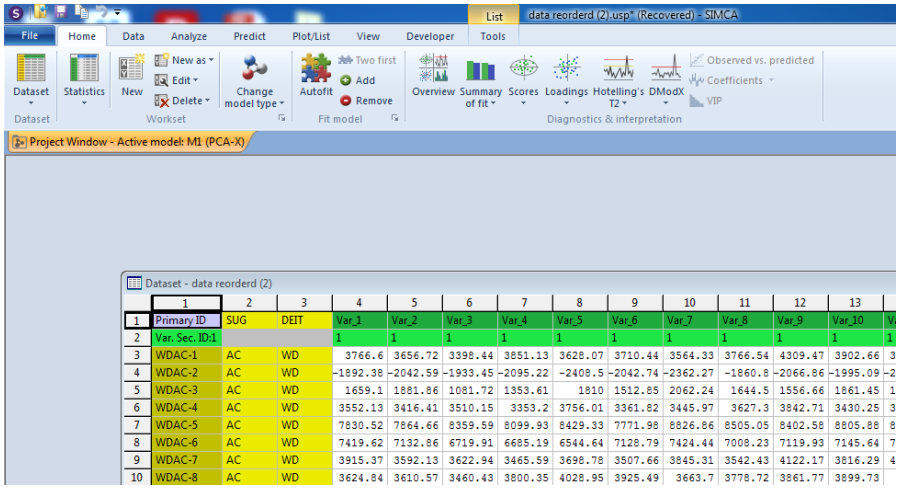

	1	2	3	4	5	6	7	8	9	10	11	12	13
1	Primary ID	SUG	DEIT	Var_1	Var_2	Var_3	Var_4	Var_5	Var_6	Var_7	Var_8	Var_9	Var_10
2	Var. Sec. ID:1			1	1	1	1	1	1	1	1	1	1
3	WDAC-1	AC	WD	3766.6	3656.72	3398.44	3851.13	3628.07	3710.44	3564.33	3766.54	4309.47	3902.66
4	WDAC-2	AC	WD	-1892.38	-2042.59	-1933.45	-2095.22	-2408.5	-2042.74	-2362.27	-1860.8	-2066.86	-1995.09
5	WDAC-3	AC	WD	1659.1	1881.86	1081.72	1353.61	1810	1512.85	2062.24	1644.5	1556.66	1861.45
6	WDAC-4	AC	WD	3552.13	3416.41	3510.15	3353.2	3756.01	3361.82	3445.97	3627.3	3842.71	3430.25
7	WDAC-5	AC	WD	7830.52	7864.66	8359.59	8099.93	8429.33	7771.98	8826.86	8505.05	8402.58	8805.88
8	WDAC-6	AC	WD	7419.62	7132.86	6719.91	6685.19	6544.64	7128.79	7424.44	7008.23	7119.93	7145.64
9	WDAC-7	AC	WD	3915.37	3592.13	3622.94	3465.59	3698.78	3507.66	3845.31	3542.43	4122.17	3816.29
10	WDAC-8	AC	WD	3624.84	3610.57	3460.43	3800.35	4028.95	3925.49	3663.7	3778.72	3861.77	3899.73

B.

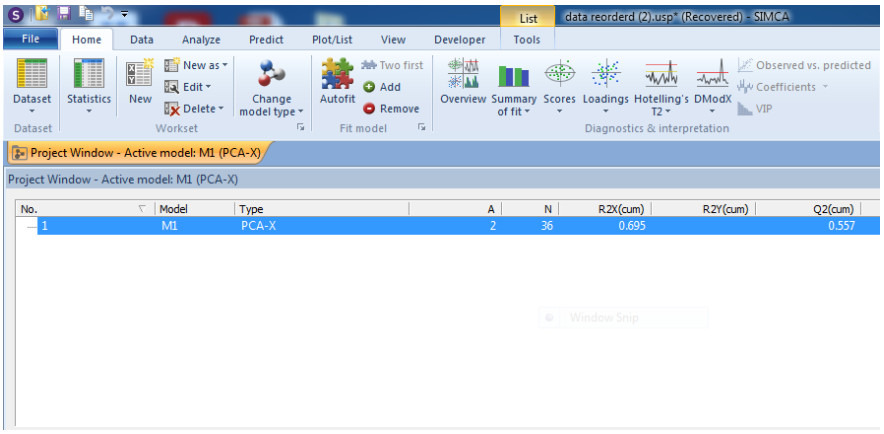

No.	Model	Type	A	N	R2X(cum)	R2Y(cum)	Q2(cum)
1	M1	PCA-X	2	36	0.695		0.557

Figure: (A) Importing NMR-spectra data to the Simca work sheet and defining the primary and secondary observation ID. In this data set, observations (N) =36 (Sprague-Dawley rats) and variables (K) = 1983 (^{1}H-NMR chemical shift region integrals). The observations (rats) are separated in four groups or classes; WDAC = 13 rats, WDSHAM = 11 rats, SDAC = 7 rats, (B) Defining the PCA model of the project.

Step 2: Defining the "workset". Selected the PCA-X model, M1and opened the "workset" box.

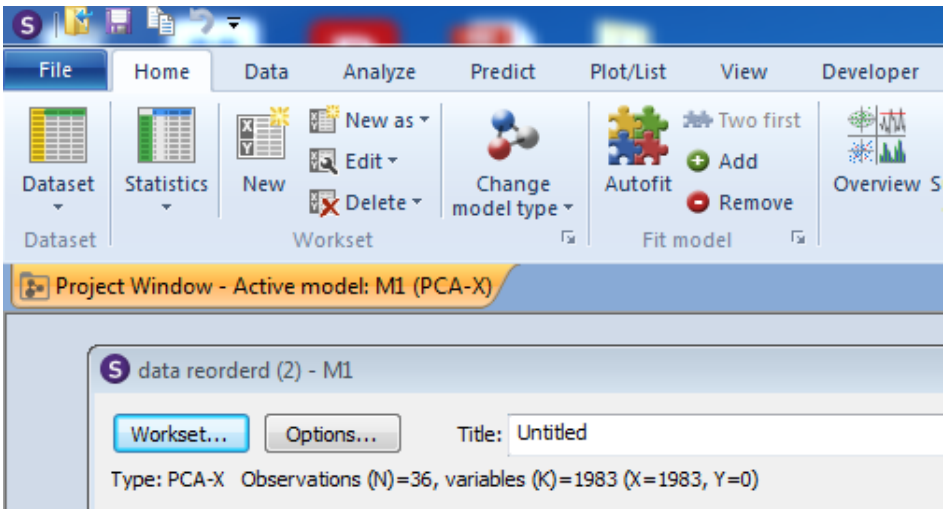

Figure: Creation of "workset" using PCA-X model, M1

Step 3: Scaling the variables: On the "workset" window, opened the scale button and selected the all variables. Under "set scaling type" selected "ParN" as a default for scaling the data that automatically generated the mean-centres of the data as shown in figure.

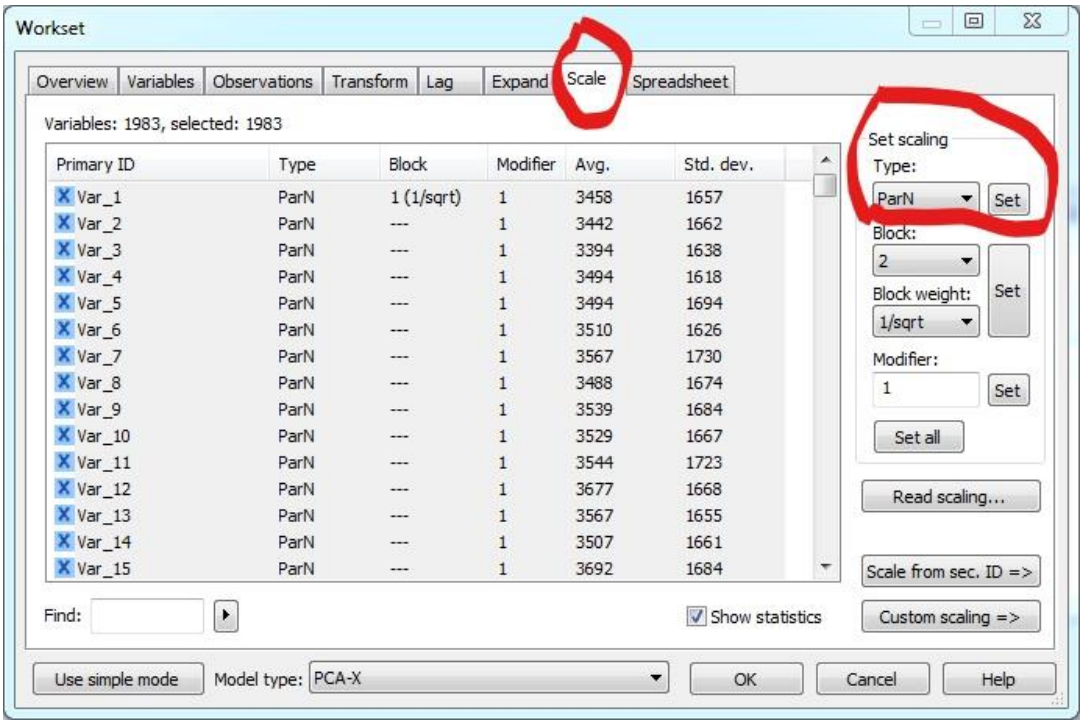

Figure: Selected the "ParN" scaling type to generate the mean centres of the data

Step 4: Set up observations (obs): On "workset" window selected the observation button and set up the class ID. The data were categorised in to four observation primary ID and their corresponding four observation Class ID (Obs Primary ID (Obs Class ID)); WDAC (1), WDS (3), SDAC (2) and SDS (4).

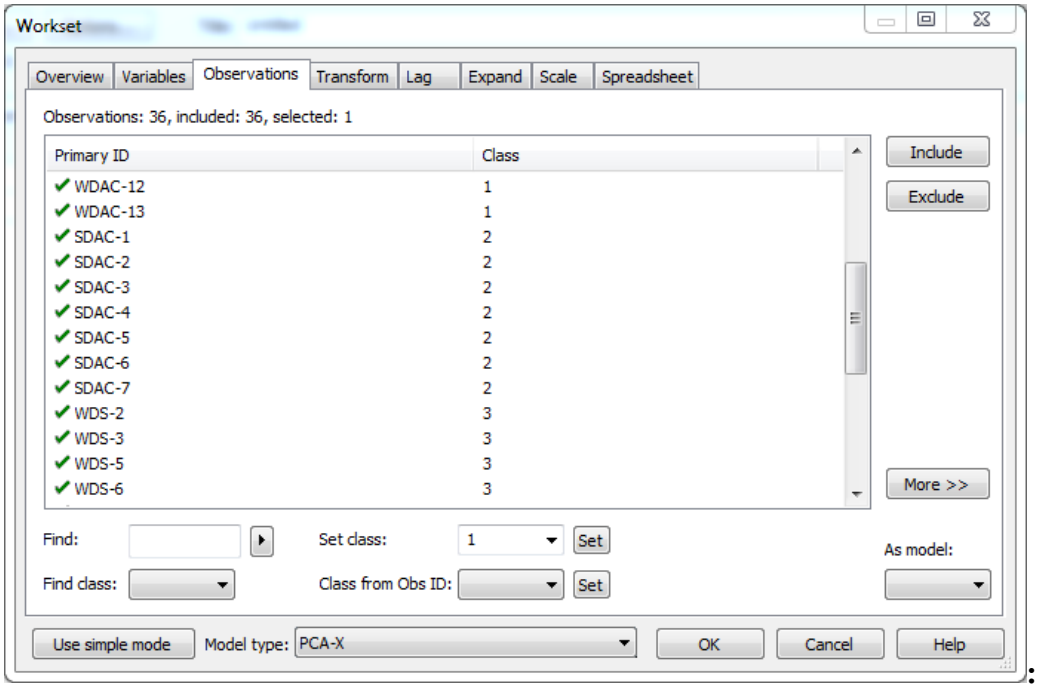

Figure: Defining the observations as primary ID and Class ID

Step 5: **Selection of PCA model type**. For this, used button "Change Model Type" to select PCA-X as shown in figure and then created PCA model as shown in below figure.

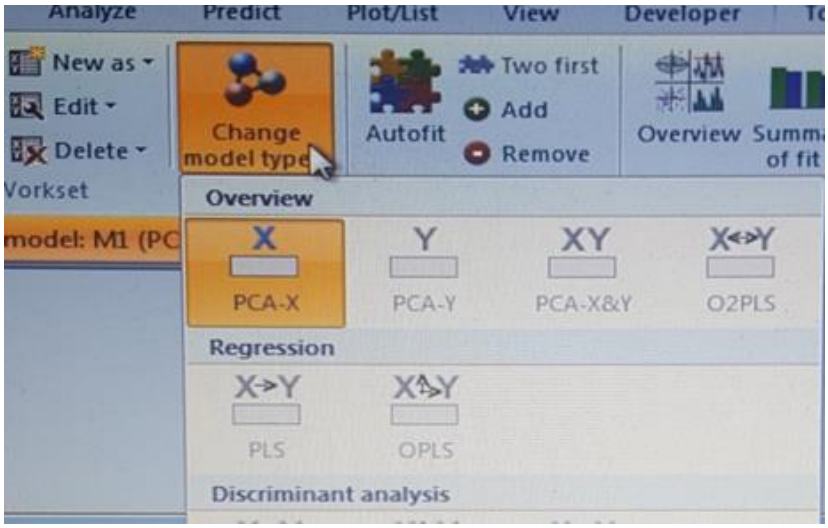

Figure: Selection and creation of PCA model using button “Change Model Type”

Step 6: PCA-X model summary (M1): PCA model summary of fit generated automatically using “Autofit”.

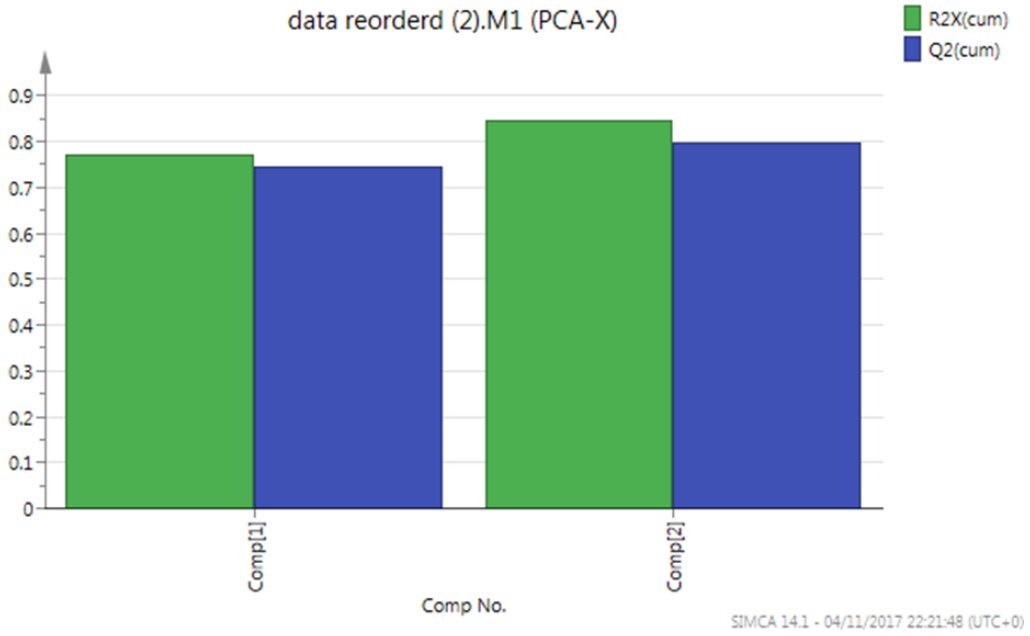

Figure: Plot displays the cumulative R2 and Q2 for the X-model matrix, after each component. R2X is the percentage of the variations of all the X explained by the model and Q2 is percentage of the variation of all the X that can be predicted by the model.

Step 7: Model details of PCA-X: Double clicking on PCA model (M1), the statistics was generated.

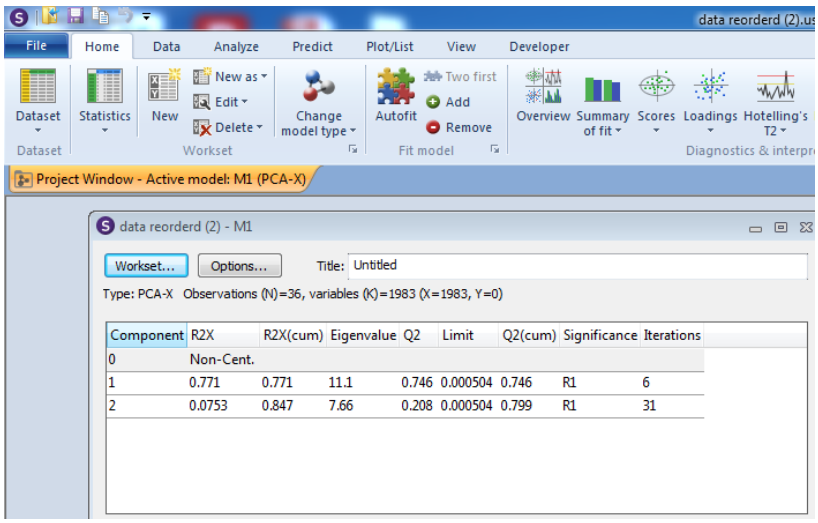

Figure: PCA-X model has an ability to fit the data and the explained variation described by the parameter R2 and the predictive model of PCA-X is estimated by the parameter Q2. In PCA-X model, R2 always increase with number of PC's calculated until it is close to the optimal value of 1.0. However, Q2 will reach an optimal value, after which the predictive power decreases ie. there is a trade-off between fit and prediction ability.

Step 8: **Overview of the plots of PCA-X model:** After evaluating the statistics, clicked button “overview” on Home window and obtained four different plots including “score scatter plot”, “Loading scatter plot”, “DModX line plot” and “X/Y plots”.

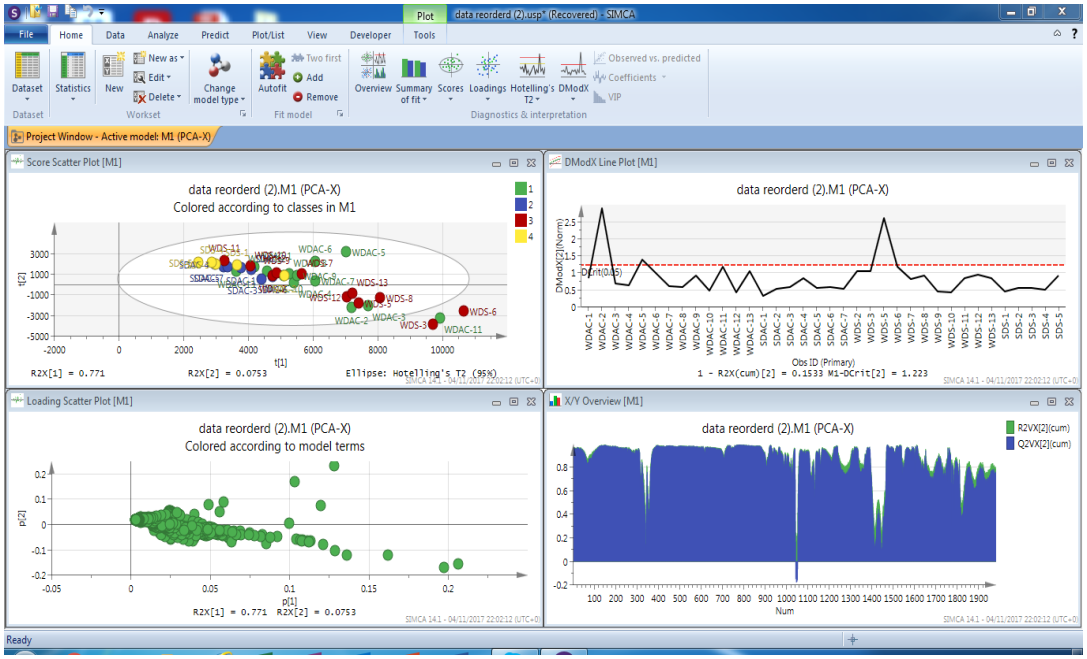

Figure: The score plot defines the separation between variables. The loading plot suggests which variables contribute to the formation of the score. DMod X line plot indicates the residual standard deviation (RSD) of the observations in the X space. X/Y plot displays the cumulative R2VX and Q2VX for each X variable. R2VX is the cumulative percent of the variation of the X variable explained by the model after the last component. Q2VX is the cumulative percent of the variation of the X variable predicted by the model, after the last component.